

UCSF

UC San Francisco Electronic Theses and Dissertations

Title

Mitotic chromosome and spindle dynamics in saccharomyces cerevisiae

Permalink

<https://escholarship.org/uc/item/9q30t1r7>

Author

Straight, Aaron French

Publication Date

1998

Peer reviewed|Thesis/dissertation

MITOTIC CHROMOSOME AND SPINDLE DYNAMICS IN SACCHAROMYCES CEREVISIAE

by

AARON FRENCH STRAIGHT

DISSERTATION

Submitted in partial satisfaction of the requirements for the degree of

DOCTOR OF PHILOSOPHY

in

BIOCHEMISTRY

in the

GRADUATE DIVISION

of the

UNIVERSITY OF CALIFORNIA

San Francisco



This thesis is dedicated to my parents,
Mary and Richard Straight

Acknowledgements

I would first like to thank the Murray Lab as the most amusing scientific environment imaginable. Doug Kellogg was invaluable both personally and scientifically in every aspect of graduate school. He offered endless advice, reagents and bad jokes and will always be an excellent friend. Jeremy Minshull will never be matched as a baymate. He taught me the utilitarian value of surliness, brutally rigorous scientific method and was an endless source of amusement. William Arnold Este Bartholomew Wells Esq. was a fantastic classmate and comrade as we waded through our years in the Murray Lab. Dana Smith was always a shoulder to lean on, helped me with numerous computer problems, and provided the solid support for this thesis. Kevin Hardwick taught me the value of actually doing experiments rather than just talking about doing them. Adam Rudner was uniquely able to construct models to explain scientific problems and was the prototype for generations of pork eating vegetarians. Lena Hwang was an endless source of beer due to her support for Colorado sports teams and an endless source of cheer and enthusiasm. Sue Biggins tried to teach me sensitivity and was very gracious when she failed. Marion Shonn was always there to remind me that there was someone crustier than me in the world. Alex Szidon served as an excellent example of how not to play squash and was always able to make me laugh when I needed it. Cathy Mistrot kept the lab running as well as being an expert source of barbeque information. Hiro Funabiki introduced me to the wonderful world of sake and when he wasn't drinking sake was one of the best critical minds I have met.

Many students at UCSF made graduate school bearable. Kurt Zingler and Pratima Raghunathan fed me through the years and were the best of

friends. Jeremy Minshull and Abby Dernburg also kept my belly full of delicious food and chocolates and were exceptionally generous. Anita Sil was the person I wanted to talk to whenever things turned grim and helped me through a number of difficult times.

John Sedat, Wallace Marshall and Andy Belmont were the best collaborators one could hope for. Andy was always generous with reagents and advice and was insightful concerning experiments throughout the development stages of the chromosome tagging system. Wallace taught me most of what I know about 3D time lapse microscopy and iterative deconvolution, everything I know about Death Metal and is one of the rare people who fully understand the importance of eating animal flesh. John welcomed me into his lab, offered me a place to go when I thought I was out on the street, opened my eyes to the incredible world of microscopy, and took me on my first salmon fishing expedition.

David Morgan and the Morgan Lab deserve special credit. Dave was my surrogate PI for the many instances of Andrew's absence and offered excellent advice on both personal and scientific matters. Dave was also a stellar example of how to be good-natured even in the face of adversity. The Morgan Lab was always a source of reagents, conversation and friendship throughout graduate school.

Thanks also go to the members of the computer graphics lab at UCSF. In particular Leslie Taylor, Chris Botka, Graham Redgrave and Tom Ferrin offered me the opportunity to learn sequence analysis and computer programming. The members of the CGL made the work presented in Appendix A of this thesis possible.

The members of my thesis committee were extraordinary. I would first like to thank Ira Herskowitz, who started on my thesis committee. Ira is

a true geneticist and helped to get me through the dark days of DNA replication.

Sandy Johnson was both a thesis committee member and a good friend. Sandy is one of the best critical thinkers at UCSF and taught me that science can be rigorous and enjoyable at the same time. Sandy also has one of the finest senses of humor at UCSF and was never afraid to use it. Sandy's rigorous logic and his approach to scientific problems helped me a great deal.

Tim Mitchison will use any means necessary to pull unsuspecting fish from their watery beds and his fishing skills translate to his scientific method. I thank Tim for his ingenious approach to science and his critical mind. Tim was always brutally honest and objective when it came to analyzing data and making conclusions. He is in a large part responsible for my decision to abandon a project that was not working and starting the work that resulted in this thesis.

Andrew Murray is a riddle, wrapped in a mystery, inside an enigma. I was never sure whether I should view Andrew as a friend or as an advisor so I did both. Andrew is one of the most imaginative and creative people I have ever encountered. His ideas and example are the fuel for the special character of his lab. Even when I wanted to throttle him I still admired him for his intellect and for his love of science. As a result of Andrew's influence I know that I have become a better scientist.

Alison Farrell was my closest friend and confidant through all the good and the bad times. Alison supported me when times were difficult, was a sage advisor when my thoughts were muddled and helped me bolster my strengths and overcome my weaknesses. Most important, I would like to thank my family for their unending support, for knowing the difference between right and wrong, and for always setting the right example, my Dad

Abstract

Mitotic Chromosome and Spindle Dynamics in *Saccharomyces cerevisiae*.

Aaron F. Straight

Studies of chromosome dynamics in *Saccharomyces cerevisiae* have been hampered by the inability to visualize individual chromosomes in living yeast cells. We have developed a system that makes it possible to monitor the movement of a single chromosome in living yeast. We have introduced a tandem repeat of the lac repressor binding site into sites in the yeast genome. Expression of a green fluorescent protein-lac repressor fusion allows us to visualize the locus containing the lac repressor binding site repeat. Using this system we have been able to monitor chromosome movement in interphase and chromosome segregation as cells proceed through mitosis. Additionally, we have been able to monitor the dynamics of chromosome movement in relation to the mitotic spindle using green fluorescent protein fusions to alpha tubulin.

Using our chromosome staining method we were able to demonstrate the following observations. Mutants that are defective in the spindle assembly checkpoint are able to separate their sister chromatids in the absence of any microtubule spindle. Wild type yeast cells separate their sister chromatids prior to the destruction of the mitotic cyclins and protein-protein interactions are sufficient to mediate the linkage of sister chromatids. Time lapse observation of mitosis revealed that spindle elongation and chromosome separation exhibit biphasic kinetics and that centromere separation precedes telomere separation. Furthermore, budding yeast lack a

conventional metaphase plate but do show anaphaseA chromosome to pole movement. We have examined the effect of deletions of the kinesin motors Cin8, Kip1 and Kip3 on spindle elongation and chromosome separation. We have observed very specific roles for each kinesin motor during yeast mitosis. Cells that lack Cin8 are defective in the rapid phase of spindle elongation while cells that lack Kip1 are defective in the slower phase of elongation. Furthermore, Kip3 deleted cells show normal kinetics of anaphase but the timing of spindle disassembly is disrupted. Our observations demonstrate that kinesin molecules that have genetically redundant functions actually have specific roles during mitosis. We also show that the cell monitors both the timing and extent of spindle elongation to ensure proper chromosome segregation.

A Murray 2/10/98

Table of Contents

Introduction		1-24
Chapter One	GFP tagging of budding yeast chromosomes reveals that protein-protein interactions can mediate sister chromatid cohesion.	25-63
Chapter Two	Mitosis in living budding yeast: anaphase A but no metaphase plate.	64-89
Chapter Three	Time lapse microscopy reveals unique roles for kinesins during anaphase in budding yeast.	90-137
Appendix A	Identification of Cyclosome/APC substrates by regular expression pattern matching of protein families.	138-163
Appendix B	The spindle assembly checkpoint in budding yeast.	164-194

List of Figures and Tables

Chapter 1	Description	Page
Table I	Table of yeast strains	56
Figure 1	Construction of the LacO/LacI system	57
Figure 2	Chromosome staining of cells after α -factor release	58
Figure 3	Timing of sister chromatid separation, Clb2 protein expression and DNA replication	59
Figure 4	Premature sister chromatid separation in checkpoint mutants	60
Figure 5AB	Quantitation of premature sister chromatid separation and cell death in checkpoint mutants	61
Figure 5C	Distance of sister chromatid separation in <i>mad2-1</i>	62
Figure 6	Lac repressor tetramerization can mediate sister chromatid separation	63

List of Figures and Tables (cont.)

Chapter 2	Description	Page
Figure 1A	Visualization of spindle and chromosome staining in living yeast	80
Figure 1B	Stages of mitosis in yeast	81
Figure 2	Centromeres oscillate along the spindle prior to anaphase	82
Figure 3A	Time lapse depiction of sister chromatid separation and spindle elongation	83
Figure 3B	Anaphase has two kinetic phases in yeast	84
Figure 3C	Yeast exhibit anaphase A chromosome to pole movement ⁸⁵	85
Figure 4A	Sister chromatids separate in the absence of a mitotic spindle	86
Figure 4B	Quantitation of sister chromatid separation in <i>mad1</i> treated with nocodazole	87
Figure 5A	Centromeres separate prior to telomeres	88
Figure 5B	Measurement of centromere and telomere separation during anaphase	89

List of Figures and Tables (cont.)

Chapter 3	Description	Page
Table I	Yeast strains	124
Table II	Summary of spindle dynamics in wild type and kinesin mutants	125
Figure 1A	Spindle pole separation in <i>cin8Δ</i>	126
Figure 1B	Centromere separation in <i>cin8Δ</i>	127
Figure 2	Average duration of anaphase in wild type and kinesin mutants	128
Figure 3A	Spindle pole separation in <i>kip1Δ</i>	129
Figure 3B	Centromere separation in <i>kip1Δ</i>	130
Figure 4	Average length of metaphase spindle in wild type and kinesin mutants	131
Figure 5A	Spindle pole separation in <i>kip3Δ</i>	132
Figure 5B	Centromere separation in <i>kip3Δ</i>	133
Figure 5C	Spindle length in <i>kip3Δ</i>	134
Figure 5D	Excessive elongation of <i>kip3Δ</i> spindle	135
Figure 6	Average spindle breakdown length in wild type and kinesin mutants	136
Figure 7	<i>cin8Δ</i> delays anaphase	137

List of Figures and Tables (cont.)

Appendix A	Description	Page
Figure 1	Alignment of destruction boxes and construction of scoring matrix	157
Figure 2	List of eukaryotic destruction boxes	158-159
Figure 3	PERL program to identify destruction boxes	160-162
Figure 4	Results from destruction box searches	163
Appendix B	Description	Page
Figure 1	Plate assay for benomyl sensitivity	185
Figure 2	Rapid death assay	186
Figure 3	Measurement of cyclin levels and cyclin associated kinase activity	187
Figure 4	Mad1 hyperphosphorylation assay	188
Figure 5	FACS analysis	189
Figure 6	Rebudding assay	190
Figure 7	Microcolony assay	191
Figure 8	Pedigree analysis	192
Figure 9	Sister chromatid separation assay using GFP tagging of chromosomes	193
Table I	Reagent Table	194

Introduction

Introduction

The study of mitotic chromosome behavior was born in the late 19th century with the work of Walther Flemming, Eduard Strasburger, Edouard van Beneden and Wilhelm Roux. Flemming's careful observations of chromosomes showed that the chromosomes split longitudinally and are distributed equally between the two daughter cells during what he called mitosis. The characterization of the stages of mitosis led Flemming, Strasburger and van Benden to name those stages: prophase, metaphase and anaphase. Accompanied by Roux's theory of the role of chromosomes in heredity, it became clear that the accurate distribution of chromosomes to daughter cells during mitosis was essential to the survival of the cell and the organism (Darlington 1932). In the intervening century we have learned a great deal concerning the cytological structures required for chromosome distribution in mitosis: the mitotic spindle, the centrosomes and the kinetochores. Although many of the molecules that comprise the important structural components of the mitotic apparatus have now been identified and characterized, a molecular explanation for chromosome distribution during mitosis is far from realization.

This thesis is not concerned with identifying more molecules that play roles during mitosis. Instead, the experiments described can be divided into three parts. First, we developed modern tools that allowed visualization of chromosomes and spindles in living cells of the budding yeast, *Saccharomyces cerevisiae*. Second, using these modern reagents, we reinvestigated some of the cytological observations in yeast in order to better understand chromosome and spindle dynamics during yeast mitosis. Finally,

we use the information gained from our observations of yeast mitosis to understand the roles of kinesin motor proteins during mitosis.

The study of mitosis in yeast and in higher eukaryotes.

Characterization of mitosis in vertebrate, insect and plant cells has defined the important events that regulate proper chromosome segregation (reviewed in Wadsworth 1993; Nicklas 1997). Complementary genetic studies in yeast have discovered a large number of proteins that affect mitosis (reviewed in Hoyt & Geiser 1996). These two approaches, however, have serious limitations. The inability to genetically manipulate higher eukaryotic cells makes dissecting the roles of individual proteins and protein complexes difficult. The lack of cytology in yeast severely limits the analysis of proteins discovered through genetics. Rather than develop genetic approaches in higher eukaryotic cells, we have developed new cytological techniques in yeast in order to capitalize on the advantages provided by yeast genetics and existing yeast mutants affecting mitosis. Here we describe the stages of mitosis and the contributions to their understanding from yeast studies and cell biological approaches in higher organisms. In order to provide a contextual framework for our studies, we also describe problems in studying mitosis and some of the outstanding questions that require attention.

Chromosome condensation and spindle assembly.

The first events of mitosis are the condensation of the chromosomes and the assembly of the bipolar spindle around the condensed chromatin.

Virtually all of our understanding of chromosome condensation comes from studies in higher eukaryotes. Early cytological observations of condensing chromosomes pointed out that the nucleus increased in its 'granularity' until chromosome fibers became apparent. Furthermore, it was suggested that these granules were assembling 'coiled threads' prior to the appearance of the chromatids (Belar 1929). More recent analysis of chromosome condensation has shown that complex three dimensional organization of the DNA strand is required for proper condensation (Marsden & Laemmli 1979; Mirkovitch et al 1984). The histones that make up the nucleosome core are required for the proper condensation of the chromosome (Billett & Barry 1974; Gurley et al 1974). Many non-histone proteins participate in the assembly of the chromatin into looped domains around a scaffold structure resulting in the compacted metaphase chromosome (Earnshaw & Laemmli 1983). Recently, a new family of ATPases that directly regulate and mediate chromosome condensation has been identified biochemically in *Xenopus* egg extracts and genetically in budding yeast (Hirano et al 1997; Hirano & Mitchison 1994; Strunnikov et al 1995). These proteins, known as the SMC family, are able to bind to DNA and introduce positive supercoils into circular DNA molecules (Kimura & Hirano 1997; Sutani & Yanagida 1997). It is still not clear how the cell signals condensation or how it recruits the SMC proteins to the DNA to initiate condensation. The observation that yeast exhibit chromosome condensation like higher eukaryotes opens the door for genetic analysis of the process (Guacci et al 1994). Combining new cytological approaches in *S. cerevisiae* with genetic approaches and biochemical approaches in higher eukaryotes should allow a comprehensive analysis of the process of chromosome condensation.

The assembly of the bipolar spindle is thought to be directed by multiple independent pathways (Waters & Salmon 1997). In the best understood model of spindle formation, microtubules nucleated from two centrosomes interact with chromosomes resulting in the capture and stabilization of the microtubules and the establishment of a bipolar spindle array (Kirschner & Mitchison 1986). Although centrosomes direct assembly of the spindle in some systems, bipolar spindle formation can also occur in the absence of centrosomes. Condensed chromatin can serve as a nucleating site for bipolar spindle assembly. In this system, a bipolar array of microtubules is formed around chromatin and cytoplasmic dynein crosslinks and sorts microtubules into spindle poles (Heald et al 1996; Heald et al 1997). It has been demonstrated in both vertebrates and in yeast that the establishment and maintenance of centrosome separation and bipolar microtubule arrays involves kinesin related proteins (Hoyt et al 1992; Rodionov et al 1993; Saunders & Hoyt 1992; Sawin et al 1992; Vernos et al 1995; Walczak et al 1996).

Chromosome congression to the metaphase plate

Concomitant with the assembly of the spindle, chromosomes establish bipolar attachment of their sister kinetochores to the spindle poles. Following attachment to the spindle, chromosomes congress to a position midway between the spindle poles to establish the metaphase plate. Chromosomes nearer one spindle pole than the other at the time of nuclear envelope breakdown establish a monopolar attachment to the spindle pole. Generally, these chromosomes do not initiate congression to the metaphase plate until the unattached kinetochore captures a microtubule from the opposite pole to

establish a bipolar attachment (Rieder & Salmon 1994). Earlier models for chromosome congression assumed that the positioning of the chromosome on the metaphase plate was the result of antagonistic forces acting on sister kinetochores pulling them toward opposite poles (Nicklas 1971; Östergren 1951). It is now understood that even when only one kinetochore is attached to a pole the chromosome pair can exhibit motion both away from and toward its attached pole (Skibbens et al 1993).

The oscillatory motions of kinetochores may be explained by a number of different forces acting at the kinetochore and along the chromosome arms. One possibility is that plus and minus-end microtubule motors acting at the kinetochore are responsible for moving the kinetochores toward and away from the pole (Hyman & Mitchison 1991). Another alternative is that the kinetochore is able to couple the force provided by the polymerization and depolymerization of kinetochore microtubules to produce kinetochore movement on the spindle (Desai & Mitchison 1995). In addition to forces applied directly at the kinetochore, the array of spindle microtubules also exert a pushing force on the chromosome arms, forcing the chromosome away from the spindle pole. It is now thought that a balance between these forces is responsible for the proper positioning of chromosomes on the metaphase plate (Hyman & Karsenti 1996; Inoue & Salmon 1995; Rieder & Salmon 1994).

The metaphase to anaphase transition

Following proper alignment of all the chromosomes in metaphase, the chromosomes are separated and move to the poles and the spindle poles separate from one another in anaphase. It is now understood that the

transitions between the different cell cycle stages are driven by the activity of the cyclin dependent kinases (CDK's). Activation of CDK's by the synthesis of A and B-type cyclins, drives cells into mitosis and initiates spindle assembly and chromosome condensation (Morgan 1997). The initiation of anaphase is then triggered by the proteolytic destruction of the cyclin subunits of the CDK's and the destruction of proteins responsible for holding sister chromatids together (for a detailed discussion see Appendix A) (King et al 1996). The release of the bond between the sister chromatids and the removal of CDK activity results in spindle elongation and chromosomes separation. During anaphase there are three events that are important for chromosome segregation. First, the link between the sister chromatids must be removed so that the spindle can segregate the chromatids into the daughter cells. Second, the chromatids must move to the spindle poles utilizing the kinetochore microtubules. Third, the non-kinetochore microtubules must elongate and slide along one another to separate the spindle poles.

The role of sister chromatid separation in mitosis has recently received a great deal of attention. It was known that the separation of sister chromatids required the ubiquitin mediated proteolysis of protein (s) other than the mitotic cyclins (Holloway et al 1993; Irniger et al 1995). The most likely candidates for these proteins were identified in fission and in budding yeast. The Cut2 protein and the Pds1 protein were both shown to be degraded by the ubiquitin degradation pathway and mutated versions of these proteins that could not be destroyed blocked the separation of sister chromatids in both yeasts (Cohen-Fix et al 1996; Funabiki et al 1996a; Funabiki et al 1996b). Although the Pds1 and Cut2 proteins need to be degraded to separate the sister chromatids they do not appear to be responsible for holding the sister chromatids together. The identification of another protein in budding yeast,

Mcd1/Scc1, that binds to the chromatin and dissociates at the time of sister chromatid separation is likely to be responsible for the link between chromatids. Mutations in the Mcd1/Scc1 protein cause premature separation of sister chromatids (Guacci et al 1997; Michaelis et al 1997). How is the destruction of Pds1 linked to the dissociation of Mcd1/Scc1 from the chromosomes? A third protein, Esp1 in budding yeast and Cut1 in fission yeast, seems to be responsible for initiating sister chromatid separation. Mutants in the Esp1/Cut1 protein are defective in sister chromatid separation. Furthermore, the Pds1/Cut2 protein binds tightly to the Esp1/Cut1 protein effectively sequestering it from other interactions. The proteolysis of the Pds1/Cut2 protein during mitosis releases the Esp1/Cut1 protein which can then carry out its function in anaphase initiation (Ciosk et al manuscript submitted; Funabiki et al 1996b). An intriguing question is whether the separation of sister chromatids is responsible for triggering anaphase by releasing the link between the two centrosomes thereby allowing spindle elongation. In metaphase, if one kinetochore of a chromosome is destroyed or the link between the sister kinetochores is severed, the kinetochores move toward the poles suggesting that the removal of the link between the chromatids is sufficient for anaphase A chromosome movement (McNeill and Berns 1981, Skibbens et al 1995). One important argument against this hypothesis comes from the study of mitosis in grasshopper spermatocytes. In spindles where metaphase was established but all the chromosomes were removed by micromanipulation, the spindle length and the timing of spindle pole separation were the same as cells that contained chromosomes (Zhang & Nicklas 1996).

Two distinct steps of chromosome and spindle movement occur during anaphase; anaphase A, the movement of the chromosomes to the

poles and anaphase B, the separation of the spindle poles and elongation of the spindle. Studies of a symbiotic protist (*Barbulanympha ufalula*) that inhabits the hindgut of the wood-eating cockroach (*Cryptocereus punctulatus*) provided the most elegant demonstration of the two discrete phases of anaphase. *Barbulanympha* mitosis exhibits a complete temporal separation of chromosome to pole movement from spindle elongation, clearly showing that the two steps are discrete (Inoue & Ritter 1978).

The exact mechanism for anaphase A chromosome to pole movement is still under discussion. The first models to explain the movement of chromosomes toward the spindle poles invoked a "traction fiber" model (Östergren 1951). This model and its variations argue that chromosomes attached to microtubules by their kinetochores are pulled toward the spindle pole by the movement of the kinetochore microtubules toward the pole. Although this model was widely accepted after its introduction, experiments in somatic cells suggested an alternative mechanism. Kinetochore microtubules that were labeled at their plus ends lost the label after the initiation of anaphase, suggesting that depolymerization of the microtubules was occurring at the kinetochore (Mitchison et al 1986). Photobleaching of kinetochore microtubules showed that they remained quite stable during anaphase and were not transported toward the pole. Furthermore, chromosomes moved toward and through the photobleached regions of the spindle suggesting that microtubules depolymerized primarily at the kinetochore and not at the spindle pole (Gorbsky et al 1987; Gorbsky et al 1988). Microdissection experiments demonstrated that the spindle could actually be severed and the pole removed thereby eliminating a large part of the traction fiber but chromosomes would still move poleward (Nicklas 1989). Finally, kinetochore microtubules that were labeled and photobleached or

labeled by photoactivation were used to demonstrate that the majority of chromosome to pole movement is the result of the depolymerization of the microtubules at the kinetochore (Mitchison & Salmon 1992; Zhang & Nicklas 1996).

The discovery of poleward flux of microtubules provides another possible explanation for the anaphaseA movement of chromosomes. Photolabeling of kinetochore microtubules in metaphase demonstrated that the kinetochore microtubules polymerize at the kinetochores and depolymerize at the spindle poles resulting in net microtubule flux toward the spindle pole (Mitchison 1989). The preferential stabilization of kinetochore microtubules at their plus ends with the drug taxol resulted in the stretching of the centromeric DNA as a result of minus end microtubule depolymerization; demonstrating that microtubule flux can produce poleward force (Waters et al 1996). Recent experiments argue that unlike the situation in some somatic cell types, microtubule flux can be the primary mechanism for the movement of the chromosomes to the poles. In *Xenopus* egg extracts, the rate of chromosome to pole movement could be explained by the rate of microtubule flux and inhibition of microtubule flux blocked chromosome to pole movement. Furthermore, taxol treated extracts that have stabilized microtubule plus ends still show microtubule flux and still show chromosome to pole movement (Desai et al manuscript submitted).

How does the kinetochore link the depolymerization of the kinetochore microtubules to the movement of chromosomes to the poles? The two models of chromosome to pole movement mentioned above can be explained in terms of the actions of microtubule motor proteins at the kinetochore. In the first model, the motor activity of microtubule motor proteins would be responsible for towing the chromosome along the

kinetochore spindle fibers toward the pole. The plus ends of the microtubules would depolymerize as the motor protein moved along the microtubule, catalyzed by either the motor protein or other proteins at the kinetochore (Inoue & Salmon 1995; Rieder & Salmon 1994). Alternatively, it has been demonstrated that microtubule motors can couple the plus-end depolymerization of microtubules to the movement of chromosomes toward the minus end of the microtubule (Desai & Mitchison 1995; Lombillo et al 1995a; Lombillo et al 1995b). In the flux model, the motor proteins at the kinetochore would mediate the attachment of the kinetochore to the microtubules. The flux of the microtubule toward the pole could then carry the chromosomes poleward (Desai et al manuscript submitted; Mitchison & Salmon 1992; Sawin et al 1992; Waters et al 1996).

The final separation of the chromosomes into the daughter cells at mitosis is achieved by a combination of anaphase A and anaphase B. McIntosh postulated in 1969 that the movement of the chromosomes to the poles and the separation of the poles could be explained by forces produced by the antiparallel sliding of microtubules (McIntosh et al 1969). Although this hypothesis is probably not correct for the movement of chromosomes to the poles it is almost certainly involved in pole separation. Analysis of diatom spindles demonstrated that the metaphase spindle consisted of antiparallel overlapping microtubules but that the overlap zone decreased as the spindle fibers elongated in anaphase (Inoue 1981; McDonald et al 1977; McDonald et al 1979). Experiments from a number of laboratories have implicated the kinesin family of microtubule motor proteins in the antiparallel sliding of microtubules in anaphase. Disruption of motor proteins blocks nuclear division and spindle elongation in *Aspergillus* (Enos & Morris 1990), fission yeast (Hagan & Yanagida 1990; Hagan & Yanagida 1992), *Drosophila* (Heck et

al 1993), *Xenopus* (Boleti et al 1996; Sawin et al 1992), and budding yeast (Hoyt et al 1992; Saunders & Hoyt 1992). Furthermore, separation of diatom spindles can be blocked with either ATP analogs that affect kinesins or with kinesin specific anti-peptide antibodies (Hogan et al 1992; Hogan et al 1993).

What is the role of kinesin motors in spindle elongation? Experiments in budding yeast demonstrated that the maintenance of the preanaphase bipolar spindle required an outward directed force on the spindle poles caused by the plus-end directed kinesin motors Cin8p and Kip1p. The balance of this outward directed force against an inward directed force caused by the Kar3p motor protein resulted in the proper length of the preanaphase spindle (Saunders & Hoyt 1992). Once cells entered anaphase, the actions of Cin8 and Kip1, in combination with the actions of dynein, resulted in the proper elongation of the mitotic spindle (Saunders et al 1995). The authors put forth the model that Cin8 and Kip1 form crossbridges between the antiparallel microtubules and slide them apart. Purification of the KLP61F kinesin from *Drosophila* and analysis by electron microscopy demonstrated that this kinesin was a bipolar rod with two kinesin motor domains at each end. The bipolar kinesin was able to form bridges between microtubules thus giving biochemical credence to the previous models for kinesin in the microtubule overlap zone (Kashina et al 1996a; Kashina et al 1996b; Saunders et al 1995). The fact that dynein was also required for the separation of the spindle poles in anaphase suggests that kinesin driven pushing forces may not be the only mechanism for spindle elongation. The observation in newt lung cells that anaphase B continues even when there is no microtubule overlap argues strongly that pulling forces directed through the astral microtubules may also be responsible for separating the centrosomes (Rieder & Salmon 1994; Waters et al 1993).

The first chapter of this thesis describes techniques we use to bridge some of the gap between the beautiful cytology available in higher eukaryotes and the powerful genetics afforded by yeast. We establish techniques for visualizing individual yeast chromosomes in living cells and use these techniques to investigate the checkpoint that controls the progression of cells from metaphase into anaphase. We show that mutants in the checkpoint for the metaphase to anaphase transition prematurely separate their sister chromatids when challenged with spindle depolymerization. We also show that the link between sister chromatids can be mediated by interactions between proteins and that in wild type cells the link between chromatids is destroyed prior to the destruction of the cyclin molecules that control mitosis.

In the second chapter we use the chromosome staining technique coupled with a new method for fluorescently labeling the mitotic spindle in living cells to analyze mitosis in budding yeast. Through time lapse observation of dividing yeast cells we are able to compare yeast mitosis with the mitosis of higher cells. We demonstrate that yeast show oscillations of chromosomes prior to sister separation but that unlike higher eukaryotes these oscillations do not result in the alignment of the chromosomes on the metaphase plate. We also demonstrate that once anaphase initiates, yeast exhibit a clear anaphase A movement of the chromosomes to the poles followed by anaphase B separation of the spindle poles and that anaphase B has two kinetic phases. Finally we show that the separation of yeast centromeres precedes the separation of yeast telomeres and that chromosome separation does not require spindle forces.

The final chapter of this thesis utilizes the genetics of yeast in order to clarify the roles of microtubule motors during anaphase. By deleting

individual kinesin motors we demonstrate that different kinesins control different phases and parameters of mitosis. The Cin8 motor protein regulates the fast phase of anaphase B and the Kip1 motor regulates the slow phase of anaphase B. The Kip3 motor regulates the dynamics of microtubules during anaphase and assists spindle breakdown at the end of anaphase. From our analysis of motor proteins it appears that the cell monitors the final length of the spindle as well as the total time that the cell spends in anaphase in order to ensure that mitosis is properly executed.

References

Belar, K. 1929. Beitrage zur Kausalanalyse der Mitose III. Untersuchungen an den Staubfaden, Haarzellen und Blattmeristemzellen von *Tradescantia virginica*. *Zeits. Zellforsch. u. mikr. Anat.* 10:73-134

Billett, M. A., Barry, J. M. 1974. Role of histones in chromatin condensation. *Eur J Biochem* 49:477-84

Boleti, H., Karsenti, E., Vernos, I. 1996. Xklp2, a novel *Xenopus* centrosomal kinesin-like protein required for centrosome separation during mitosis. *Cell* 84:49-59

Ciosk, R., Michaelis, C., Zachariae, W., Shevchenko, A., Mann, M., Nasmyth, K. manuscript submitted. An Esp1/Pds1 complex regulates loss of sister chromatid cohesion at the metaphase to anaphase transition in yeast.

Cohen-Fix, O., Peters, J. M., Kirschner, M. W., Koshland, D. 1996. Anaphase initiation in *Saccharomyces cerevisiae* is controlled by the APC-dependent degradation of the anaphase inhibitor Pds1p. *Genes Dev* 10:3081-93

Darlington, C. D. 1932. *Recent advances in cytology* London: J. & A. Churchill. 559 pg.

Desai, A., Maddox, P. S., Mitchison, T. J., Salmon, E. D. manuscript submitted. Anaphase A chromosome movement and poleward spindle microtubule flux occur at similar rates in *Xenopus* extract spindles.

Desai, A., Mitchison, T. J. 1995. A new role for motor proteins as couplers to depolymerizing microtubules. *J Cell Biol* 128:1-4

Earnshaw, W. C., Laemmli, U. K. 1983. Architecture of metaphase chromosomes and chromosome scaffolds. *J Cell Biol* 96:84-93

Enos, A. P., Morris, N. R. 1990. Mutation of a gene that encodes a kinesin-like protein blocks nuclear division in *A. nidulans*. *Cell* 60:1019-27

Funabiki, H., Kumada, K., Yanagida, M. 1996a. Fission yeast Cut1 and Cut2 are essential for sister chromatid separation, concentrate along the metaphase spindle and form large complexes. *Embo J* 15:6617-28

Funabiki, H., Yamano, H., Kumada, K., Nagao, K., Hunt, T., Yanagida, M. 1996b. Cut2 proteolysis required for sister-chromatid separation in fission yeast. *Nature* 381:438-41

Gorbsky, G. J., Sammak, P. J., Borisy, G. G. 1987. Chromosomes move poleward in anaphase along stationary microtubules that coordinately disassemble from their kinetochore ends. *J Cell Biol* 104:9-18

Gorbsky, G. J., Sammak, P. J., Borisy, G. G. 1988. Microtubule dynamics and chromosome motion visualized in living anaphase cells. *J Cell Biol* 106:1185-92

Guacci, V., Hogan, E., Koshland, D. 1994. Chromosome condensation and sister chromatid pairing in budding yeast. *J Cell Biol* 125:517-30

Guacci, V., Koshland, D., Strunnikov, A. 1997. A direct link between sister chromatid cohesion and chromosome condensation revealed through the analysis of MCD1 in *S. cerevisiae*. *Cell* 91:47-57

Gurley, L. R., Walters, R. A., Tobey, R. A. 1974. Cell cycle-specific changes in histone phosphorylation associated with cell proliferation and chromosome condensation. *J Cell Biol* 60:356-64

Hagan, I., Yanagida, M. 1990. Novel potential mitotic motor protein encoded by the fission yeast *cut7+* gene. *Nature* 347:563-6

Hagan, I., Yanagida, M. 1992. Kinesin-related *cut7* protein associates with mitotic and meiotic spindles in fission yeast. *Nature* 356:74-6

Heald, R., Tournebize, R., Blank, T., Sandaltzopoulos, R., Becker, P., et al. 1996. Self-organization of microtubules into bipolar spindles around artificial chromosomes in *Xenopus* egg extracts. *Nature* 382:420-5

- Heald, R., Tournebize, R., Habermann, A., Karsenti, E., Hyman, A. 1997. Spindle assembly in *Xenopus* egg extracts: respective roles of centrosomes and microtubule self-organization. *J Cell Biol* 138:615-28
- Heck, M. M., Pereira, A., Pesavento, P., Yannoni, Y., Spradling, A. C., Goldstein, L. S. 1993. The kinesin-like protein KLP61F is essential for mitosis in *Drosophila*. *J Cell Biol* 123:665-79
- Hirano, T., Kobayashi, R., Hirano, M. 1997. Condensins, chromosome condensation protein complexes containing XCAP-C, XCAP-E and a *Xenopus* homolog of the *Drosophila* Barren protein. *Cell* 89:511-21
- Hirano, T., Mitchison, T. J. 1994. A heterodimeric coiled-coil protein required for mitotic chromosome condensation in vitro. *Cell* 79:449-58
- Hogan, C. J., Stephens, L., Shimizu, T., Cande, W. Z. 1992. Physiological evidence for involvement of a kinesin-related protein during anaphase spindle elongation in diatom central spindles. *J Cell Biol* 119:1277-86
- Hogan, C. J., Wein, H., Wordeman, L., Scholey, J. M., Sawin, K. E., Cande, W. Z. 1993. Inhibition of anaphase spindle elongation in vitro by a peptide antibody that recognizes kinesin motor domain. *Proc Natl Acad Sci U S A* 90:6611-5
- Holloway, S. L., Glotzer, M., King, R. W., Murray, A. W. 1993. Anaphase is initiated by proteolysis rather than by the inactivation of maturation-promoting factor. *Cell* 73:1393-402

Hoyt, M. A., Geiser, J. R. 1996. Genetic analysis of the mitotic spindle. *Ann Rev Genet* 30:7-33

Hoyt, M. A., He, L., Loo, K. K., Saunders, W. S. 1992. Two *Saccharomyces cerevisiae* kinesin-related gene products required for mitotic spindle assembly. *J Cell Biol* 118:109-20

Hyman, A. A., Karsenti, E. 1996. Morphogenetic properties of microtubules and mitotic spindle assembly. *Cell* 84:401-10

Hyman, A. A., Mitchison, T. J. 1991. Two different microtubule-based motor activities with opposite polarities in kinetochores. *Nature* 351:206-11

Inoue, S. 1981. Cell division and the mitotic spindle. *J Cell Biol* 91:131s-147s

Inoue, S., Ritter, H., Jr. 1978. Mitosis in *Barbulanympha*. II. Dynamics of a two-stage anaphase, nuclear morphogenesis, and cytokinesis. *J Cell Biol* 77:655-84

Inoue, S., Salmon, E. D. 1995. Force generation by microtubule assembly/disassembly in mitosis and related movements. *Mol Biol Cell* 6:1619-40

Irniger, S., Piatti, S., Michaelis, C., Nasmyth, K. 1995. Genes involved in sister chromatid separation are needed for B-type cyclin proteolysis in budding yeast. *Cell* 81:269-78

Kashina, A. S., Baskin, R. J., Cole, D. G., Wedaman, K. P., Saxton, W. M., Scholey, J. M. 1996a. A bipolar kinesin. *Nature* 379:270-2

Kashina, A. S., Scholey, J. M., Leszyk, J. D., Saxton, W. M. 1996b. An essential bipolar mitotic motor. *Nature* 384:225

Kimura, K., Hirano, T. 1997. ATP-dependent positive supercoiling of DNA by 13S condensin: a biochemical implication for chromosome condensation. *Cell* 90:625-34

King, R. W., Deshaies, R. J., Peters, J. M., Kirschner, M. W. 1996. How proteolysis drives the cell cycle. *Science* 274:1652-9

Kirschner, M., Mitchison, T. 1986. Beyond self-assembly: from microtubules to morphogenesis. *Cell* 45:329-42

Lombillo, V. A., Nislow, C., Yen, T. J., Gelfand, V. I., McIntosh, J. R. 1995a. Antibodies to the kinesin motor domain and CENP-E inhibit microtubule depolymerization-dependent motion of chromosomes in vitro. *J Cell Biol* 128:107-15

Lombillo, V. A., Stewart, R. J., McIntosh, J. R. 1995b. Minus-end-directed motion of kinesin-coated microspheres driven by microtubule depolymerization. *Nature* 373:161-4

Marsden, M. P., Laemmli, U. K. 1979. Metaphase chromosome structure: evidence for a radial loop model. *Cell* 17:849-58

- McDonald, K., Pickett-Heaps, J. D., McIntosh, J. R., Tippit, D. H. 1977. On the mechanism of anaphase spindle elongation in *Diatoma vulgare*. *J Cell Biol* 74:377-88
- McDonald, K. L., Edwards, M. K., McIntosh, J. R. 1979. Cross-sectional structure of the central mitotic spindle of *Diatoma vulgare*. Evidence for specific interactions between antiparallel microtubules. *J Cell Biol* 83:443-61
- McIntosh, J. R., Hepler, P. K., Van Wie, D. G. 1969. Model for mitosis. *Nature* 224:659-663
- McNeill, P.A., Berns, M.W., 1981. Chromosome behavior after laser microirradiation of a single kinetochore in mitotic PtK2 cells. *J. Cell Biol* 88:543-53
- Michaelis, C., Ciosk, R., Nasmyth, K. 1997. Cohesins: chromosomal proteins that prevent premature separation of sister chromatids. *Cell* 91:35-45
- Mirkovitch, J., Mirault, M. E., Laemmli, U. K. 1984. Organization of the higher-order chromatin loop: specific DNA attachment sites on nuclear scaffold. *Cell* 39:223-32
- Mitchison, T., Evans, L., Schulze, E., Kirschner, M. 1986. Sites of microtubule assembly and disassembly in the mitotic spindle. *Cell* 45:515-27

- Mitchison, T. J. 1989. Polewards microtubule flux in the mitotic spindle: evidence from photoactivation of fluorescence. *J Cell Biol* 109:637-52
- Mitchison, T. J., Salmon, E. D. 1992. Poleward kinetochore fiber movement occurs during both metaphase and anaphase-A in newt lung cell mitosis. *J Cell Biol* 119:569-82
- Morgan, D. O. 1997. Cyclin-dependent kinases: engines, clocks and microprocessors. *Ann. Rev. Cell Dev. Biol.* 13:261-91
- Nicklas, R. B. 1971. Mitosis. *Adv Cell Biol* 2:225-97
- Nicklas, R. B. 1989. The motor for poleward chromosome movement in anaphase is in or near the kinetochore. *J Cell Biol* 109:2245-55
- Nicklas, R. B. 1997. How cells get the right chromosomes. *Science* 275:632-7
- Östergren, G. 1951. The mechanism of co-orientation in bivalents and multivalents. The theory of orientation by pulling. *Hereditas* 31:498
- Rieder, C. L., Salmon, E. D. 1994. Motile kinetochores and polar ejection forces dictate chromosome position on the vertebrate mitotic spindle. *J Cell Biol* 124:223-33
- Rodionov, V. I., Gelfand, V. I., Borisy, G. G. 1993. Kinesin-like molecules involved in spindle formation. *J Cell Sci* 106:1179-88

- Saunders, W. S., Hoyt, M. A. 1992. Kinesin-related proteins required for structural integrity of the mitotic spindle. *Cell* 70:451-8
- Saunders, W. S., Koshland, D., Eshel, D., Gibbons, I. R., Hoyt, M. A. 1995. *Saccharomyces cerevisiae* kinesin- and dynein-related proteins required for anaphase chromosome segregation. *J Cell Biol* 128:617-24
- Sawin, K. E., LeGuellec, K., Philippe, M., Mitchison, T. J. 1992. Mitotic spindle organization by a plus-end-directed microtubule motor. *Nature* 359:540-3
- Skibbens, R. V., Rieder, C. L., Salmon, E. D. 1995. Kinetochore motility after severing between sister centromeres using laser microsurgery: evidence that kinetochore directional instability and position is regulated by tension. *J Cell Sci* 108:2537-48
- Skibbens, R. V., Skeen, V. P., Salmon, E. D. 1993. Directional instability of kinetochore motility during chromosome congression and segregation in mitotic newt lung cells: a push-pull mechanism. *J Cell Biol* 122:859-75
- Strunnikov, A. V., Hogan, E., Koshland, D. 1995. SMC2, a *Saccharomyces cerevisiae* gene essential for chromosome segregation and condensation, defines a subgroup within the SMC family. *Genes Dev* 9:587-99
- Sutani, T., Yanagida, M. 1997. DNA renaturation activity of the SMC complex implicated in chromosome condensation. *Nature* 388:798-801

Vernos, I., Raats, J., Hirano, T., Heasman, J., Karsenti, E., Wylie, C. 1995. Xklp1, a chromosomal *Xenopus* kinesin-like protein essential for spindle organization and chromosome positioning. *Cell* 81:117-27

Wadsworth, P. 1993. Mitosis: spindle assembly and chromosome motion. *Curr Opin Cell Biol* 5:123-8

Walczak, C. E., Mitchison, T. J., Desai, A. 1996. XKCM1: a *Xenopus* kinesin-related protein that regulates microtubule dynamics during mitotic spindle assembly. *Cell* 84:37-47

Waters, J. C., Cole, R. W., Rieder, C. L. 1993. The force-producing mechanism for centrosome separation during spindle formation in vertebrates is intrinsic to each aster. *J Cell Biol* 122:361-72

Waters, J. C., Mitchison, T. J., Rieder, C. L., Salmon, E. D. 1996. The kinetochore microtubule minus-end disassembly associated with poleward flux produces a force that can do work. *Mol Biol Cell* 7:1547-58

Waters, J. C., Salmon, E. 1997. Pathways of spindle assembly. *Curr Opin Cell Biol* 9:37-43

Zhang, D., Nicklas, R. B. 1996. 'Anaphase' and cytokinesis in the absence of chromosomes. *Nature* 382:466-8

Chapter 1

**GFP tagging of budding yeast chromosomes
reveals that protein-protein interactions can
mediate sister chromatid cohesion**

GFP tagging of budding yeast chromosomes reveals that protein-protein interactions can mediate sister chromatid cohesion

Aaron F. Straight*, Andrew S. Belmont‡, Carmen C. Robinett‡, and Andrew W. Murray*

Addresses: *Department of Physiology Box0444
School of Medicine
University of California San Francisco
San Francisco, CA 94143-0444

‡Department of Cell and Structural Biology,
506 Morrill Hall, 505 S. Goodwin Ave.
University of Illinois, Urbana-Champaign
Urbana, IL 61801 USA.

Editorial Correspondence: A. Murray
E-mail: amurray@cgl.ucsf.edu
FAX: 415-476-4929
PHONE: 415-476-0364

Correspondent after publication: Aaron F. Straight
E-mail: straight@cgl.ucsf.edu
FAX: 415-476-4929
PHONE: 415-476-6970

Background: Precise control of sister chromatid separation is essential for the accurate transmission of genetic information. Sister chromatids must remain linked to each other from the time of DNA replication until the onset of chromosome segregation, when the linkage must be promptly dissolved. Recent studies suggest that the machinery that is responsible for the destruction of mitotic cyclins also degrades proteins that play a role in maintaining sister chromatid linkage, and that this machinery is regulated by the spindle assembly checkpoint. Studies on these problems in budding yeast are hampered by the inability to resolve its chromosomes by light or electron microscopy.

Results: We have developed a novel method for visualizing specific DNA sequences in fixed and living budding yeast cells. A tandem array of 256 copies of the Lac operator is integrated at the desired site in the genome and detected by binding of a green fluorescent protein (GFP)-Lac repressor fusion expressed from the *HIS3* promoter. Using this method we show that sister chromatid segregation precedes the destruction of cyclin B. In *mad* or *bub* cells, which lack the spindle assembly checkpoint, sister chromatid separation can occur in the absence of microtubules. Expressing a tetramerizing form of the GFP-Lac repressor which can bind Lac operators on two different DNA molecules can hold sister chromatids together under conditions in which they would normally separate.

Conclusions: We conclude that sister chromatid separation in budding yeast can occur in the absence of microtubule dependent forces and that protein complexes that can bind two different DNA molecules are capable of holding sister chromatids together.

Background

Controlling the linkage between sister chromatids is essential for accurate chromosome segregation. Sister chromatids must remain linked to each other from the time of DNA replication until the onset of chromosome segregation. At the transition between metaphase and anaphase, this linkage must be promptly dissolved to allow sisters to separate to opposite poles of the mitotic spindle. Several lines of evidence suggest that the principal trigger of chromosome segregation is sister separation, rather than any change in the structure of the spindle or the forces acting on the chromosomes [1, 2, 3].

Sister chromatid separation is controlled by the machinery that regulates the eukaryotic cell cycle. Mitosis is induced by the activation of MPF (maturation or mitosis promoting factor) a protein kinase composed of three subunits: Cdc2 (known as Cdc28 in budding yeast), cyclin B, and a small subunit named Suc1 in fission yeast (reviewed in [4]). Cells normally exit from mitosis by destroying cyclin B and thus inactivating MPF [5]. Cyclin destruction requires ubiquitination of the protein [6, 7], which depends on the activity of a multiprotein complex known as the cyclosome or anaphase promoting complex (APC) [8, 9, 10] and a short stretch of amino acids in the N-terminus of cyclin called the destruction box [6]. Although the destruction of cyclin B is not required for the onset of anaphase, experiments in frog egg extracts suggest that the cyclin proteolysis machinery induces anaphase by destroying other proteins that are required to maintain the linkage between sister chromatids [3]. Genetic analysis of chromosome segregation in yeast has identified proteins whose destruction regulates sister chromatid separation. In fission yeast, the proteolysis of Cut2, which contains a cyclin destruction

box, is required for sister separation [11]. In budding yeast, the Pds1 protein, which is weakly homologous to Cut2, has similar properties, and the absence of Pds1 allows sister chromatids to separate in cells arrested in mitosis by depolymerization of the mitotic spindle or inactivation of the cyclin proteolysis machinery [12]. We do not know whether Pds1 and Cut2 directly link sister chromatids by forming a proteinaceous linkage between them or link them indirectly by inhibiting activities that can dissolve the linkage between sisters. The observation that topoisomerase II activity is required at mitosis for sister chromatid segregation in both vertebrates [13, 14] and fungi [15, 16], suggests that there is a topological component to sister linkage, although this linkage appears to be absent from very small chromosomes [17].

Studies on chromosome behavior in budding yeast have been hampered by the inability to resolve individual chromosomes in intact cells by either light or electron microscopy. This problem has been partially solved by the development of in situ hybridization techniques [18], but these depend on fixation and proteolysis and are thus unsuitable for detailed studies on cell morphology or analysis of living cells. We have developed a method that reveals the localization of a defined DNA segment in living yeast by expressing a protein fusion between green fluorescent protein (GFP) [19] and the Lac repressor in cells containing 256 tandem repeats of the Lac operator integrated into the genome. We have visualized the binding of the GFP-Lac repressor fusion to the operator array in both living and fixed cells and used it to show that sister chromatid separation can occur in the absence of microtubule-dependent forces. In addition, by using versions of the GFP-Lac repressor fusion that can bind to two operators simultaneously we have shown that protein-protein interactions can maintain sister chromatid linkage.

Results

A novel assay for sister chromatid separation

We exploited the intrinsic fluorescence of green fluorescent protein and the highly specific binding of the Lac repressor to the Lac operator to visualize a specific segment of the budding yeast genome in living cells. To ensure an adequate signal, we used a 10 kb segment of DNA that contains 256 tandem repeats of the Lac operator [20], which can be cloned into yeast vectors and integrated into any site in the genome by homologous recombination. For the majority of experiments in this paper, the repeat was integrated at the *LEU2* locus, which is located 22 kb to the left of the centromere of chromosome III (Figure 1A) [21]. Despite the large number of tandemly repeated sequences the Lac operator array is not a frequent substrate for mitotic recombination events: the size of the array does not change detectably during the approximately 25 cell divisions required for a single cell to form a macroscopic colony (data not shown). In meiosis, a single Lac operator repeat segregates to two of the four spores and remains tightly linked to the selectable marker used to integrate it into chromosome III.

The Lac operator repeats were recognized by a hybrid protein that consists of GFP fused to the N-terminus of the Lac repressor (Figure 1B). Each Lac repressor dimer binds to a single operator sequence. Since wild-type Lac repressor tetramerizes, it can bind two operators allowing it to link two segments of DNA to each other [22]. To investigate the potential role of such linkage we constructed GFP-Lac repressor fusions that contained either wild-type repressor or a C terminal truncation that allows normal dimerization but

prevents tetramerization [23]. We found that the *HIS3* promoter, which normally drives the expression of b-isopropyl malate dehydrogenase, a gene involved in histidine biosynthesis, gave the optimal level of expression of the GFP-Lac repressor fusion for efficient detection of the Lac operator array. This promoter is expressed at very low levels when cells are grown in the presence of histidine, at low levels when cells are grown in histidine free medium, and at moderate levels in the presence of 3-aminotriazole, an inhibitor of histidine biosynthesis [24]. For all the experiments reported here, cells were placed in histidine-free medium containing 10 mM aminotriazole for 30 minutes to induce expression of the GFP-Lac repressor, and then returned to medium containing histidine before any other experimental manipulations.

We used the Lac operator tagged chromosome III to monitor sister chromatid separation as a population of cells proceeded synchronously through the cell cycle. An *a*-mating strain containing both the Lac operator array and the non-tetramerizing GFP-Lac repressor fusion was cultured until it was proliferating exponentially in histidine-containing medium. The culture was then treated with α -factor, which arrests cells in G1 of the cell cycle by activating the mating pheromone signaling pathway (reviewed in [25]). α -factor arrested cells were then incubated in media lacking histidine and containing 10 mM aminotriazole for 30 minutes to induce the GFP-Lac repressor fusion. After induction of the GFP-Lac repressor the cells were washed free of a factor and aminotriazole into medium containing histidine allowing them to escape from the G1 arrest and proceed synchronously through the cell cycle. To restrict our observations to a single cell cycle we arrested cells at G1 of the next cell cycle, by adding a factor back to the culture 60 minutes after the initial release from

a factor. Samples were fixed at 15 minute intervals and subjected to fluorescence microscopy to determine the localization of the GFP-Lac repressor fusion. We monitored progress through the cell cycle by analyzing overall cell morphology, DNA content, and the level of Clb2, one of the yeast B-type cyclins that rises as cells enter mitosis and falls as they leave mitosis.

During the early part of the cell cycle each cell contains a single green fluorescent dot, corresponding to the unreplicated marked copy of chromosome III. After 75 minutes cells containing two dots appear and by 90 minutes constitute the majority of the population (Figure 2A, 3A). To confirm that the two fluorescent dots in these cells are due to separated sister chromatids, we released cells from a factor arrest into conditions that would block the onset of anaphase. Releasing cells into hydroxyurea, which blocks DNA synthesis leads to a uniform population of large budded cells that contain a single fluorescent dot (Figure 2B), as expected from the ability of this drug to block the onset of anaphase by activating the cell cycle checkpoint that detects unreplicated DNA [26, 27].

By monitoring sister separation relative to Clb2 levels and DNA content we determined the timing of sister separation relative to DNA synthesis, cyclin proteolysis, and cytokinesis (Figure 3). As expected, sister separation does not occur until cells have completed DNA replication and accumulated mitotic cyclins, indicating that they have assembled a spindle. Sister separation is first detectable at 75 minutes after release from a factor (Figure 3A) but Clb2 levels do not begin to fall until at least 90 minutes after release from α -factor (Figure 3B), suggesting that sister separation precedes the bulk destruction of the mitotic cyclins. This finding is consistent with the existence of mutants, such as *cdc15*, that allow sister separation to occur but prevent the complete inactivation of MPF and destruction of mitotic cyclins

[28]. Cytokinesis and cell separation produce G1 cells with a 1C DNA content and this event occurs between 105 and 120 minutes (Figure 3C).

Checkpoint mutants and sister separation

The spindle assembly checkpoint prevents the onset of anaphase in cells that have defects in spindle assembly or chromosome alignment on the spindle [29, 30, 31, 32]. Mutations that inactivate this checkpoint allow cells whose spindles have been depolymerized by anti-microtubule drugs to proceed through mitosis into the next cell cycle. Previous experiments in yeast have monitored passage through mitosis by detecting the inactivation of MPF, the destruction of mitotic cyclins, or the round of budding and DNA replication that occurs after the exit from mitosis [29, 30, 33, 34].

We wished to examine the role of microtubule-dependent forces in sister chromatid separation by determining whether sister separation would occur in checkpoint mutants proceeding through mitosis in the absence of microtubules. We used the non-tetramerizing form of GFP-Lac repressor to follow sister separation in cultures of wild type cells and a variety of checkpoint-defective mutants. Cells were grown to mid log phase before inducing the GFP-Lac repressor by shifting the cells into histidine-free medium containing 10 mM 3-aminotriazole. After 30 minutes of induction, the cells were shifted back into medium with histidine containing 15 mg/ml of nocodazole, a level that reduces microtubules below detectable levels in the W303 strain background used for these experiments. Samples of each culture were fixed every three hours and examined for the pattern of GFP fluorescence. Cells with two dots were scored as having undergone sister chromatid separation.

Wild type cells incubated in nocodazole-containing medium proceed through the cell cycle until they arrest as large budded cells with a single green fluorescent dot (Figure 4A, 5A). This result is consistent with those obtained using in situ hybridization to determine whether sister separation occurs in cells that lack microtubules ([18] and A. Rudner and A.W.M.) unpublished results). One interpretation of these experiments is that the failure to observe sister separation is due to activation of the spindle assembly checkpoint, but it is difficult to eliminate the possibility that the only factor preventing sister separation is a requirement for microtubule-dependent forces that can physically pull the sisters apart. To test this possibility, we examined sister separation in two classes of checkpoint defective mutants: the *mad1-mad3* (mitotic arrest defective [30]) and *bub1-bub3* (budding uninhibited by benzimidazole [29]) mutants. In all six mutants, cells treated with nocodazole show an increase in the number of separated spots in comparison to wild type (Figure 4C,D, 5A) showing that sister chromatid separation can occur in the absence of the spindle. We also examined the behavior of the *tub1-801* mutant whose microtubules are more susceptible to depolymerization than those of wild type cells (K. Richards and D. Botstein, personal communication). Nocodazole treatment of this mutant did not induce sister separation, indicating that the separation seen in the checkpoint mutants is not simply a consequence of their sensitivity to anti-microtubule drugs (Figures 4B and 5A). Unlike cells proceeding through a normal anaphase, in which the separation between dots is closely correlated with extent of spindle elongation, the distance of separation between the dots in nocodazole treated checkpoint mutants reflects the lack of spindle forces. *mad2-1* cells that proceed through anaphase in the absence of nocodazole separate their sister chromatids up to 8 microns as a result of spindle

elongation (Figure 5C, filled bars). In the presence of nocodazole, *mad2-1* cells passively separate their sister chromatids showing separation distances of 1 micron or less (Figure 5C, open bars) with both chromatids remaining in the mother cell (data not shown). It is clear that although sister chromatid separation occurs in *mad* mutants in the presence of nocodazole, mitotic spindle elongation is the primary force behind proper distribution of the sister chromatids to the mother and daughter cells.

Previous analysis of *mad* and *bub* mutants has shown that their cell cycle continues despite the absence of a spindle, leading to the death of these mutants as they pass through mitosis [29, 30]. In our experiments the onset of sister separation correlates with the decline in viability, but it remains to be determined whether sister separation in the absence of a spindle is the event that prevents the generation of viable progeny. Our analysis of chromosome behavior in cells lacking the spindle assembly checkpoint makes two points: sister separation can occur in the absence of detectable microtubules and thus in the absence of microtubule-dependent forces, and this checkpoint prevents the initiation of sister separation in cells with spindle defects.

Lac repressor tetramerization can link sister chromatids

The observation that sister chromatids can separate in the absence of microtubules prompted us to investigate the minimum requirements to maintain the linkage between sisters. In vitro, tetrameric Lac repressor can bind two Lac operators simultaneously, thus linking two different DNA molecules or two distant segments of the same piece of DNA [22]. We therefore asked whether a tetramerizing GFP-Lac repressor fusion could hold a pair of sister chromatids together by linking their Lac operator repeats.

mad2-1 cells containing the Lac operator array on chromosome III were grown to mid log phase. Following GFP-Lac repressor induction, the cells were transferred to nocodazole-containing medium and examined for the pattern of GFP fluorescence at 3 hour intervals. Comparing Figures 6A and 5A shows that unlike *mad* mutants which express the non-tetramerizing form of the Lac repressor, those expressing the tetramerizing form contain only one fluorescent dot, despite the inactivation of the spindle assembly checkpoint.

To confirm that the sister chromatids are being held together by the Lac repressor binding to the operator array, we repeated this experiment in the presence of isopropyl- β -D thio galactopyranoside (IPTG). The binding of IPTG to the Lac repressor reduces its affinity for the Lac operator 1000-fold, without affecting its affinity for non-specific DNA [35]. Log phase cells were incubated in medium containing nocodazole and 20 mM IPTG. When the living cells were examined in the presence of IPTG, no discrete pattern of fluorescence was observed. To determine whether sister chromatids were linked, samples of the culture were removed at 3 hr intervals and the cells were transferred to IPTG-free medium for 30 minutes before fixation and observation. Figure 6A shows that *mad2-1* cells cultured in the presence of IPTG and nocodazole separate their sister chromatids. To eliminate the possibility that the tetramerizing GFP-Lac repressor was affecting the cell cycle, we examined the ability of *mad2-1* cells containing this molecule to pass through mitosis, as determined by their ability to rebud in the presence of nocodazole. Figure 6B shows that the tetrameric GFP-Lac repressor has no effect on the progression of the cell cycle in *mad* mutants in the presence or absence of IPTG. Two conclusions can be drawn from the effects of the tetramerizing GFP-Lac repressor on sister separation. First, the ability of the tetramerizing form of

the Lac repressor to link sister chromatids depends on its binding to the Lac operator array rather than non-specific DNA. Second, that activating the binding activity of the Lac repressor cannot restore the linkage of sister chromatids that have already separated from each other.

Discussion

We have developed a new method that uses the intrinsic fluorescence of a GFP-Lac repressor to localize a repeated array of the Lac operator incorporated into various DNA molecules within living or fixed budding yeast cells. This technique reveals that sister chromatid separation is under the control of the spindle assembly checkpoint and can occur in the absence of microtubule-dependent forces. The tetramerization of the Lac repressor can hold sister chromatids together by binding to repeated arrays of the Lac operator.

The Lac operator array has a number of advantages over in situ hybridization [18] for following chromosome behavior in yeast cells. Because the operator is detected by a GFP-Lac repressor fusion expressed within the cells, it can be observed in living cells and followed by time lapse video microscopy (our unpublished observations). The fluorescence of GFP survives fixation allowing the location of the Lac operator array to be determined relative to proteins visualized by immunofluorescence. Experiments in mammalian cells that use GFP-lac repressor and in situ hybridization to see the same Lac operator arrays show that chromosome morphology is degraded by the conditions required to denature double stranded DNA prior to hybridization [20]. One advantage of in situ hybridization is that by using differently labeled probes it is possible to determine the localization of up to three different DNA segments within the

same cell . Although we can create strains which have the Lac operator array integrated at two or more sites in the genome, and see multiple spots within cells (data not shown), we cannot determine which spot corresponds to which segment of DNA. Varying the length of the operator repeat may allow us to distinguish different loci within the cell based on differences in fluorescent intensity.

Analyzing the behavior of the Lac operator array reveals that it is an accurate marker for sister chromatid segregation. Experiments on synchronous populations of cells show that sister chromatid separation occurs within a brief window and that treatments that prevent the onset of anaphase block sister separation. There is no change in the appearance of the GFP dots during the cell cycle, suggesting that any cell cycle-dependent changes in local chromatin structure occur below the resolution of the light microscope. By constructing chromosomes that have two or more widely separated Lac repressor arrays, it should be possible to determine whether the changes in chromosome condensation seen by in situ hybridization [18] can also be detected in living cells.

We determined the timing of sister separation relative to cyclin proteolysis and cytokinesis (Figure 3). Sister separation appears to precede cyclin proteolysis by about 15 minutes and cytokinesis by about 30 minutes. The relative timing of sister separation and cyclin proteolysis thus seems to differ between yeast and multicellular eukaryotes, where the onset of cyclin proteolysis clearly precedes detectable sister separation [14, 36]. This difference may reflect the different relationship between the orientation of the spindle and the cleavage plane in these different organisms. In animals, the orientation of the spindle determines the orientation of cleavage [37]. In contrast, in budding yeast the cleavage plane is specified by the position of the

bud neck and is independent of the orientation of the spindle [38]. To ensure that both mother and daughter cells inherit DNA, cells must make sure that one pole of the anaphase spindle lies in the mother and one in the daughter before cytokinesis begins. One way of satisfying this requirement is to delay cytokinesis by delaying the proteolysis of mitotic cyclins and the inactivation of MPF until one pole of the spindle has entered the daughter cell [39].

Treating cells with microtubule inhibitors activates the spindle assembly checkpoint and prevents sister chromatid separation as monitored by in situ hybridization or the GFP-tagged Lac operator array. To eliminate the possibility that sister separation can only occur if the sisters are physically pulled apart, we demonstrated that inactivation of the spindle assembly checkpoint allows sisters to separate in the absence of microtubules. The separation of the GFP dots in these cells is variable and substantially smaller than the separation observed in cells not treated with nocodazole. This suggests that the separation occurs by diffusion, unlike the uniform sister separation seen in telophase of cells that contain a functional spindle.

The wild type Lac repressor can form a tetramer that can hold two DNA molecules together because each of the two dimers it contains can bind one Lac operator [22]. If a tetramerizing GFP-Lac repressor is expressed from the beginning of the cell cycle it can hold sister chromatids together in a *mad* mutant that lacks a spindle. Intriguingly, once sister separation has occurred, the tetramerizing Lac repressor is unable to restore the linkage of sister chromatids, suggesting that their mobility within the nucleus is restricted. In the presence of microtubules the binding of the tetramerizing GFP-Lac repressor to the Lac operator repeats fails to prevent chromosome separation (data not shown). This observation suggests that microtubule dependent forces can overcome the association between two DNA molecules mediated

by multiple copies of the Lac repressor. The linkage between sister chromatids is stable in cells, such as unfertilized vertebrate eggs or yeast mutants in the cyclin proteolysis machinery [9], that are arrested in metaphase for long periods. This observation suggests the natural linkage between sisters is considerably more robust than the artificial linkage due to tetramerization of the Lac repressor.

Conclusions

We have demonstrated that the interaction of a DNA-binding protein with its specific recognition sequence can be used to determine the location of a particular DNA molecule within a living cell. By making the DNA binding protein fluorescent, we have shown that the technique can be used to investigate the behavior of chromosomes throughout the cell cycle. This technology will allow a detailed comparison of the dynamic behavior of the chromosomes and spindle of budding yeast with those of animal and plant cells.

Materials and Methods

Strains and media

All yeast strains are isogenic derivatives of strain W303 (AFS34) and their genotypes are listed in Table I. For all experiments yeast were grown in YPD (10g/l yeast extract, 20g/l Bacto-Peptone, 20g/l Dextrose) supplemented with 50 μ g/l adenine-HCl and 50 μ g/l l-tryptophan. Complete synthetic medium lacking histidine (CSM-HIS) [40] was supplemented with 50 μ g/l

adenine-HCl, 50µg/l l-tryptophan and 6.5g/l NaCitrate. All experiments were performed at 23°C. Yeast transformations were performed using the lithium acetate method [41]. All plasmids were propagated in E. coli strain TG1 in medium containing 100µg/ml ampicillin.

Expression of GFP-Lac repressor fusions in yeast

To express GFP in yeast, wild type GFP was cloned into pDK20 (Doug Kellogg, unpublished), a plasmid that contains the bidirectional *GAL1-GAL10* promoter cloned into pRS306 [42], by PCR using oligos with overhanging XhoI (5'CGCCTCGAGGAGATGAGTAAAGGAGAAGAAGACTT3') and EcoRI (5'GCGGAATTCTTTGTATAGTTCATCCATGCC3') sites to yield pGAL-GFP. Oligonucleotides encoding the SV40 nuclear localization sequence (5'GGGGGATCCTGTACTCCACCAAAGAAGAAGAGAAAGGTTGCCTAATCTAGAGGG3') were inserted into the BamHI and XbaI sites of pGAL-GFP to give an in frame fusion with GFP(pAFS50). The Lac repressor was then cloned into the BamHI site of pAFS50 by PCR with oligos containing overhanging BamHI sites (5'CGCGGATCCATGGTGAAACCAGTAACG3', 5'GCGGGATCCCTGCCCGCTTTCCA3') to give pAFS51. Serine 65 of GFP was then mutated to threonine to shift the excitation peak to 495 nm followed by replacement of the KpnI-XhoI GAL promoter fragment with a KpnI-XhoI HIS3 promoter fragment [24] to give pAFS67. The carboxyl terminal 11 amino acids were then deleted from the Lac repressor to prevent tetramerization as previously described [23] resulting in pAFS78. Yeast strain AFS168 was made by linearizing pAFS78 by Nhe1 digestion and integrating into the HIS3 locus of yeast strain AFS34.

Introduction of Lac-operator repeat into yeast

The 256 Lac operator repeat was introduced into yeast by cloning the KpnI-SphI fragment of pSV-DHFR-8.32 [20] into the yeast integrating plasmid YIplac128 [43] to yield pAFS59. pAFS59 was linearized with EcoRV which cuts within LEU2 and transformed into yeast strain AFS168 resulting in strain AFS173. Transformants were selected for leucine prototrophy, and integration at the *LEU2* locus was verified by Southern blotting [44]. For experiments on *tub1-801*, which is marked with *LEU2*, pAFS52, which carries the Lac operator array on a plasmid bearing *TRP1*, was integrated at the *TRP1* locus of chromosome IV. Control experiments showed that the Lac operator arrays on chromosomes III and IV behaved identically, with respect to the timing of sister separation (data not shown).

Growth Conditions

For all experiments yeast were grown to mid log phase in YPD before manipulation. For experiments with synchronous cultures, cells were arrested with 10 μ g/ml of α -factor for three hours and then released into medium lacking α -factor. The GFP-Lac repressor was induced during the last 30 min of the α -factor arrest by transferring the cells to CSM-HIS containing 10 μ g/ml α -factor and 10 mM 3-aminotriazole to induce the *HIS3* promoter. Cells were then transferred to YPD and samples were taken every 15 minutes and fixed for 30 minutes in 3.7% formaldehyde. Hydroxyurea was added to 10 mM where indicated.

For nocodazole arrest experiments log phase cells were induced for 30 minutes in CSM-HIS containing 10 mM 3-aminotriazole to induce GFP-Lac repressor expression. The cells were then resuspended in YPD containing 15µg/ml nocodazole. Samples were collected at 3 hour intervals and fixed as above.

Western Blotting

Western blotting were performed as described [45]. Clb2 antibody was diluted 1:2000 and protein was detected using chemiluminescence (ECL, Amersham).

FACS Analysis

To determine DNA content, yeast cells were fixed for 60 minutes in 70% ethanol at 24°C. Cells were then washed twice in 50 mM Tris pH 7.5 and resuspended in 1 mg/ml RNaseA in 50 mM Tris pH 7.5. RNaseA digestion was performed for 4 hours at 37°C. Cells were then washed in 50 mM Tris pH 7.5, resuspended in 40µg/ml proteinase K, and incubated for 1 hour at 55°C. The cells were harvested and resuspended in 50µg/ml propidium iodide in PBS, pH 7.2 and then sonicated. Determination of DNA content was performed on a Becton-Dickinson FACScan.

Visualization of Lac operator staining in yeast

Cells were imaged on a Nikon Microphot SA microscope using a 60x, 1.4 NA oil immersion lens. Fluorescence was visualized with a conventional

FITC excitation filter and a long pass emission filter. Images were acquired with a MTI-SIT68 camera using MaxVision-AT software. All images were averages of 128 optical frames of 33 msec each.

ACKNOWLEDGEMENTS

We wish to thank Kristen Richards and David Botstein for plasmid pKR16-1, Kathleen Matthews for advice, Kevin Struhl for the HIS3 promoter, Kurt Zingler, Jeff Cox, Karen Oegema, Tim Mitchison, and Arshad Desai for expert technical assistance and Alison Farrell and members of the Murray labs for assistance and critical review. We are especially indebted to Adam Rudner whose in situ hybridization experiments played an important role in validating GFP labeling. This work was supported by grants from NIH, the Packard Foundation, and the March of Dimes to AWM. AWM is a David and Lucile Packard Fellow.

REFERENCES

1. Nicklas, RB. **Measurements of the force produced by the mitotic spindle in anaphase:** *J. Cell Biol.* 1983, **97**:542-548.
2. McNiell, PA, Berns, MW. **Chromosome behavior after laser microirradiation of a single kinetochore in mitotic PtK2 cells.:** *J. cell Biol.* 1984, **88**:543-553.
3. Holloway, SL, Glotzer, M, King, RW, Murray, AW. **Anaphase is initiated by proteolysis rather than by the inactivation of MPF:** *Cell* 1993, **73**:1393-1402.
4. Morgan, DO. **Principles of CDK regulation.:** *Nature* 1995, **374**:131-134.
5. Murray, AW, Solomon, MJ, Kirschner, MW. **The role of cyclin synthesis and degradation in the control of maturation promoting factor activity:** *Nature* 1989, **339**:280-286.
6. Glotzer, M, Murray, AW, Kirschner, MW. **Cyclin is degraded by the ubiquitin pathway:** *Nature* 1991, **349**:132-138.
7. Hershko, A, Ganoth, D, Pehrson, J, Palazzo, RE, Cohen, LH. **Methylated ubiquitin inhibits cyclin degradation in clam embryo extracts.:** *J. Biol. Chem.* 1991, **266**:16376-16379.

8. Sudakin, V, Ganoth, D, Dahan, A, Heller, H, Hersko, J, Luca, F, Ruderman, JV, Hershko, A. **The cyclosome, a large complex containing cyclin-selective ubiquitination ligase activity, targets cyclins for destruction at the end of mitosis.:** *Mol. Biol. Cell* 1995, **6**:185-198.
9. Irniger, S, Piatti, S, Michaelis, C, Nasmyth, K. **Genes involved in sister chromatid separation are needed for B-type cyclin proteolysis in budding yeast.:** *Cell* 1995, **77**:1037-1050.
10. King, RW, Peters, JM, Tugendreich, S, Rolfe, M, Hieter, P, Kirschner, MW. **A 20S complex containing CDC27 and CDC16 catalyzes the mitosis-specific conjugation of ubiquitin to cyclin B:** *Cell* 1995, **81**:279-88.
11. Funabiki, H, Yamano, H, Kumada, K, Nagao, K, Hunt, T, Yangida, M. **Cut2 proteolysis required for sister-chromatid separation in fission yeast.:** *Nature* 1996, **381**:438-441.
12. Yamamoto, A, Guacci, V, Koshland, D. **Pds1p, an inhibitor of anaphase in budding yeast, plays a critical role in the APC and checkpoint pathway(s):** *J Cell Biol* 1996, **133**:99-110.
13. Downes, CS, Mullinger, AM, Johnson, RT. **Inhibitors of DNA topoisomerase II prevent chromatid separation in mammalian cells but do not prevent exit from mitosis:** *Proc. Natl. Acad. Sci., USA* 1991, **88**:8895-8899.

14. Shamu, CE, Murray, AW. **Sister chromatid separation in frog egg extracts requires DNA topoisomerase II activity during anaphase.:** *J. Cell Biol.* 1992, **117**:921-934.
15. Uemura, T, Ohkura, H, Adachi, Y, Morino, K, Shiozaki, K, Yanagida, M. **DNA topoisomerase II is required for condensation and separation of mitotic chromosomes in *S. pombe*:** *Cell* 1987, **50**:917-25.
16. Holm, C, Stearns, T, Botstein, D. **DNA topoisomerase II must act at mitosis to prevent non-disjunction and chromosome breakage.:** *Molec. Cell Biol.* 1989, **9**:159-168.
17. Koshland, D, Hartwell, LH. **The structure of sister minichromosome DNA before anaphase in *Saccharomyces cerevisiae*:** *Science* 1987, **238**:1713-6.
18. Guacci, V, Hogan, E, Koshland, D. **Chromosome condensation and sister chromatid pairing in budding yeast.:** *J. Cell Biol.* 1994, **125**:517-530.
19. Prasher, DC, Eckenrode, VK, Ward, WW, Prendergast, FG, Cormier, MJ. **Primary structure of the *Aequorea victoria* green-fluorescent protein:** *Gene* 1992, **111**:229-33.
20. Robinett, CC, Straight, AF, Li, G, Wilhelm, C, Sudlow, G, Murray, AW, Belmont, A. **In vivo localization of DNA sequences and visualization of large scale chromatin organization using lac operator/repressor recognition.:** *J. Cell Biol.* 1996,

21. Oliver, SG, van, der, Aart, Qj, Agostoni, CM, Aigle, M, Alberghina, L, Alexandraki, D, Antoine, G, Anwar, R, Ballesta, JP, Benit, P, et, al. **The complete DNA sequence of yeast chromosome III.:** *Nature* 1992, 357:38-46.
22. Kramer, H, Niemoller, M, Amouyal, M, Revet, B, von Wilcken-Bergmann, B, Muller-Hill, B. **lac repressor forms loops with linear DNA carrying two suitably spaced lac operators:** *Embo J* 1987, 6:1481-91.
23. Chen, J, Matthews, KS. **Subunit Dissociation Affects DNA Binding in a Dimeric Lac Repressor Produced by C-Terminal Deletion:** *Biochemistry* 1994, 33:8728-8735.
24. Struhl, K, Kill, DE. **Two Related Regulatory Sequences Are Required for Maximal Induction of *Saccharomyces cerevisiae* HIS3 Transcription:** *Mol Cell Biol* 1987, 7:104-110.
25. Herskowitz. **MAP Kinase Pathways in Yeast: For Mating and More:** *Cell* 1995, 80:187-197.
26. Weinert, TA. **Dual cell cycle checkpoints sensitive to chromosome replication and DNA damage in the budding yeast *Saccharomyces cerevisiae*:** *Radiat Res* 1992, 132:141-3.
27. Allen, JB, Zhou, Z, Siede, W, Freidberg, EC, Elledge, SJ. **The SAD1/RAD53 protein kinase controls multiple checkpoints and DNA damage-induced transcription in yeast.:** *Genes and Dev.* 1994, in press:

28. Surana, U, Amon, A, Dowzer, C, McGrew, J, Byers, B, Nasmyth, K. **Destruction of the CDC28/CLB mitotic kinase is not required for the metaphase to anaphase transition in budding yeast.** *EMBO J.* 1993, **12**:1969-1978.
29. Hoyt, MA, Trotis, L, Roberts, BT. **S. cerevisiae genes required for cell cycle arrest in response to loss of microtubule function.** *Cell* 1991, **66**:507-517.
30. Li, R, Murray, AW. **Feedback control of mitosis in budding yeast.** *Cell* 1991, **66**:519-531.
31. Li, X, Nicklas, RB. **Mitotic forces control a cell cycle checkpoint.** *Nature* 1995, **373**:630-632.
32. Wells, WAE, Murray, AW. **Aberrantly segregating centromeres activate the spindle assembly checkpoint in budding yeast.** *J. Cell Biol.* 1996, **133**:75-84.
33. Hardwick, K, Murray, AW. **Mad1p, a phosphoprotein component of the spindle assembly checkpoint in budding yeast.** *J. Cell Biol.* 1995, **131**:709-720.
34. Minshull, J, Straight, A, Rudner, A, Dernburg, A, Belmont, A, Murray, AW. **Protein Phosphatase 2A Regulates MPF Activity and Sister Chromatid Cohesion in Budding Yeast.** *Curr. Biol.* 1996, Submitted.:

35. Riggs, AD, Newby, RF, Bourgeois, S. **lac repressor--operator interaction. II. Effect of galactosides and other ligands:** *J Mol Biol* 1970, **51**:303-14.
36. Lehner, CF, O'Farrell, PH. **The roles of Drosophila cyclins A and B in mitotic control:** *Cell* 1990, **61**:535-547.
37. Rappaport, R. **Repeated furrow formation from a single mitotic apparatus in cylindrical sand dollar eggs:** *J Exp Zool* 1985, **234**:167-71.
38. Chant, J, Herskowitz, I. **Genetic control of bud site selection in yeast by a set of gene products that constitute a morphogenetic pathway:** *Cell* 1991, **65**:1203-12.
39. Yeh, E, Skibbens, RV, Cheng, JW, Salmon, ED, Bloom, K. **Spindle dynamics and cell cycle regulation of dynein in the budding yeast, Saccharomyces cerevisiae:** *J Cell Biol* 1995, **130**:687-700.
40. Sherman, F, Fink, G, Lawrence, C. **Methods in Yeast Genetics.** Cold Spring Harbor Laboratory Press. Cold Spring Harbor, New York. 1974.
41. Ito, H, Fukuda, Y, Murata, K, Kimura, A. **Transformation of Intact Yeast Cells Treated with Alkali Cations:** *J Bacteriol* 1983, **153**:163-168.
42. Sikorski, RS, Hieter, P. **A system of shuttle vectors and yeast host strains designed for efficient manipulation of DNA in Saccharomyces cerevisiae.:** *Genetics* 1989, **122**:19-27.

43. Gietz, RD, Sugino, A. **New yeast-Escherichia coli shuttle vectors constructed with in vitro mutagenized yeast genes lacking six-base pair restriction sites:** *Gene* 1988, 74:527-34.
44. Southern, E. **Detection of specific sequences among DNA fragments separated by gel electrophoresis:** *J. Mol. Biol.* 1975, 98:503-517.
45. Kellogg, DR, Kikuchi, A, Fujii-Nakata, T, Turck, CW, Murray, AW. **Members of the NAP/SET family of proteins interact specifically with B-type cyclins.:** *J. Cell Biol.* 1995, 130:661-673.

FIGURE LEGENDS

Figure 1 - Yeast chromosomes can be tagged by directed integration of Lac operator repeats.

A) Lac operator repeats were integrated by homologous recombination near the centromere of chromosome III in *S. cerevisiae*. Plasmid pAFS59 was cut with EcoRV to target integration to the LEU2 locus which lies 22 kb to the left of the centromere. B) Schematic structure of the GFP-Lac repressor fusion.

Figure 2 - GFP-Lac repressor staining shows separation of sister chromatids in yeast.

WT yeast cells (AFS173) containing integrated Lac operator repeats were arrested in a factor then released into rich medium after induction of GFP-Lac repressor. (A) GFP fluorescence (GFP-LacI, left panels) and DIC (differential interference contrast) images of yeast (right panels) every 15 minutes after α -factor release. Cells at the 0 and 30 minute time points are unbudded and contain a single fluorescent dot per cell. Cells at 60 and 75 minutes have small buds and a single fluorescent dot, whereas those at 90, 105, and 120 minutes have large buds and a pair of widely separated dots. Cells at 135 and 150 minutes have completed cytokinesis and cell separation and each individual G1 cell contains a single fluorescent dot. In this experiment α -factor was added back at 60 minutes after release to prevent cells from proceeding beyond G1 of the second cell cycle. (B) Yeast cells released from an α -factor arrest for 120 minutes into the medium containing 10 mM

hydroxyurea. Each cell has a large bud but only a single fluorescent dot, indicating that preventing DNA replication blocks the onset of sister chromatid separation.

Figure 3 - Separation of sister chromatids occurs in mitosis.

WT yeast cells (AFS173) were scored for sister chromatid separation, Clb2 levels and DNA content after α -factor release. The cells analyzed in this figure are from the same experiment as the cells depicted in Figure 2. (A) Separation of sister chromatids as assayed by GFP-Lac repressor staining. At least 100 cells were scored for each time points. (B) Western blot of Clb2 protein. The Clb2 band is indicated with an arrow, bands above and below it are background bands. (C) DNA content from FACS analysis. Similar results to those shown here were obtained in 5 other independent experiments.

Figure 4 - Checkpoint deficient mutants prematurely separate sister chromatids.

Wild type (WT, AFS173), *mad2-1* (AFS387), and *tub1-801* (AFS396) cells were treated with nocodazole and assayed for sister chromatid separation. GFP fluorescence (left panels) and DIC (differential interference contrast) images (right panels) are shown. (A) WT yeast cells treated with nocodazole for 3 hours. Both cell pairs show a single fluorescent dot. (B) *tub1-801* cells treated with nocodazole for 3 hours. Both cell pairs show a single fluorescent dot. (C) *mad2-1* cells treated with nocodazole for 3 hours. Two cell pairs show two

fluorescent dots and one shows a single dot. (D) A *mad2-1* cell pair treated with nocodazole for 6 hours. The sisters have separated and one of the two cells has rebudded.

Figure 5 - Premature sister chromatid separation in nocodazole treated cells correlates with rapid death.

Logarithmically growing cultures of wild type (WT, AFS173), *mad2-1* (AFS387), *mad1-181* (AFS386), *mad3-152* (AFS388), *bub1-242* (AFS389), *bub2-257* (AFS390), *bub3-305* (AFS391), and *tub1-801* (AFS396) were treated with nocodazole and assayed for sister chromatid separation. (A) Separation of sister chromatids assayed as the percentage of cells with two fluorescent dots at 0, 3, and 6 hours after nocodazole treatment. (B) Percentage of viable cells at 3, and 6 hours after nocodazole treatment relative to the number of viable cells in that strain at time 0. (C) α -factor arrested *mad2-1*(AFS387) cells were released in the presence (open bars) or absence (filled bars) of nocodazole. The distances between separated sister chromatids were scored 120 minutes after release from α -factor arrest. Separation distances less than 0.6 μ m were difficult to resolve and thus were scored as unseparated.

Figure 6 - Lac repressor binding can hold sister chromatids together.

Wild type (WT, AFS173) and *mad2-1* (AFS387) yeast strains containing the tetramerizing GFP-Lac repressor were treated with nocodazole in the presence (+IPTG) or absence of 20 mM IPTG. In the IPTG containing cultures, the cells

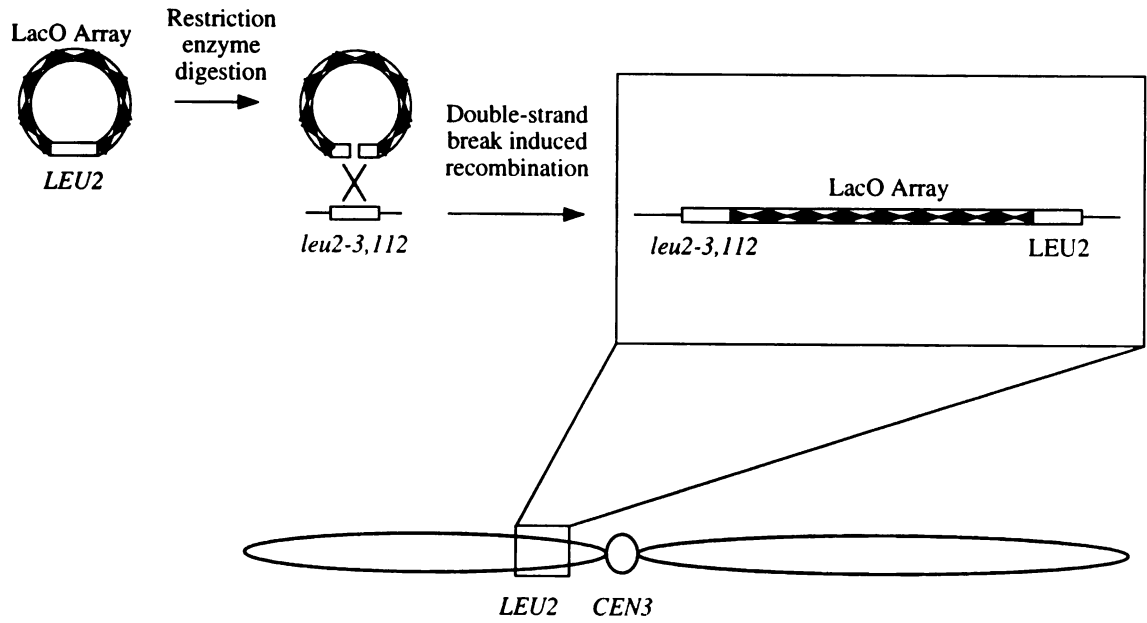
were transferred to medium lacking IPTG for 30 minutes before assaying the pattern of fluorescence (A) Sister chromatid separation at 0, 3 and 6 hours after drug treatment as assayed by the percentage of cells containing two fluorescent dots. (B) The percentage of cells that have rebudded as a measure of passage through mitosis in the presence of nocodazole. Cells are scored as rebudding if they form a cluster containing at least three distinct projections.

Table I. Yeast strains

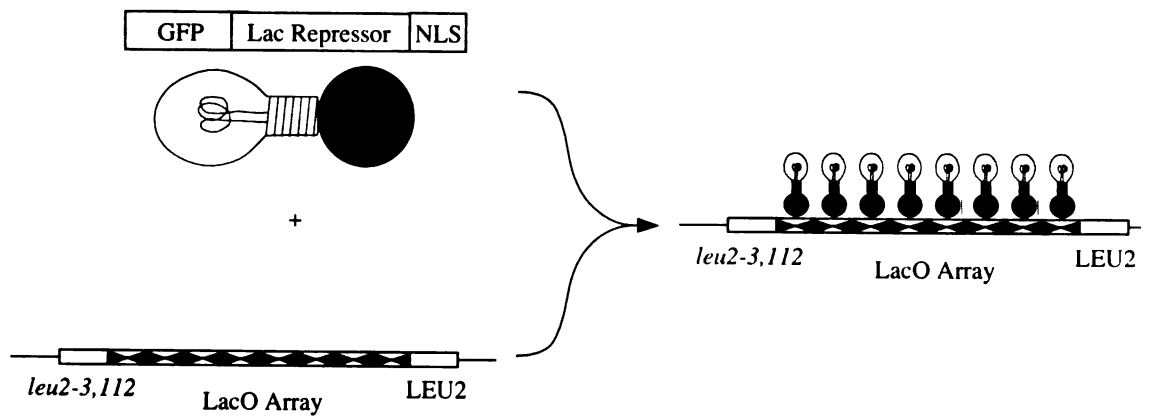
Strain Number	Relevant Genotype	Plasmid	Source
AFS34 (W303-1a)	<i>MATa ade2-1 can1-100 ura3-1 leu2-3,112 his3-11,15 trp1-1</i>		Rothstein
AFS168	<i>MATa his3-11,15::GFP-LacI-HIS3</i>	pAFS78	This work
AFS173	<i>MATa his3-11,15::GFP-LacI-HIS3 leu2-3,112::lacO-LEU2</i>	pAFS78, pAFS59	"
AFS386	<i>MATa mad1-181 his3-11,15::GFP-LacI-HIS3 leu2-3,112::lacO-LEU2</i>	"	"
AFS387	<i>MATa mad2-1 his3-11,15::GFP-LacI-HIS3 leu2-3,112::lacO-LEU2</i>	"	"
AFS388	<i>MATa mad3-152 his3-11,15::GFP-LacI-HIS3 leu2-3,112::lacO-LEU2</i>	"	"
AFS389	<i>MATa bub1-242 his3-11,15::GFP-LacI-HIS3 leu2-3,112::lacO-LEU2</i>	"	"
AFS390	<i>MATa bub2-257 his3-11,15::GFP-LacI-HIS3 leu2-3,112::lacO-LEU2</i>	"	"
AFS391	<i>MATa bub3-305 his3-11,15::GFP-LacI-HIS3 leu2-3,112::lacO-LEU2</i>	"	"
AFS396	<i>MATa tub1-801::LEU2 his3-11,15::GFP-LacI-HIS3 ltrp1-1::lacO-TRP1</i>	pAFS52, pAFS 78, pKR16-1	"
AFS292	<i>MATa his3-11,15::GFP-LacI(tet+)-HIS3 leu2-3,112::lacO-LEU2</i>	pAFS67, pAFS59	"
AFS397	<i>MATa mad2-1 his3-11,15::GFP-LacI(tet+)-HIS3 leu2-3,112::lacO-LEU2</i>	"	"

All strains are isogenic to AFS34, and only those parts of the genotype that differ from that of AFS34 are indicated. *LacI(tet+)* indicates the tetramerizing form of the Lac Repressor.

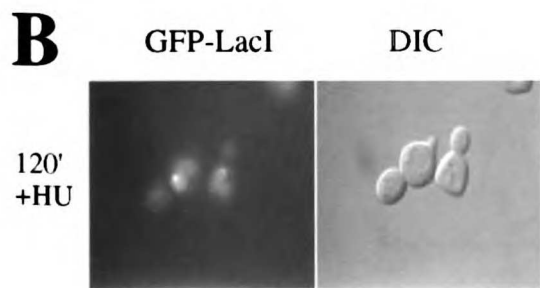
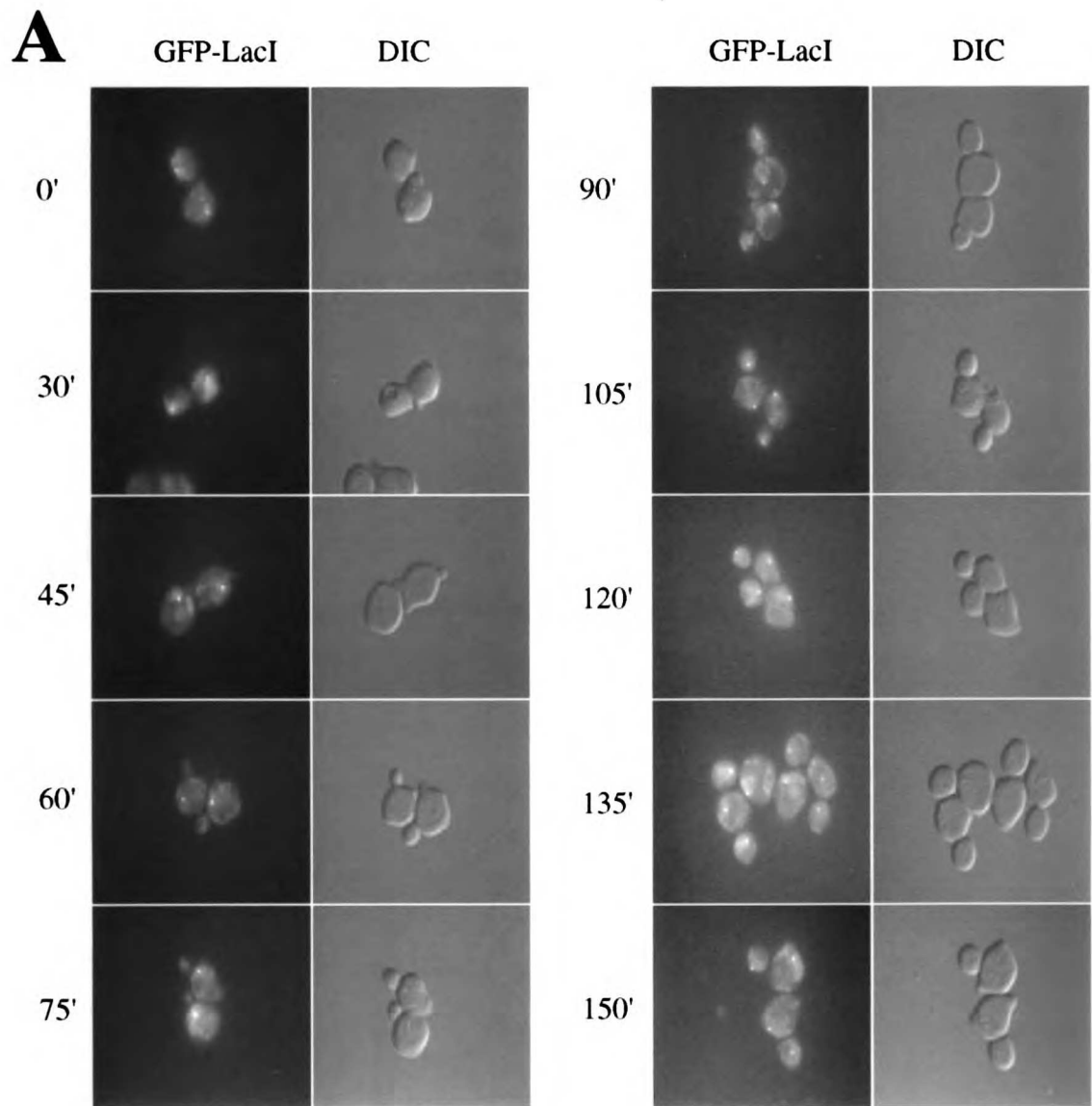
A



B



Straight et al. Figure 1



Straight et al. Figure 2

INCE LIBRARY

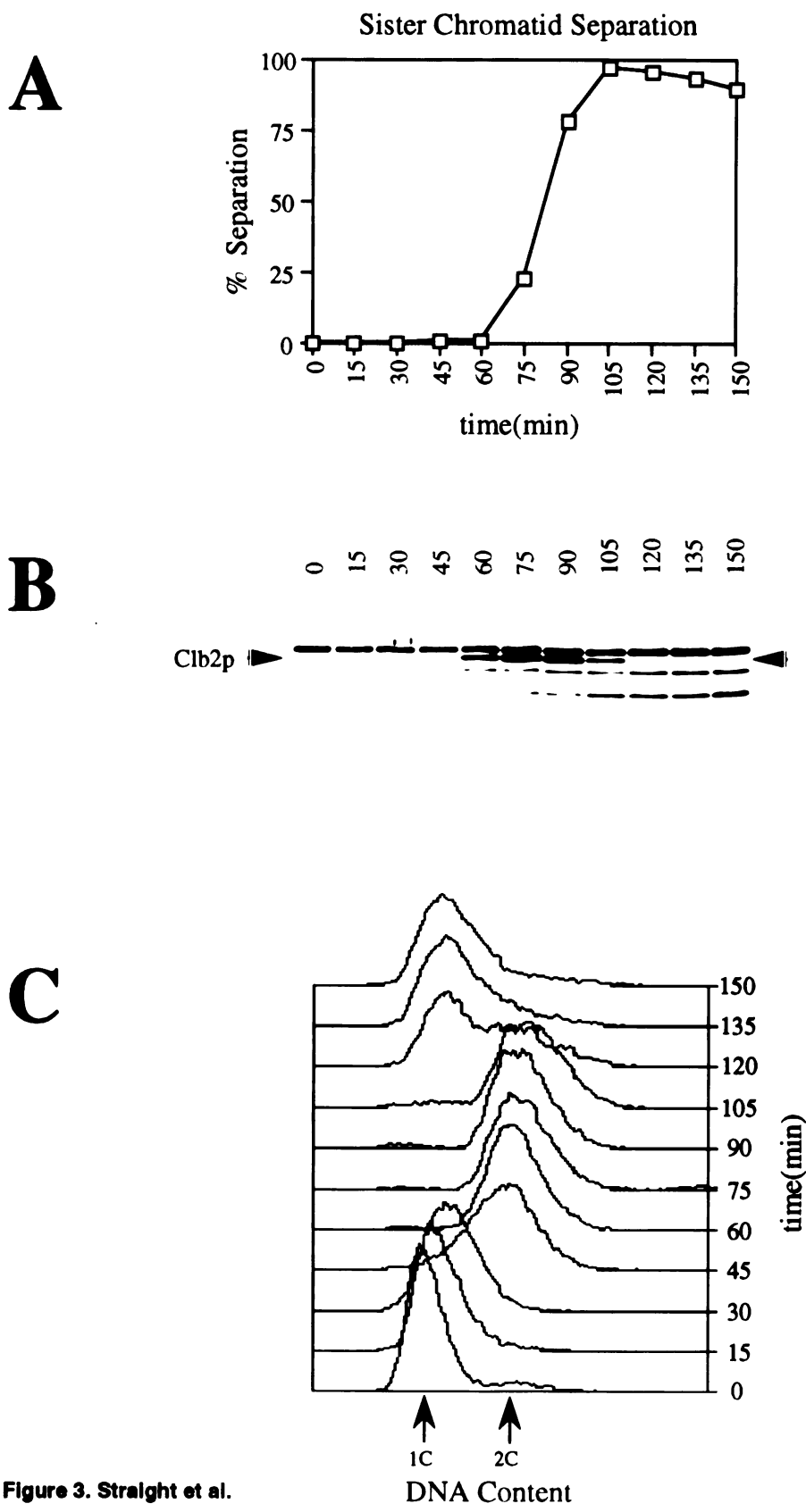
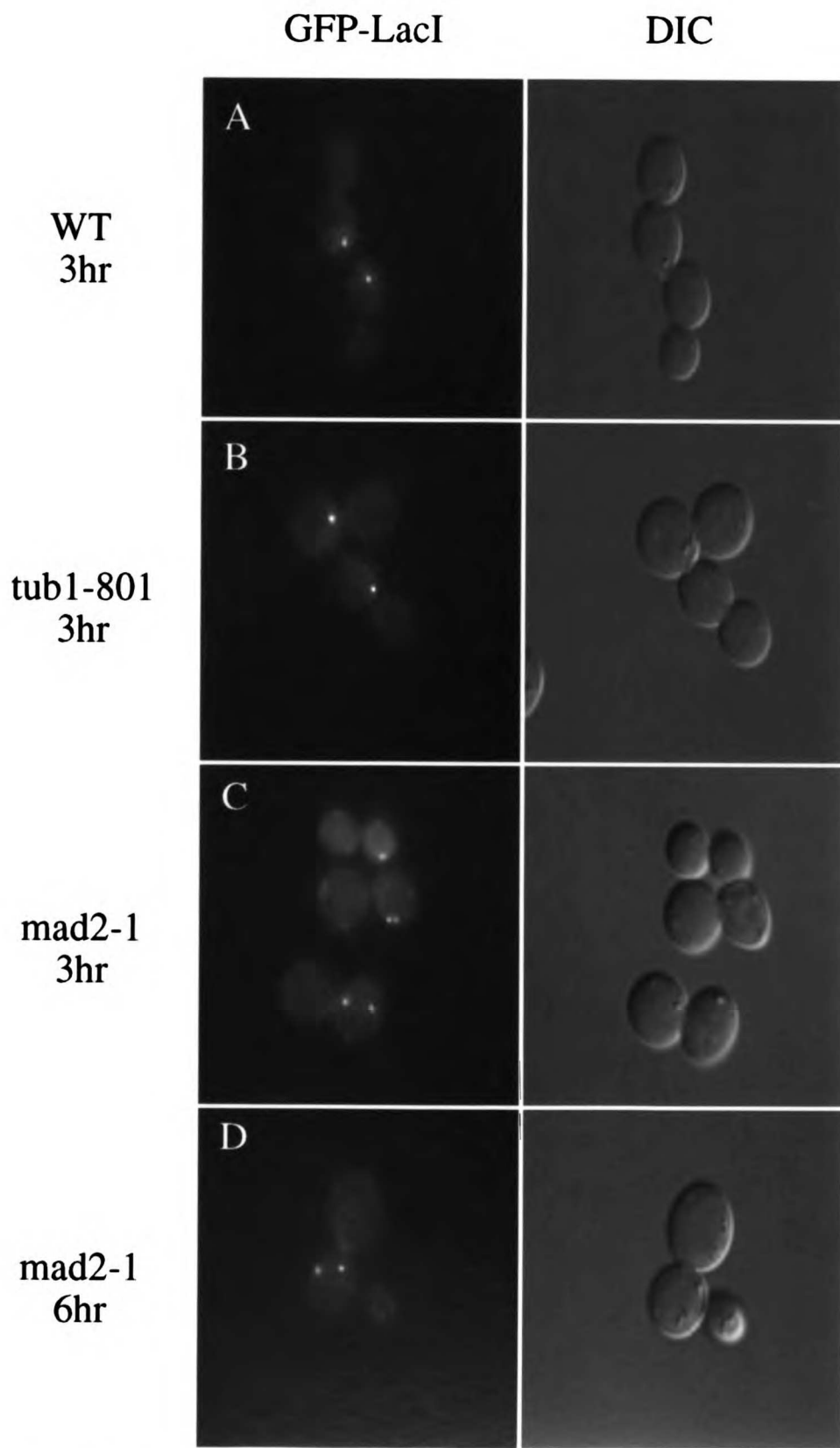
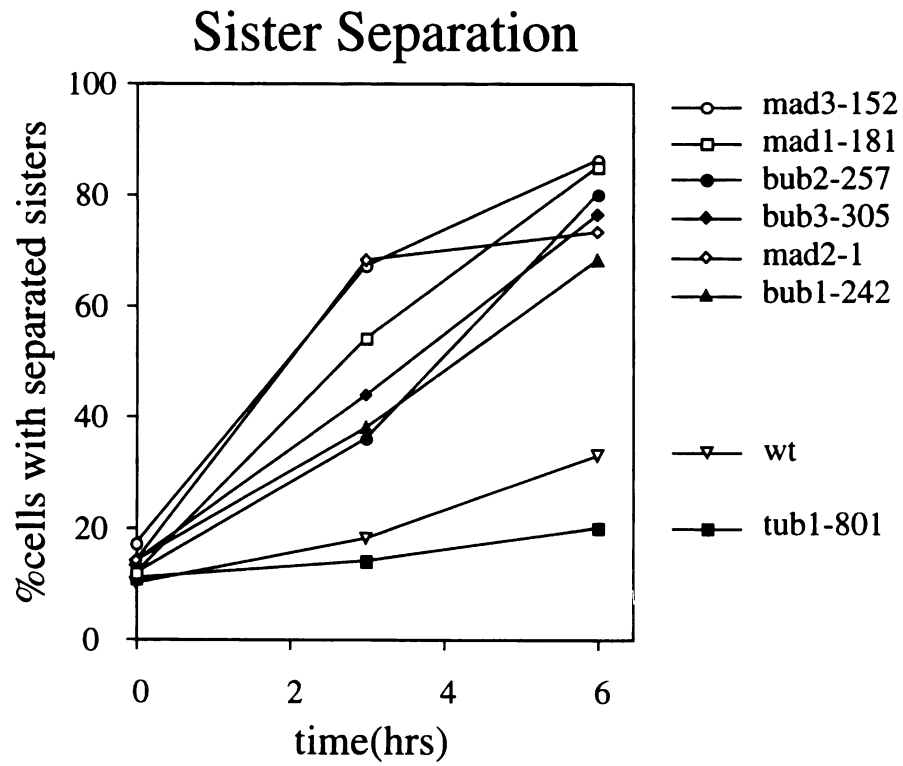
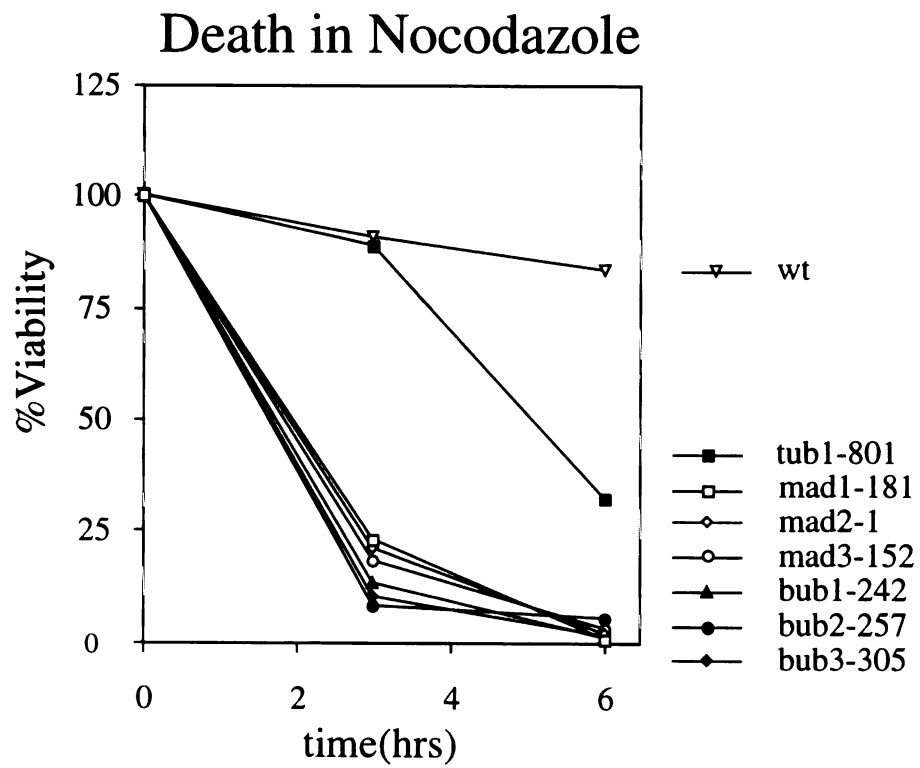


Figure 3. Straight et al.



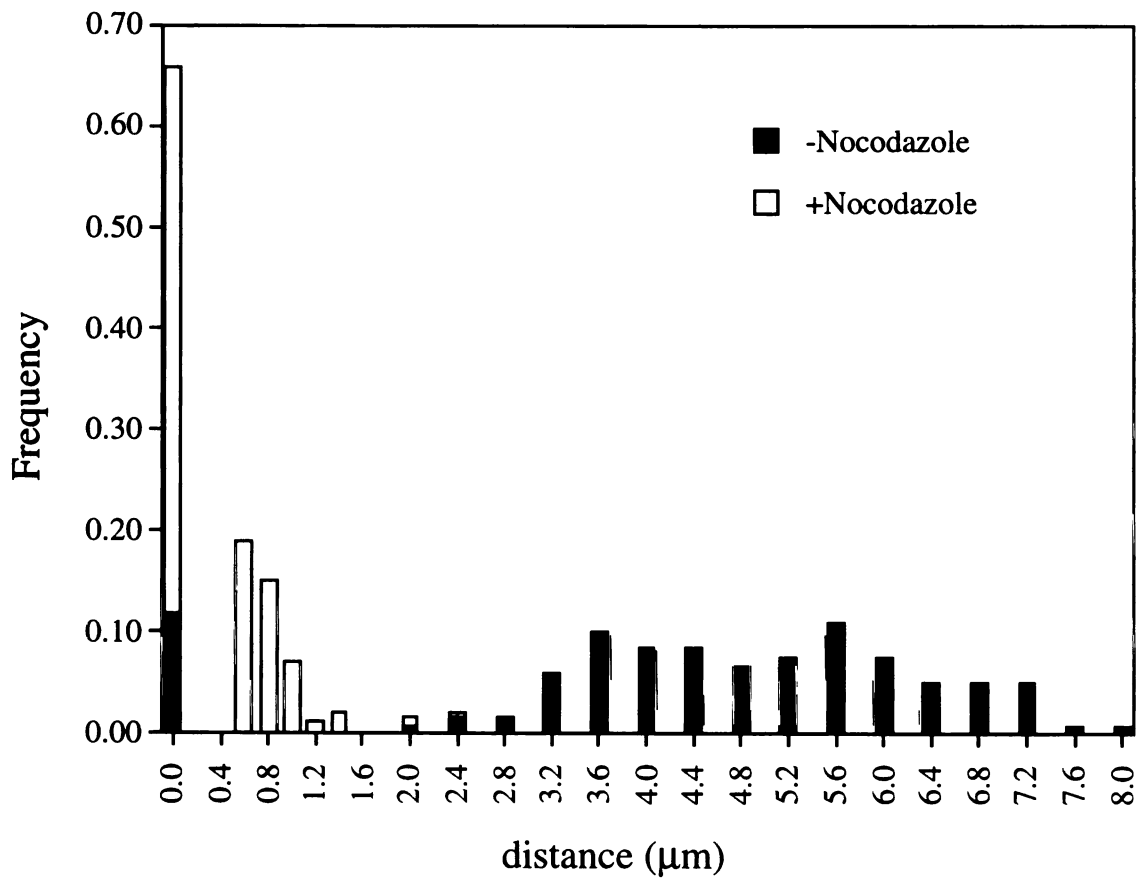
Straight et al. Figure 4

A**B**

Straight et al. Figure 5

C

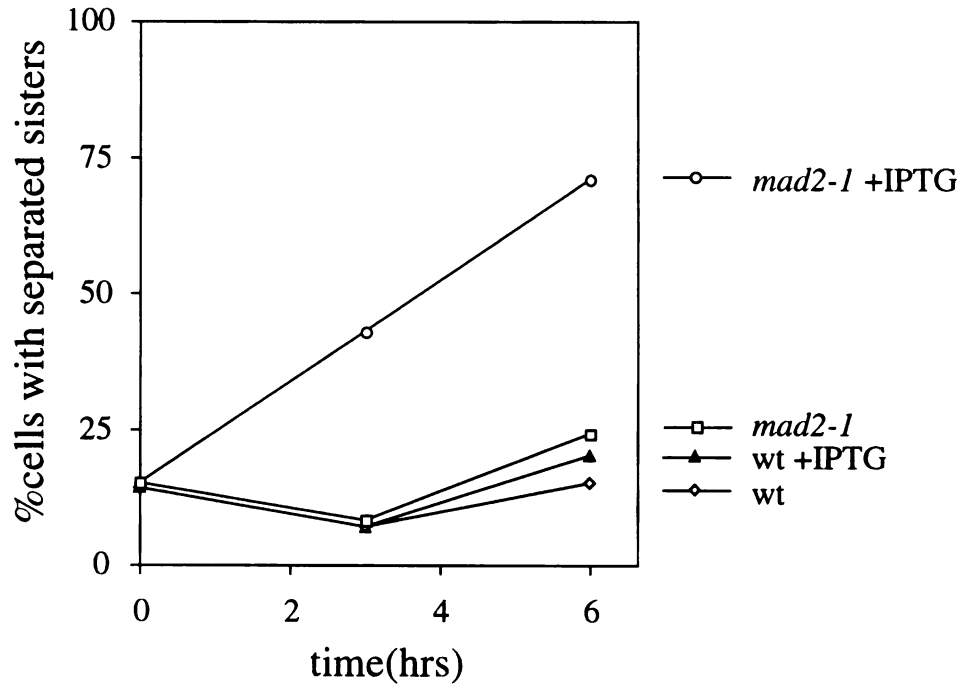
Separation Distance in mad2-1



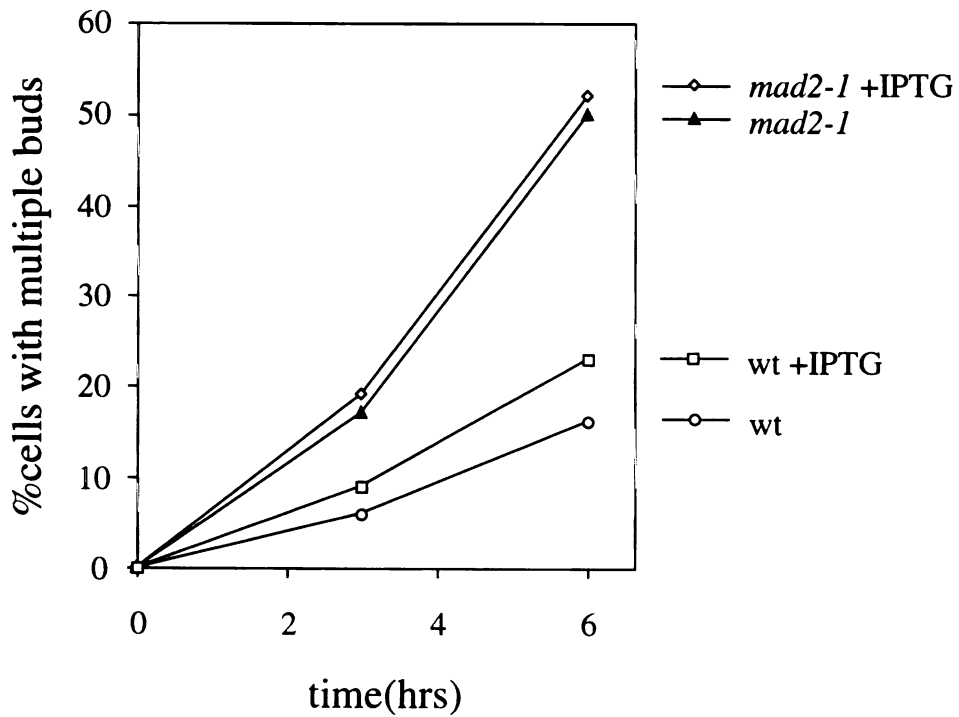
Straight et al. Figure 5

A

Sister Separation

**B**

Rebudding



Straight et al. Figure 6

Chapter 2

**Mitosis in living budding yeast: anaphase A
but no metaphase plate**

Mitosis in living budding yeast: Anaphase A but No Metaphase Plate

Aaron F. Straight, Wallace F. Marshall, John W. Sedat,
and Andrew W. Murray

A.F. Straight and A.W. Murray
Department of Physiology Box 0444
School of Medicine
University of California San Francisco
San Francisco, CA 94143-0444, USA.

W.F. Marshall and J.W. Sedat
Department of Biochemistry Box 0448
School of Medicine
University of California San Francisco
San Francisco, CA 94143-0448, USA.

ABSTRACT

Chromosome movements and spindle dynamics were visualized in living cells of the budding yeast *Saccharomyces cerevisiae*. Individual chromosomal loci were detected by expressing a protein fusion between green fluorescent protein (GFP) and the Lac repressor, which bound to an array of Lac operator binding sites integrated into the chromosome. Spindle microtubules were detected by expressing a protein fusion between GFP and Tub1, the major alpha tubulin. Spindle elongation and chromosome separation exhibited biphasic kinetics and centromeres separated before telomeres. Budding yeast did not exhibit a conventional metaphase chromosome alignment but did show anaphase A, movement of the chromosomes to the poles.

The reproduction of eukaryotic cells depends on the ability of the mitotic spindle to segregate the replicated chromosomes into two identical sets. As cells enter mitosis they organize microtubules into a bipolar spindle. In most eukaryotes, the kinetochore, a specialized region of the chromosome, binds microtubules and in higher eukaryotes the condensed chromosomes move to a position equidistant from the spindle poles called the metaphase plate. Once all sister chromatids are properly aligned in metaphase, the linkage between the sister chromatids is dissolved causing two changes that segregate the sisters from each other: chromosomes move toward the spindle pole (Anaphase A) and elongation of the spindle separates the spindle poles (Anaphase B).

Knowledge of mitosis comes from three sources: microscopic observation and manipulation of animal and plant cells (1), studies in cell cycle extracts (2), and genetic analysis, especially in budding and fission yeast (3). To integrate the findings of these different approaches, we need to know if the basic features of mitosis are conserved among eukaryotes. Although the budding yeast, *Saccharomyces cerevisiae*, is an excellent organism for genetic analysis, its mitotic spindle is small and difficult to see in living cells. Individual mitotic yeast chromosomes are not visible by conventional light or electron microscopy and can only be seen by in situ hybridization to fixed cells (4, 5). We have simultaneously visualized the mitotic spindle and individual chromosomes in living yeast cells. These studies show that budding yeast chromosomes do not align on a metaphase plate, that spindle elongation and chromosome separation exhibit biphasic kinetics, that yeast exhibit anaphase A chromosome to pole movement, that chromosomes are under polewards force as they separate, and that centromeres separate before

telomeres.

We used green fluorescent protein (GFP) (6) to follow chromosome and spindle movements in living yeast cells by fluorescence microscopy. We visualized the spindle with a protein fusion between GFP and the major alpha tubulin (Tub1) (7). Specific loci were marked by binding of a protein fusion between GFP and the Lac repressor (GFP-LacI) to an integrated array of the Lac operator (LacO) (8, 9). We observed synchronized cells passing through mitosis, taking vertical stacks of images every 26s and subjecting them to iterative deconvolution (10, 11). The top panel of Fig. 1A shows a series of optical sections after deconvolution projected as a stereo pair to reveal the structure of the entire spindle and the staining of the centromeres in three dimensions and the bottom panel shows a three dimensional model of the same cells. Although the chromosomal LacO array and microtubules are both marked with GFP, the two structures are easily distinguished: the LacO array is a spherically symmetrical dot whereas the spindle is a straight, rod-shaped structure that stains more intensely at its two ends. Although, subsequent images are two dimensional projections of the three dimensional data, all distances are true distances between objects in three dimensional space.

Fig 1B shows mitosis in a living yeast cell. Even in the shortest spindles, the GFP-tagged centromeres were close to the spindle's long axis (Fig. 1B). The centromeric staining was not restricted to the central region of the spindle and was often found near one of the spindle poles. Once anaphase began, sister chromatids moved rapidly toward opposite spindle poles along the spindle axis. Finally, spindle elongation distributed one sister chromatid to the mother cell and its partner to the daughter cell.

In animal and plant cells, once the two kinetochores of a pair of sister

chromatids have attached to opposite spindle poles, the chromatid pair moves to a point equidistant from the two poles (12, 13). This congression is thought to be achieved by a balance between opposing forces on chromosomes: a poleward force applied at the kinetochore, a polar ejection force or the 'polar wind' acting along the length of the chromosome, and forces acting on the attached sister kinetochore (12). We examined yeast cells to see if congression occurred in these very small spindles, which appear to lack the non-kinetochore microtubules that have been postulated to be responsible for the polar wind (14). We observed multiple cells (6 out of 14) in which the centromeric staining moved back and forth along the long axis of the spindle (Fig. 2A and B). The oscillations spanned the length of the spindle (1.5 to 2.0 μm), and continued until anaphase began ($t=0$ seconds). Animal and plant chromosomes also oscillate along the the spindle axis and the absolute magnitude of the of the oscillations is similar to that seen in yeast. Unlike yeast spindles, however, the relative amplitude of these movements is much less than the length of the spindle so that the oscillations do not bring chromosomes near the poles. Centromere oscillation along the spindle axis implies that either kinetochores detach from and reattach to spindle microtubules or that microtubules lengthen and shorten while attached to the kinetochore, as occurs in higher eukaryotes (15). Detachment and reattachment of kinetochores to microtubules seems unlikely because yeast appear to have a single microtubule per kinetochore (16, 17) and unattached kinetochores would activate the spindle assembly checkpoint (18). Thus, chromosome oscillations suggest that an individual microtubule can polymerize and depolymerize while maintaining attachment to a yeast kinetochore.

Yeast cells often initiate anaphase when the centromeres are closer to

one pole than the other. Fig. 2A shows a chromosomal spot abutting one spindle pole immediately prior to anaphase chromosome separation. Ten out of 17 cells (59%) initiated anaphase when the centromere was within the terminal 25% of the spindle, and 7 (41%) did so when the centromere was between 25% and 75% of the distance along the spindle. This observation suggests that budding yeast lack a conventional metaphase plate and that chromosomal alignment on a metaphase plate is not required for anaphase chromosome separation in *S. cerevisiae*. This result is consistent with fixed cell studies that show that chromosomes are distributed along the length of the metaphase spindle and that presumptive kinetochore microtubules do not exhibit a metaphase arrangement (4, 17, 19, 20). Although the chromosomes often separated when the sister chromatid pair was near one of the spindle poles, both sister chromatids never moved to the same pole. Thus the sister kinetochores on all the observed chromosomes were attached to opposite spindle poles before the onset of anaphase, satisfying the cell cycle checkpoint that senses kinetochore attachment to the spindle microtubules (18, 21).

Successive images of anaphase in a single cell are shown in Fig. 3A. We measured all the pairwise distances between the spindle poles and the kinetochores of the sister chromatids as cells proceeded through mitosis and aligned the records from various cells by defining $t=0$ as the moment of sister chromatid separation. Fig. 3B shows the average distance between the spindle poles and the distance between the sister centromeres over time. The kinetics of anaphase were highly reproducible from cell to cell. The bipolar mitotic spindle was between 1.5 and 2.0 μm in length for many minutes before the initiation of anaphase. Two minutes before sister chromatid separation, the rate of spindle elongation gradually increased to 0.54 $\mu\text{m}/\text{min}$ and the spindle

was between 2.5 and 3.0 μm long when chromosome separation began (Fig. 3B). In contrast to this smooth increase, the separation of the centromeres showed a jump of 1.8 μm (average) in less than 26 seconds, followed by a smooth increase in separation at a rate (0.64 mm/min) similar to that of the spindle poles. The initial jump in sister separation accomplished most of anaphase A, reducing the average centromere to pole distance from 1.5 μm to 0.7 μm in less than a minute. The abrupt separation of the sister chromatids suggests that either their linkage to the poles is under poleward force before sister separation or that there is some repulsive force between the chromosomes that propels them apart once the linkage between them is dissolved. The rapid phase of elongation and separation continued until the spindle length increased to 5.0 to 6.0 μm (Fig. 3B). At this point both spindle elongation and sister separation slowed to about 0.2 mm/min, reaching a final extent of 10 to 11 μm (Fig. 3B). However, the chromosomes continued to separate with the spindle, indicating that microtubule attachment of the chromosome to the spindle pole was still intact. These results are consistent with rates of spindle elongation measured by DIC microscopy in another wild type strain (22). In the majority of cells the rapid phases of both sister separation and spindle elongation occurred through the bud neck. In two out of seventeen mitoses, however, the initial phase of separation occurred entirely within the mother cell and was followed by reorientation of the spindle and its slow elongation through the bud neck.

The unusual property that chromosomes can separate when they are much nearer one spindle pole than the other allowed us to investigate anaphase A in yeast. Fig. 3A shows images from a cell that started anaphase when chromosomes were close to one spindle pole body. At $t=0$ the chromatid pair was still joined but was very close to one spindle pole body

(Fig. 3A). At the next timepoint (t=26 seconds) the chromatid pair had clearly separated and one chromatid had moved toward the more distant spindle pole. After this chromosome to pole movement, the spindle elongated and separated the sister chromatids into the mother and daughter cells (Fig. 3A). Fig. 3C shows the distance between the sister chromatids, the distance between the chromatid that began anaphase near its spindle pole and its spindle pole and the distance between the sister chromatid that began anaphase far from its spindle pole and its spindle pole, with respect to time. Once sister chromatid separation began, the chromatid that was far away from its spindle pole moved rapidly toward that pole at a rate of at least 1.33 $\mu\text{m}/\text{min}$. The chromatid that was near its spindle pole moved little if at all.

Our analysis of chromosome movement to the spindle pole indicates that, in yeast, proximity of the sister chromatid pair to the spindle pole is not the activating signal for the mitotic checkpoint (23). Loss of tension on a kinetochore activates the spindle checkpoint in insect spermatocytes (24). Our observation that chromatid pairs close to one spindle pole appear to satisfy the spindle assembly checkpoint suggests that either there is sufficient tension on both kinetochores to prevent the activation of the checkpoint, or the yeast checkpoint monitors a parameter other than tension. Yeast are responsive to excess kinetochores (21), and in higher eukaryotic cells unattached kinetochores activate the spindle assembly checkpoint (18), but it is still unclear how yeast cells sense defects at the kinetochore.

To investigate the role of microtubule-dependent forces in chromosome separation we observed mitosis in cells that lacked a spindle but still progressed through mitosis. The spindle assembly checkpoint mutant *mad1* does not sense spindle depolymerization and proceeds through mitosis even though it cannot accurately segregate its sister chromatids. We

constructed a *mad1* yeast strain that contained the GFP-LacI tag at the centromere of chromosome III and followed mitosis in the presence of nocodazole (15 $\mu\text{g}/\text{ml}$, a concentration that depolymerizes all microtubules). The first detectable instance of sister centromere separation occurred at $t=26$ seconds (Fig. 4A), but in the absence of a spindle there was no efficient segregation of the chromosomes. Instead, the GFP-marked LacO arrays repeatedly separated into two separate dots and then approached each other so closely that they could no longer be resolved and appeared as a single dot. Sister chromatid separation in *mad1* mutants in the presence of nocodazole was compared to that in wild-type cells in the absence of nocodazole (Fig. 4B). In *mad1* cells, sister chromatids never separated more than 1.5 to 2.0 μm from each other, whereas chromatids in wild-type cells separated 2 to 2.5 μm within 52s after disjunction (Fig. 4B), demonstrating that chromosome segregation requires the microtubule-dependent forces exerted by an intact spindle.

During anaphase in higher eukaryotes, chromosomes move towards the poles with their centromeres leading and their telomeres lagging behind. To visualize the centromere and telomere of the same chromosome in yeast, we integrated the LacO array both at the centromere and near the telomere of the long arm of chromosome IV, 1000 kb apart. A fortuitous recombination event reduced the size of the telomeric LacO array, allowing us to differentiate the weaker fluorescence of the telomeric array from the centromeric one. Before separation, the centromere and telomere stained as two discernible spots (Fig. 5A), and in all cells the centromeres separated 1 to 3 minutes before the telomeres. The kinetics of centromere and telomere separation were measured as an average of 5 video sequences (Fig. 5B). The centromeres of chromosome IV separated with kinetics nearly identical to those of the

centromeres of chromosome III (Fig. 5B). The telomeres lagged in the kinetics of their separation. The distance between Centromere2 and Telomere2 increased then decreased suggesting that the chromatin strand was stretched as the centromere was dragged into the daughter cell (Fig. 5B) and that this stretch was relieved as the telomere approached the centromere. Although the centromeres separated smoothly, the rate of telomere separation varied during anaphase. This difference may result from the active pulling on the centromere region by the spindle as opposed to the elastic stretching and recoiling of the chromatin that links the centromere and telomere.

The relative importance of various mechanisms of chromosome movement in mitosis has not been established and may vary between cell types. The ability to see individual chromosome movements in living yeast should allow detailed analysis of the phenotypes of mutations in microtubule motors and components of the mitotic apparatus and contribute to understanding of the dynamics and mechanism of mitosis.

Figure Legends

Fig. 1. Visualization of microtubules and chromosomes during mitosis. Images are two-dimensional projections of three dimensional data sets. Spindle microtubule staining is the bright bar joining the chromosomal staining. (A) Top, stereo projection of yeast cells during anaphase. Scale bar, 2 μm . Bottom, a three dimensional model of the top panel constructed by tracing the fluorescence intensity in the three dimensional data. (B) Top, images from a single cell going through mitosis (arrowheads mark chromosomal staining). Bottom, cartoon of centromeres, spindle and cell outline. Scale bar, 2 μm . (a) Early mitosis. A short bipolar spindle has formed. (b) Onset of anaphase with sister chromatids at one spindle pole. (c) Early anaphase. Sister chromatids have separated and the spindle is elongating. (d) Late anaphase. Chromosomes are distantly separated and spindle has elongated into the daughter cell (10).

Fig. 2. Chromosomes oscillating along the spindle axis. (A) Images from a single sequence showing centromere oscillations. Arrowhead indicates the centromere and time is in seconds relative to centromere separation. Scale bar, 1 μm . (B) Distances during metaphase oscillation. Chromosome1-Chromosome2, distance between the two centromeres; Chromosome1-SPB1, distance between the chromosome pair and one spindle pole body; Chromosome2-SPB2, distance between the chromosome pair and the other spindle pole body.

Fig. 3. Anaphase spindle elongation and chromosome separation. (A) Anaphase video sequence. Arrowheads mark centromeres, time is in seconds

relative to sister chromatid separation, cartoon shows cell outline. Scale bar, 2 μ m. (B) Kinetics of anaphase. Distances were measured between spindle pole bodies and chromosomal spots (25). in 6 datasets aligned by defining the time of chromosome separation as $t = 0$, (arrow on the pole separation trace). Arrowhead: time when chromosomes reached the same separation as the spindle poles. Rates of movement were derived by linear regression and all correlation coefficients exceed 0.99. (C) Observation of anaphase A chromosome movement. Chromosome-to-pole distance was calculated for cells that exhibit biased anaphase initiation (n=3).

Fig. 4. Sister chromatid separation without a spindle. (A) Successive images of the *mad1* mutant strain AFS386(8) in nocodazole. Centromeres marked by arrowheads, time in seconds relative to onset of anaphase. Scale bar, 2 μ m. (B) Distance of chromosome separation in the presence and absence of nocodazole. WT -Noc, chromatid separation in the presence of a spindle, *mad1* +Noc, distances from four separate video sequences in the presence of nocodazole.

Fig. 5. Centromere and telomere separation. (A) Successive images showing the separation of the centromeres and telomeres of chromosome IV in yeast strain AFS412 (26). Centromeres: arrowheads, telomeres: barbed arrowheads. Scale bar, 2 μ m. Time is relative to centromere separation. (B) Distance between centromeres and telomeres. The figure shows the average of five video sequences of centromere and telomere separation. The centromere and telomere that remained in the mother cell are labeled Centromere1 and Telomere1 and the centromere and telomere that were distributed to the daughter cell are labeled Centromere2 and Telomere2.

References

1. R. B. Nicklas, *Science* 275, 632 (1997).
2. A. W. Murray, *Meth. Cell Biol.* 36, 573 (1991).
3. B. D. Page, M. Snyder, *Ann. Rev. Microbiol.* 47, 231 (1993).
4. V. Guacci, E. Hogan, D. Koshland, *J. Cell Biol.* 125, 517 (1994).
5. H. Scherthan, J. Loidl, T. Schuster, D. Schweizer, *Chromosoma* 101, 590 (1992).
6. D. C. Prasher, *Trends in Genetics* 11, 320 (1995).
7. The GFP-Tub1 fusion under the control of the HIS3 promoter was constructed by ligating the entire genomic TUB1 locus with Bam HI and Not I linkers into pAFS78 (8). The resultant GFP-Tub1 fusion was cloned into the Kpn I to Xho I sites of pRS306 to yield pAFS91 and integrated at the URA3 locus after StuI digestion. The GFP-Tubulin fusion was functional since it rescues a normally lethal TUB1 deletion. Strain AFS403 was constructed by transforming strain AFS173 (8) with Stu I-digested pAFS91.
8. A. F. Straight, C. C. Robinett, A. S. Belmont, A. W. Murray, *Curr. Biol.* 6, 1599 (1996).
9. C. C. Robinett, et al., *J. Cell Biol.* 135, 1685 (1996).
10. AFS403 is a *MATa* strain carrying the GFP-Tub1 and GFP-LacI fusions as well as a Lac operator array located 23kb from the centromere of chromosome III. Cells were synchronized in G1 by treatment with 10mg/ml α -factor for 3 hours, released from this arrest, induced to express the GFP-Tub1 and GFP-LacI fusions for 30 min (8) and mounted in histidine-free medium. Every 26 s, 12 optical sections (100-ms exposure time) were collected (vertical separation 0.5 μ m) by wide-field deconvolution 3D microscopy (11) with a 60X 1.4NA lens.
11. D. A. Agard, Y. Hiraoka, P. Shaw, J. W. Sedat, *Meth. in Cell Biol.* 30, 353

(1989).

12. R. V. Skibbens, V. P. Skeen, E. D. Salmon, *J. Cell Biol.* 122, 859 (1993).
13. A. S. Bajer, J. Molè-Bajer, *ibid.* 102, 263 (1986).
14. C. L. Rieder, E. D. Salmon, *ibid.* 124, 223 (1994).
15. T. J. Mitchison, *Ann. Rev. Cell Biol.* 4, 527 (1988).
16. J. B. Peterson, H. Ris, *J. Cell Sci.* 22, 219 (1976).
17. M. Winey, et al., *J Cell Biol.* 129, 1601 (1995).
18. C. L. Rieder, R. W. Cole, A. Khodjakov, G. Sluder, *ibid.* 130, 941 (1995).
19. P. Y. Goh, J. V. Kilmartin, *ibid.* 121, 503 (1993).
20. V. Guacci, E. Hogan, D. Koshland, *Mol. Biol. Cell.* 8, (1997).
21. W. A. E. Wells, A. W. Murray, *J. Cell Biol.* 133, 75 (1996).
22. E. Yeh, R. V. Skibbens, J. W. Cheng, E. D. Salmon, K. Bloom, *ibid.* 130, 687 (1995).
23. R. B. Nicklas, P. Arana, *J. Cell Sci.* 102, 681 (1992).
24. R. B. Nicklas, S. C. Ward, G. J. Gorbsky, *J. Cell Biol.* 130, 929 (1995).
25. H. Chen, D. D. Hughes, T. A. Chan, J. W. Sedat, D. A. Agard, *J. Struct. Biol.* 116, 56 (1996).
26. Strain AFS412 was constructed by integrating pAFS52 (8) at TRP1 near the centromere of chromosome IV and then integrating pAFS114 near the telomere of chromosome IV. Plasmid pAFS114 contains a Kpn I-Sac I fragment of chromosome IV spanning nucleotides 1436502-1438325 in pAFS59 (8), and was integrated into chromosome IV after digestion with Bsa BI.
27. We thank members of the Murray laboratory, D.O. Morgan, and A. Farrell for critical review of the manuscript, A. Desai, T.J. Mitchison, and H. Funabiki for insightful comments and discussion, and J. Fung and S. Parmelee for assistance during data analysis. Supported by grants from NIH

A

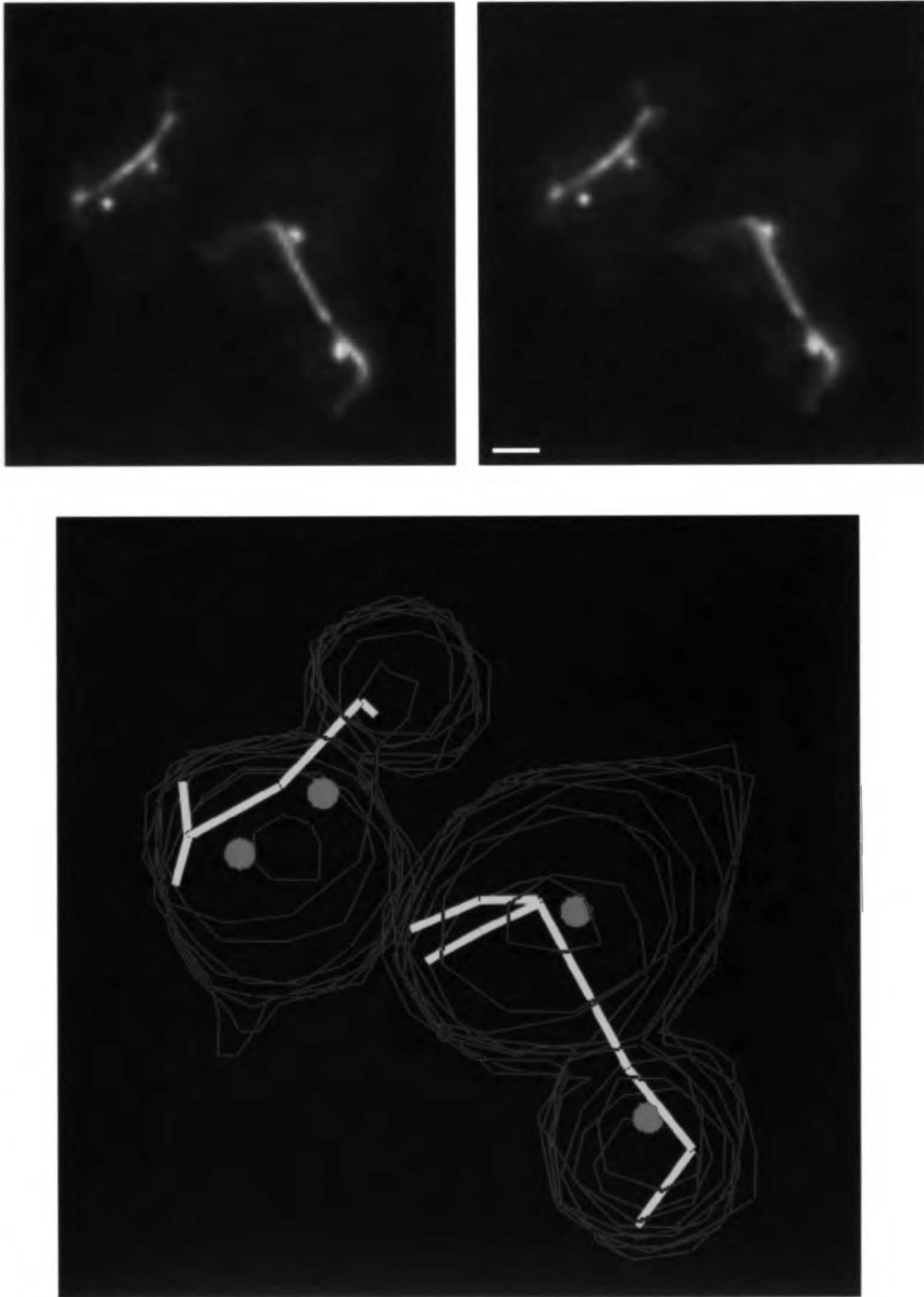


Figure 1. Straight et al.

B

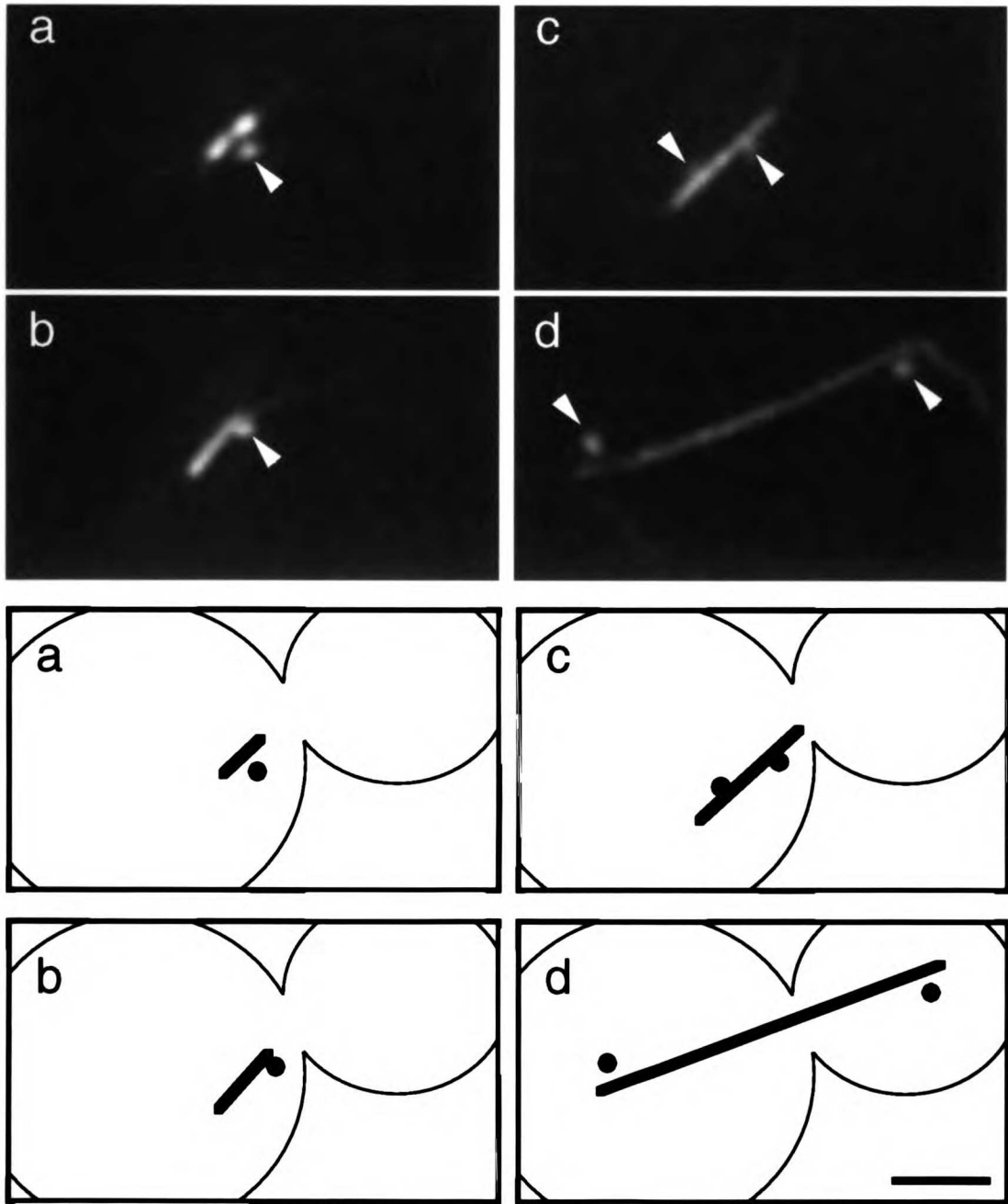


Figure 1. Straight et al.

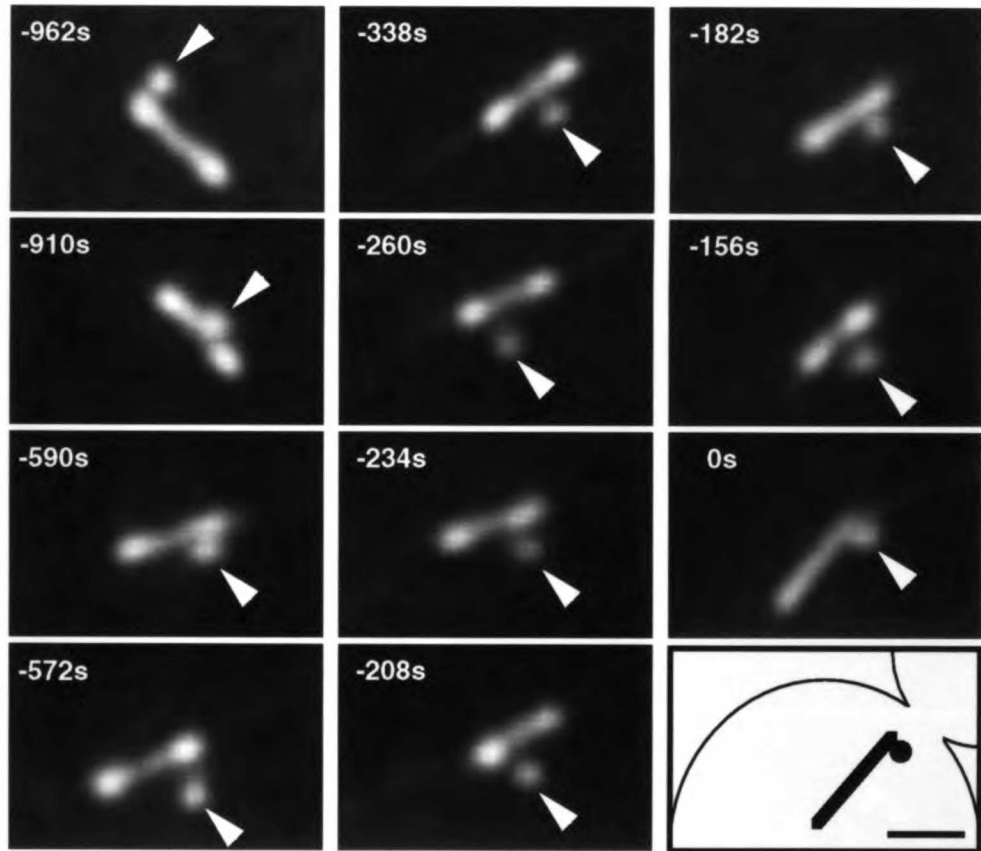
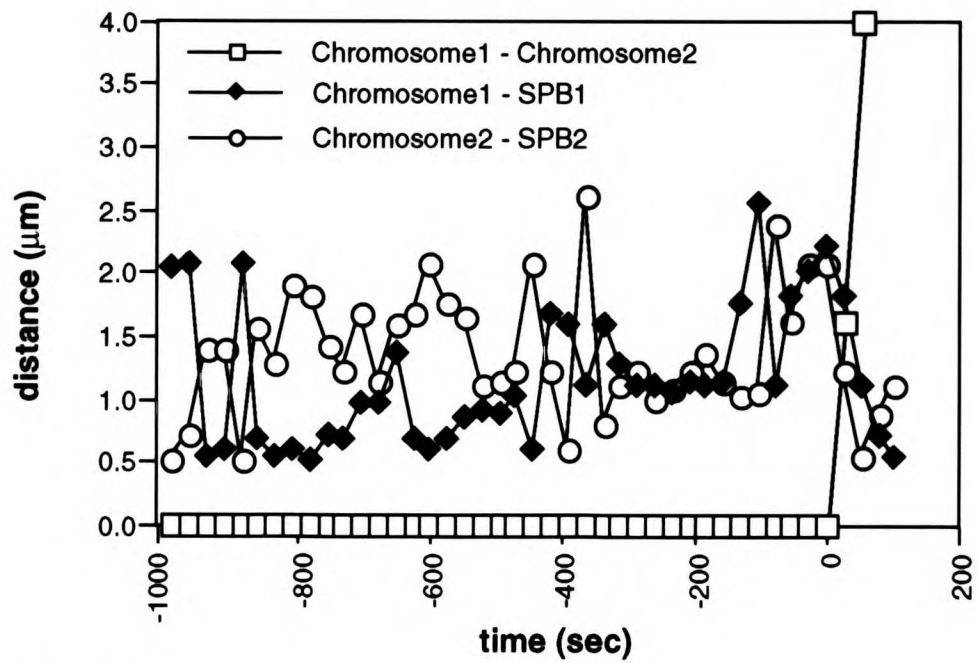
A**B**

Figure 2. Straight et al.

A

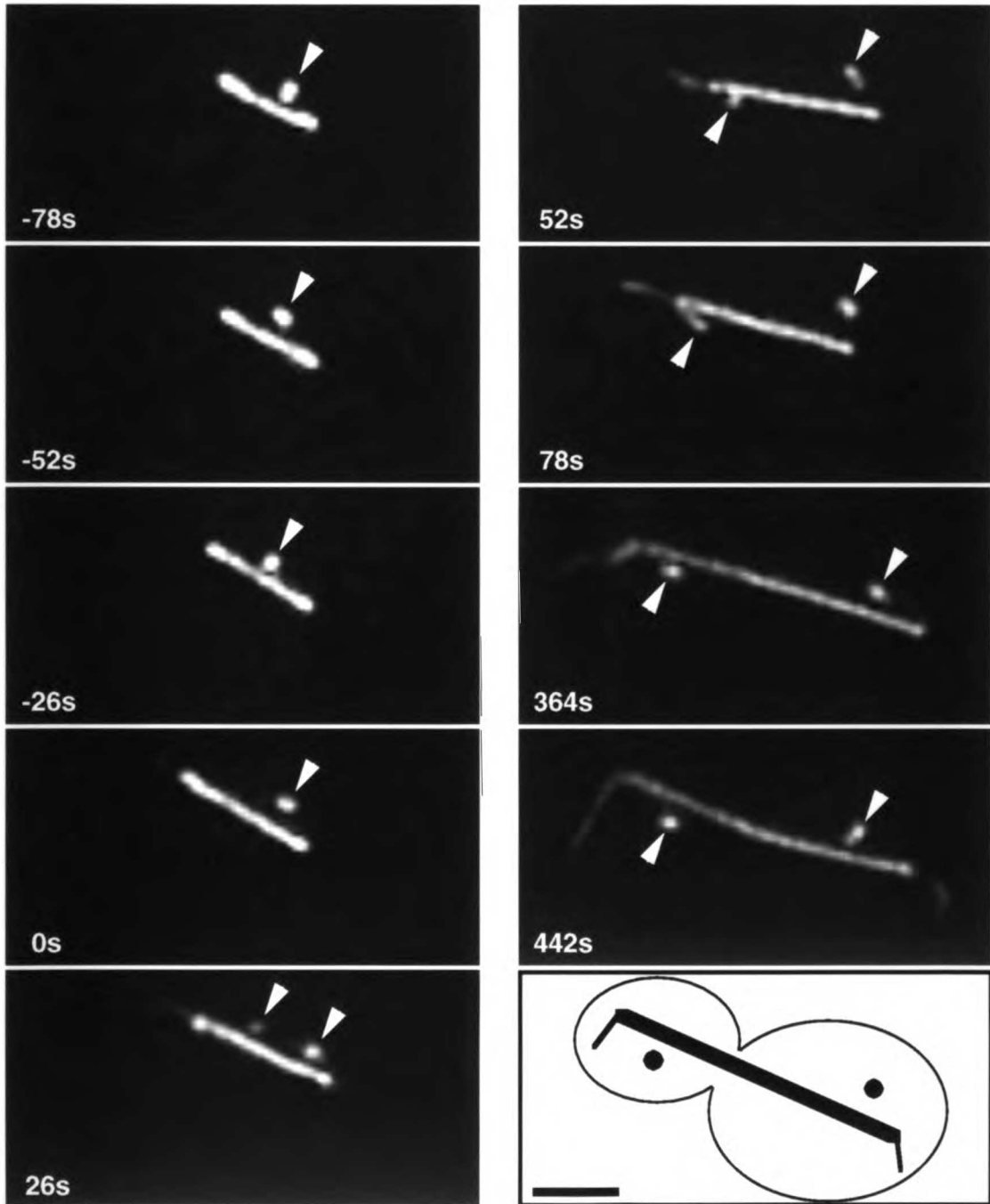


Figure 3. Straight et al.

B

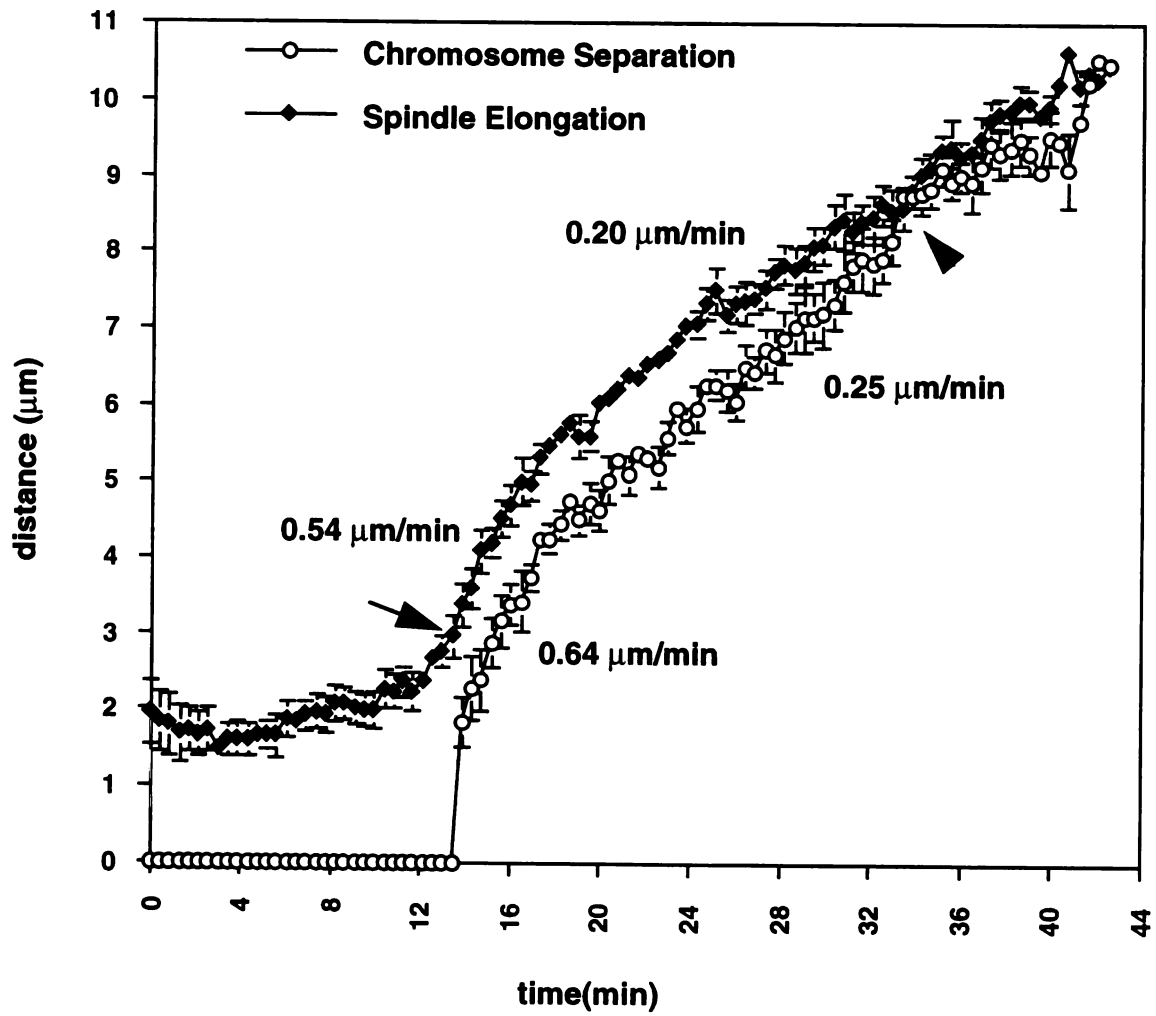
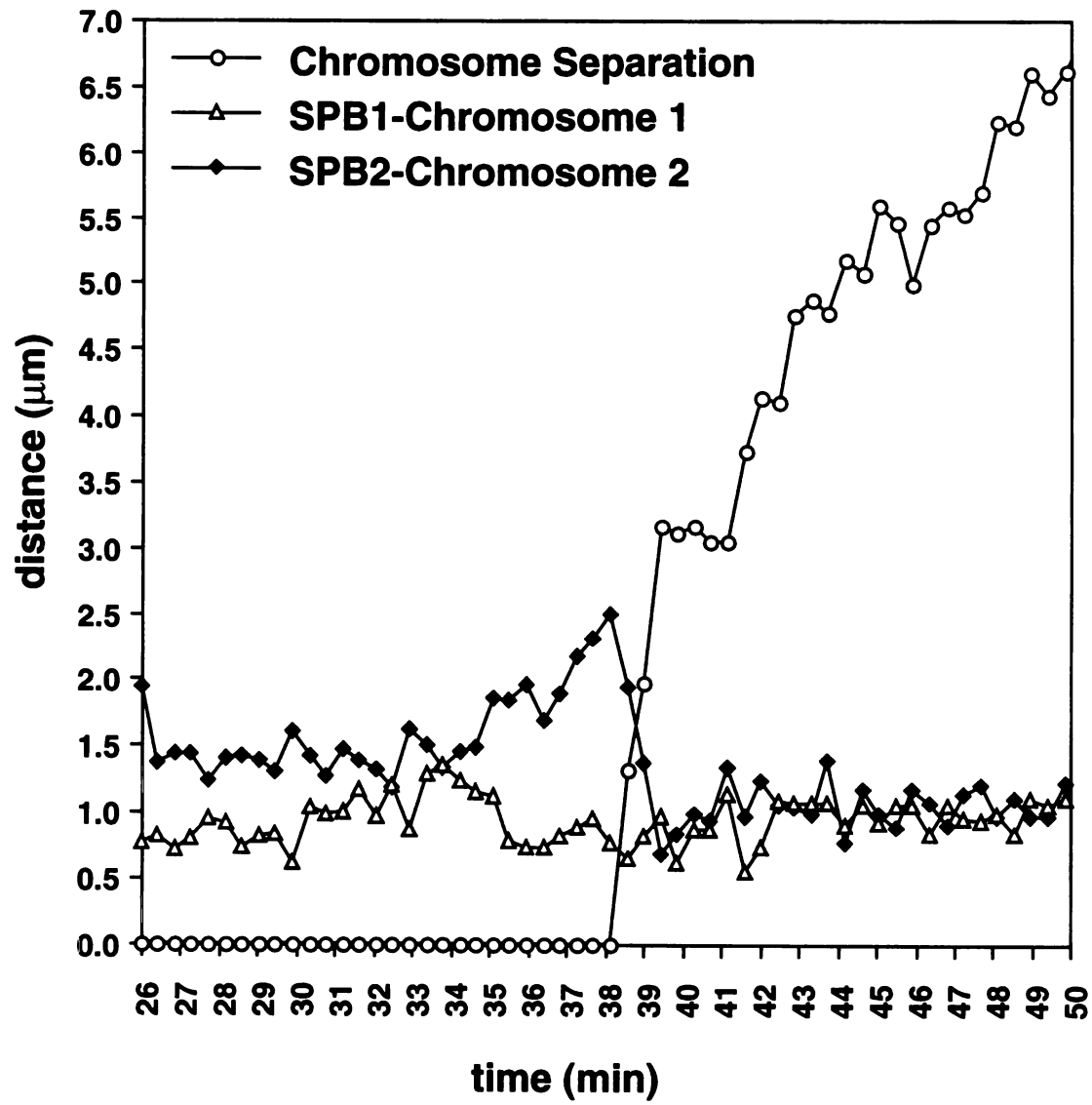


Figure 3. Straight et al.

C



UNIVERSITY OF CALIFORNIA

Figure 3. Straight et al.

A

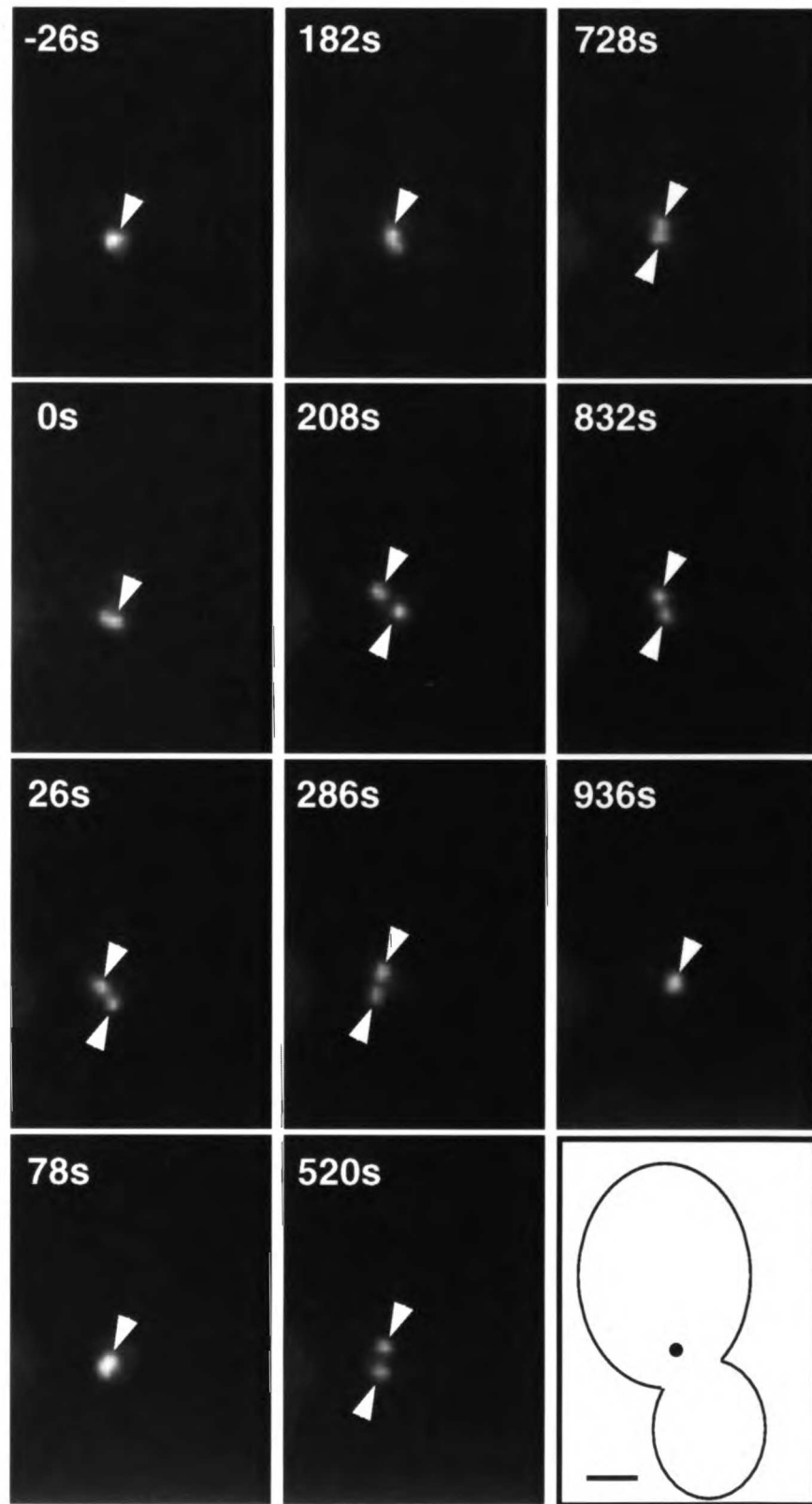


Figure 4. Straight et al.

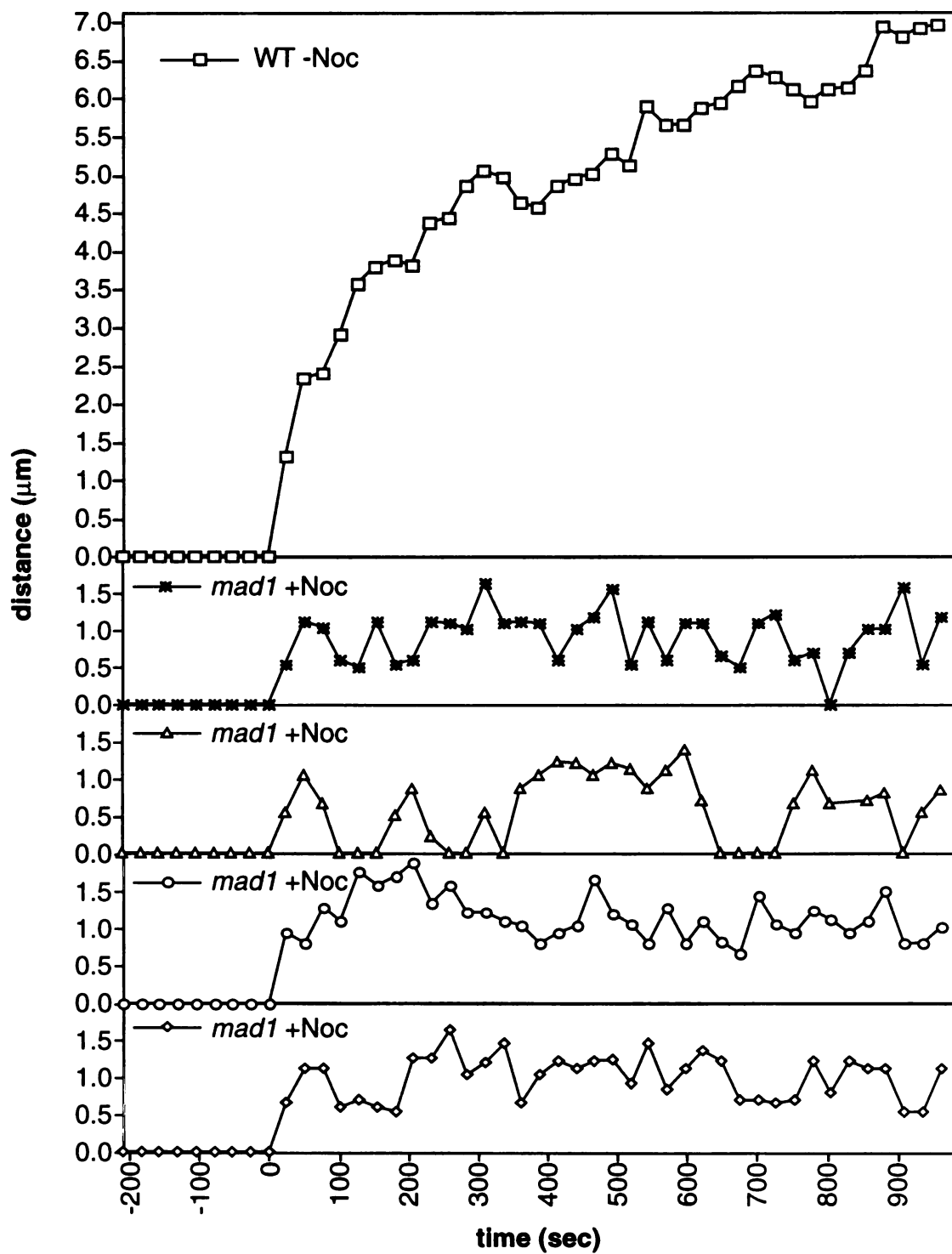
B

Figure 4. Straight et. al.

UNIVERSITY OF MICHIGAN

A

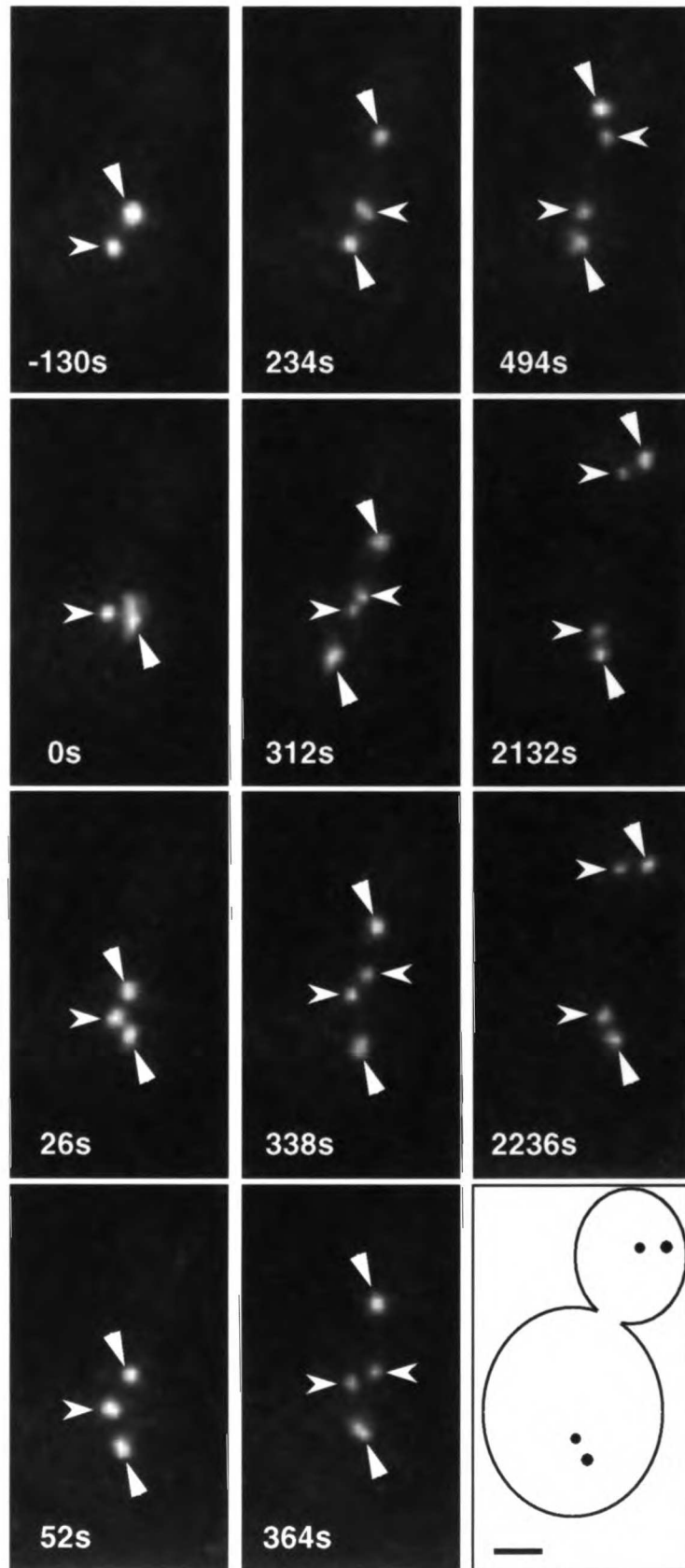


Figure 5. Straight et al.

B

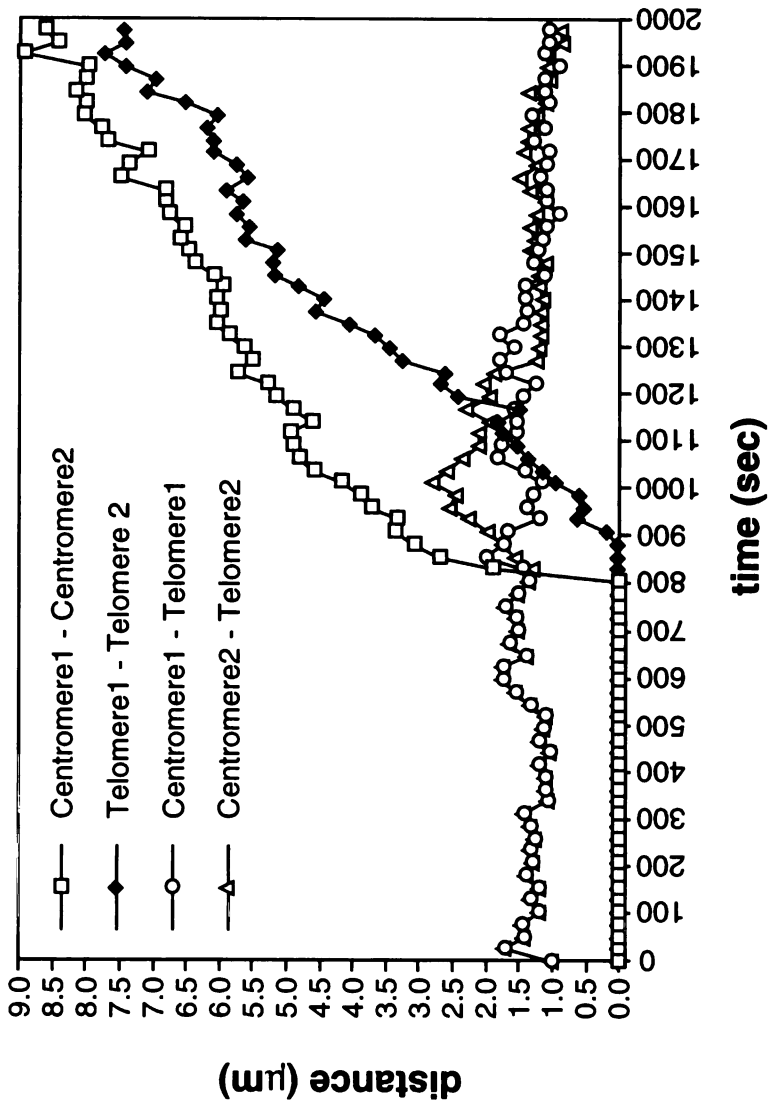


Figure 5. Straight et al.

Chapter 3

Time lapse microscopy reveals unique roles for kinesins during anaphase in budding yeast.

WEST
LAW
UNIVERSITY

Beyond redundancy: unique roles for kinesins during anaphase in budding yeast.

Aaron F. Straight, John W. Sedat and Andrew W. Murray

A.F. Straight and A.W. Murray
Department of Physiology Box 0444
School of Medicine
University of California San Francisco
San Francisco, CA 94143-0444, USA.

J.W. Sedat
Department of Biochemistry Box 0448
School of Medicine
University of California San Francisco
San Francisco, CA 94143-0448, USA.

UNIVERSITY OF CALIFORNIA
SAN FRANCISCO

Summary

The mitotic spindle is a complex and dynamic structure. Genetic analysis in budding yeast has identified two sets of kinesin-like motors, Cin8 and Kip1, and Kar3 and Kip3, that have overlapping functions in mitosis. We have studied the role of three of these motors by video microscopy of mutants cells that lack a single motor and have their microtubules and centromeres marked with green fluorescent protein. This analysis reveals that despite their functional overlap, mutants in each motor have specific defects in mitosis. *cin8Δ* mutants lack the rapid phase of anaphase B, *kip1Δ* mutants show defects in the slow phase of anaphase B, and *kip3Δ* mutants prolong the duration of anaphase to the point at which the spindle becomes longer than the cell. These findings imply that careful analysis of most groups of genes with overlapping functions will reveal specific functions for individual members of the group.

WESTERN
UNIVERSITY

Introduction

The mitotic spindle segregates the chromosomes into the daughter cells during cell division. The dynamic behavior of the spindle is controlled by motor proteins that move along microtubules and by the dynamic polymerization and depolymerization of microtubules. Motor proteins are required to assemble a bipolar spindle, to maintain the spindle prior to anaphase, to regulate microtubule dynamics, and to orient the spindle in the cell. After the spindle has formed, motor proteins mediate spindle elongation and chromosome separation during anaphase (reviewed in Inoue and Salmon, 1995; McIntosh and Pfarr, 1991; Vernos and Karsenti, 1996).

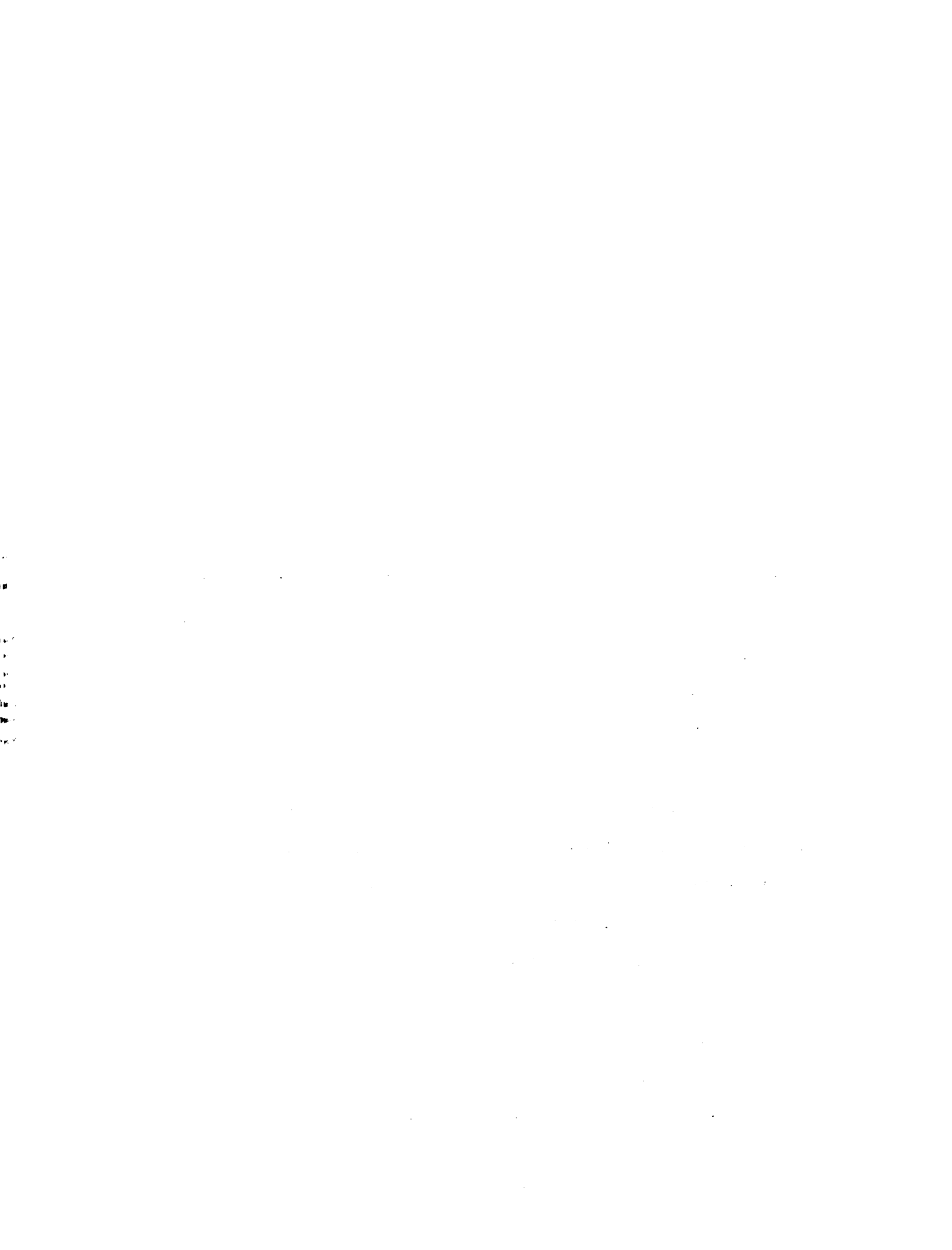
In vertebrate cells, the roles of motor proteins have been dissected by inactivating motors in living cells and by inactivating or immunodepleting them from egg extracts (Heald et al., 1997; Lombillo et al., 1995; Rodionov et al., 1993; Vaisberg et al., 1993; Walczak et al., 1996). These approaches are powerful, but can produce complex results because many motors have overlapping functions and antibody inactivation or immunodepletion experiments can also affect proteins that interact with the target motor protein. Several advances have made budding yeast an attractive alternative for studying the roles of specific motors in mitosis: the sequence of the budding yeast genome (Goffeau et al., 1996) provides a complete inventory of microtubule motors, yeast genetics allows rapid inactivation of individual motor proteins, and marking centromeres and microtubules with green fluorescent protein (GFP) makes it possible to study spindle and chromosome dynamics in living cells (Straight et al., 1997). Yeast contain six kinesin related proteins (Cin8, Kar3, Kip1, Kip2, Kip3 and Smy1) and a single dynein (Cottingham and Hoyt, 1997; DeZwaan et al., 1997; Eshel et al., 1993; Hoyt et al., 1992; Lillie and Brown, 1992; Meluh and Rose, 1990; Roof et al.,

1992) . This paper analyzes the mitotic roles of three of the six kinesin motors: Cin8, Kip1 and Kip3. We did not study Smy1 since it is likely to be involved in polarized cell growth and vesicle transport (Lillie and Brown, 1992; Lillie and Brown, 1994) or Kip2 because it primarily affects cytoplasmic microtubules rather than the intranuclear microtubules of the mitotic spindle (Miller and Rose, 1998). We were unable to study *kar3Δ* mutants, because most cells arrest in mitosis under the conditions required for microscopy.

Cin8 and Kip1 belong to the bimC/Cut7 class of microtubule motors that have been demonstrated to have roles in spindle formation and spindle elongation in other organisms (reviewed in Kashina et al., 1997). Kip3, is a novel kinesin that does not easily fit into the known kinesin subfamilies but has been shown to be important for spindle positioning (Cottingham and Hoyt, 1997; DeZwaan et al., 1997). Multiple other microtubule motor proteins have been shown to be involved in spindle positioning, assembly and elongation. The minus end directed motor Kar3 antagonizes the activity of Cin8/Kip1 to ensure proper spindle assembly and elongation (Saunders et al., 1997; Saunders and Hoyt, 1992) and is also thought to participate in the positioning of the spindle (Cottingham and Hoyt, 1997; DeZwaan et al., 1997). In addition to the kinesin family of proteins, dynein has also been shown to have a roles in spindle positioning, assembly and elongation (Carminati and Stearns, 1997; Heald et al., 1997; Li et al., 1993; Saunders et al., 1995; Shaw et al., 1997; Vaisberg et al., 1993; Yeh et al., 1995).

The Cin8 and Kip1 proteins are thought to be plus end directed motors that have overlapping roles in pushing the spindle pole bodies apart. *cin8* was isolated as a mutant that exhibited elevated chromosome loss (Hoyt et al., 1990). At 37°C *cin8Δ* mutants arrest in mitosis with duplicated spindle poles but fail to form a bipolar spindle. The defect in *cin8Δ* mutants can be overcome by the

WESTERN



overexpression of the Kip1 protein suggesting that the two motors may have redundant functions during mitosis (Hoyt et al., 1992). Furthermore, *cin8Δ kip1Δ* double mutants are inviable and fail to form a functional bipolar spindle (Hoyt et al., 1992; Roof et al., 1992). Cin8 and Kip1 are required for both the assembly and the maintenance of the bipolar spindle. Bipolar spindles in *kip1Δ* cells that carry a temperature sensitive allele of *cin8* collapse when cells are shifted to the nonpermissive temperature. Spindle collapse is partially rescued in cells lacking Kar3, suggesting that Cin8 and Kip1 push the spindle pole bodies apart during mitosis and that forces generated by Kar3 balances this outward force to maintain a constant spindle length during metaphase (Saunders and Hoyt, 1992).

Kip3 plays a role in the migration of the nucleus to the neck between the mother and daughter cells and the proper alignment of the mitotic spindle prior to anaphase (Cottingham and Hoyt, 1997; DeZwaan et al., 1997). One explanation for the defects in *kip3Δ* cells is that Kip3, like certain other motors (Endow et al., 1994; Walczak et al., 1996), can destabilize microtubules.

Since the spindle is a dynamic structure, we investigated its behavior by time lapse microscopy of wild type and mutant cells whose centromeres and microtubules were marked with GFP. Kip1 and Cin8 have distinct roles during anaphase chromosome separation and spindle elongation. Although both motors are required for normal elongation of the spindle, Cin8 is most important early in anaphase when rapid separation of the chromosomes occurs, and Kip1 is required late in anaphase for robust elongation of the spindle. Analysis of Kip3 mutants shows that Kip3 does not play a role in the absolute rates of anaphase spindle elongation but is involved in the proper timing of spindle disassembly. Thus, despite the functional overlap between them, each of the three kinesin motors is responsible for a particular event during anaphase.

UAT
UN

Results

Positioning, assembly and elongation of the yeast spindle during mitosis requires microtubule motor proteins. Anaphase has two components: anaphase A, the movement of the chromosomes towards the spindle poles and anaphase B, the separation of the poles from each other. In budding yeast, anaphase B has two phases a rapid initial elongation of the spindle that is followed by a period of slower elongation (Kahana et al., 1995; Straight et al., 1997; Yeh et al., 1995). In order to study the individual contributions of motor proteins to the process of spindle elongation and mitotic chromosome separation, we performed time lapse video microscopy on yeast cells individually deleted in three kinesin motors, Cin8, Kip1 or Kip3. We visualized the mitotic spindle using a GFP fusion to the major α -Tubulin (*TUB1*) and the centromere using a GFP-Lac repressor fusion bound to a tandem array of Lac operators integrated near the centromere of chromosome III (Straight et al., 1997). We measured the separation between the ends of the spindle and between the sister centromeres as cells went from metaphase to anaphase. These distances allow us to quantitate anaphase A chromosome to pole movement and the increase in the separation between the poles during anaphase B.

Cin8 regulates the rapid phase of mitotic spindle elongation.

Cells lacking Cin8 were recorded as they progressed through mitosis and the distance between the ends of the mitotic spindle and the distance between the centromeres were calculated over time (Figure 1A, B). During metaphase, *cin8* Δ cells had shorter spindles (1-1.5 μm) than wild type cells (1.5-2 μm) (Figure 1A, Figure 4). The suggestion that Cin8 is required for the full separation of the

spindle pole bodies during metaphase is consistent with the role for Cin8 in spindle assembly described by Saunders and Hoyt (Saunders and Hoyt, 1992)

As *cin8Δ* cells proceeded through anaphase, a defect in the rapid phase of spindle elongation became apparent. In wild type cells an initial rapid separation of the spindle pole bodies ($0.54\mu\text{m}/\text{min}$) was followed by a slower phase ($0.21\mu\text{m}/\text{min}$) (Table II) (Straight et al., 1997). *cin8Δ* cells showed a uniformly slow spindle elongation whose rate ($0.19\mu\text{m}/\text{min}$) was similar to the slow phase of anaphase B in wild type cells (Table II, Figure 1A). This defect in early anaphase suggests that Cin8 has a specific role during anaphase B in the initial separation of the spindle pole bodies but that other activities drive the slower phase of mitotic spindle elongation. The rapid initial separation of the centromeres in wild type cells was not affected in the *cin8Δ* mutant (Figure 1B) suggesting that other factors are responsible for the initial separation. These could include the activity of other motors or the release of tension as a result of dissolving the linkage between the sister chromatids.

Although, *cin8Δ* cells are defective for the rapid phase of anaphase B, the long slow phase of anaphase allows them to complete mitosis relatively normally. *cin8Δ* spindles break down at the same time after anaphase initiation as do wild type cells (Table II, Figure 2) but with a shorter length ($7.0 \pm 0.7\mu\text{m}$) than that of wild type cells ($9.5 \pm 0.5\mu\text{m}$). About $1.8\mu\text{m}$ of this difference can be accounted for by the slower elongation of *cin8Δ* spindles during the 5 minutes when wild type cells are elongating their spindle rapidly ($(0.55\mu\text{m}/\text{min}(\text{WT}) - 0.2\mu\text{m}/\text{min}(\text{cin8}\Delta)) \times 5\text{min} = 1.8\mu\text{m}$). The breakdown of the *cin8Δ* spindle at the same time as a wild type spindle suggests that spindle disassembly is in part controlled by the time since the onset of anaphase.

Kip1 regulates the slow phase of mitotic spindle elongation.

Cin8 and Kip1 have overlapping roles during spindle assembly and elongation (Saunders et al., 1997; Saunders and Hoyt, 1992). We examined *kip1Δ* cells during mitosis to determine whether differences exist between the two motors. Consistent with prior measurements in hydroxyurea arrested cells (Saunders et al., 1997), and like *cin8Δ* cells (1.2 μm), *kip1Δ* cells (1.2 μm) had shorter metaphase spindles than wild type cells (1.8 μm) (Figure 4). This result supports the idea that Cin8 and Kip1 work together to maintain the mitotic spindle at its proper metaphase length (Saunders and Hoyt, 1992). The distances we have measured are slightly larger than the distances measured in hydroxyurea arrested cells for wild type, *cin8Δ* and *kip1Δ* (Saunders et al., 1997). All the measurements of metaphase spindle length before anaphase were made using video records of the 20-30 minutes preceding sister chromatid separation. The differences between hydroxyurea arrested and G2/M cells may reflect a difference between cells arrested by the DNA replication checkpoint and mitotic cells, a difference between cells with unreplicated centromeres and replicated centromeres, or differences between measurements made on live and fixed samples.

Once anaphase began, a clear difference between *kip1Δ* and *cin8Δ* cells became apparent. In contrast to *cin8Δ* cells, whose spindles elongate slowly, *kip1Δ* cells exhibited a normal rapid elongation phase (0.51μm/min) (Figure 3A, Table II). However, once cells switched to the slow phase of spindle elongation, the *kip1Δ* cells showed a marked defect in the rate of elongation (0.12 μm/min) compared to that of wild type spindles (0.2μm/min, Figure 3A, Table II). This suggests that even though Kip1 and Cin8 both elongate the spindle, the two motors have distinct roles in anaphase B. Cin8 is required for rapid elongation at

the beginning of mitosis and Kip1 contributes to the slower completion phase of spindle elongation.

The period from the onset of anaphase to spindle breakdown was about 15 minutes longer in *kip1Δ* cells than it was in wild type or *cin8Δ* cells. The longer duration of anaphase compensated for the slower rate of spindle elongation with the result that *kip1Δ* cells elongated their spindles to the same length as wild type cells (9.5-10μm, Figure 3A, Figure 6, Table II). This difference suggests that Kip1 is involved in the timing of spindle breakdown. We cannot determine whether the absence of Kip1 slows the cell's progress through the cell cycle or slows the spindle's response to the cell cycle changes that lead to its dissolution. The failure of *cin8Δ* mutants to delay spindle breakdown suggests that defects in the rate of spindle elongation do not directly affect progress through the cell cycle. We have previously shown that anaphase A (chromosome to pole movement) occurs in budding yeast (Straight et al., 1997). The shorter metaphase spindle in *cin8Δ* and *kip1Δ* cells makes it impossible to directly determine the rate or extent of anaphase A.

Kip3 regulates microtubule length and spindle breakdown in mitosis.

Deletion of *KIP3* increases the metaphase spindle length compared to wild type cells. Spindles in *kip3Δ* cells were on average 0.4μm longer than those in wild type cells (Figure 5A, Figure 4, Table II). This increase is similar to that seen in the comparison between fixed *kip3Δ* and wild type cells arrested in S phase by treatment with hydroxyurea (Cottingham and Hoyt, 1997). Unlike Cin8 and Kip1, Kip3 opposes extension of the metaphase spindle, either by exerting an inward directed force on the spindle pole bodies or by reducing the length of spindle microtubules. One characteristic of *kip3Δ* cells is that astral microtubules

UNIVERSITY OF TORONTO

increase in length and that these cells are resistant to spindle depolymerization with the drug benomyl (Cottingham and Hoyt, 1997; DeZwaan et al., 1997). Thus, Kip3 may regulate the length of the mitotic spindle by destabilizing the central spindle microtubules.

Examination of *kip3Δ* cells during anaphase revealed a specific role for Kip3 in the regulation of spindle breakdown. Initial anaphase spindle elongation occurred normally in *kip3Δ* cells, consistent with measurements of spindle pole separation in fixed samples of *kip3Δ* cells (DeZwaan et al., 1997). *kip3Δ* cells elongated their spindles during the early rapid phase at a rate of $0.56\mu\text{m}/\text{min}$ compared to the wild type rate of $0.54\mu\text{m}/\text{min}$ (Figure 5A, Table II). The slow phase of spindle elongation in *kip3Δ* cells ($0.17\mu\text{m}/\text{min}$) was also similar to that of wild type rates ($0.21\mu\text{m}/\text{min}$) (Figure 5A, Table II). Although the rates of spindle elongation in wild type and *kip3Δ* are similar, *kip3Δ* cells broke down their spindles 12 minutes later than wild type cells (Figure 2, Table II). This observation contrasts with measurements on populations of *kip3Δ* cells, that showed that the distance between the spindle pole bodies stopped increasing at the same time wild type and *kar3Δ* cells (DeZwaan et al., 1997). However, in all but one of our video records ($n=7$), spindles persisted in *kip3Δ* cells after the time at which the spindle in wild type cells broke down. This difference is probably explained by the fact that previous measurements were made using a fluorescent spindle pole body marker. Although the distance between the spindle pole bodies in *kip3Δ* cells stopped increasing, the spindle may still have been intact in those cells and was simply not seen.

Cells lacking Kip3 elongate their spindles beyond the length of wild type cells. Although the pole to pole distance in *kip3Δ* stops increasing at around $10\mu\text{m}$ (Figure 5A), the spindles keep elongating, making them bend prior to the breakdown of the spindle (Figure 5D). Thus the spindles in *kip3Δ* cells continue

to elongate and are merely constrained by the physical dimensions of the cell. To confirm this interpretation we measured the length of the bent *kip3Δ* spindles in 3-dimensional space. Although the spindle pole bodies were only separated by 10 μm, the actual spindle length increased to more than 12 μm (Figure 5C, Figure 6, Table II). Kip3 may therefore be involved in destabilizing microtubules at the end of mitosis so that the spindle can disassemble at the proper time and at the proper length. Bowed spindles have also been observed in wild type fission yeast, although in this organism the spindle poles do not have to reach the ends of the cell for bending to occur (Hagan and Hyams, 1996).

Motor mutants delay the onset of anaphase

We investigated the effect of motor mutants on the interval between spindle assembly and the onset of anaphase. Wild type, *cin8Δ*, *kip1Δ*, and *kip3Δ* mutants that contained GFP-marked tubulin and CENIII were arrested in G1 by treatment with the yeast mating pheromone α -factor. The cells were released from this arrest and population samples were removed at intervals and scored for spindle elongation and sister chromatid separation. Cells deleted for Kip1 or Kip3 initiated anaphase at the same time as wild type cells and progressed through anaphase with similar kinetics (Figure 7). Cells lacking Cin8 showed a dramatic delay in the progression through anaphase. Ninety minutes after release from α -factor, greater than thirty percent of wild type, *kip1Δ* and *kip3Δ* cells had initiated anaphase compared to only four percent of *cin8Δ* cells. When more than eighty percent of wild type, *kip1Δ* and *kip3Δ* cells had initiated anaphase (t = 120), less than 25 percent of *cin8Δ* cells had separated their sister chromatids (Figure 7). We have also observed delays in the entry into mitosis in cells lacking the Kar3 motor protein (data not shown). The prolonged metaphase

of motor mutants is probably due to the action of the spindle checkpoint (Nicklas, 1997; Rudner and Murray, 1996), which delays anaphase until all chromosomes are correctly aligned on a bipolar spindle. Inactivation of the checkpoint allows cells with spindle defects to exit from mitosis and kills *kar3Δ* and *cin8Δ* mutants, which have the most profound delays in mitosis (Geiser et al., 1997; Roof et al., 1991).

WUOT LIBRARY

Discussion

We performed video microscopy on microtubule motor mutants whose microtubules and a centromere had been marked with GFP. Our analysis reveals that each motor mutant has distinct defects in the rates and timing of anaphase spindle elongation.

Motor proteins in yeast are involved assembly, positioning, and elongation of the mitotic spindle. We have investigated the roles of three motor proteins in the elongation of the mitotic spindle during anaphase. Two of these motors, Cin8 and Kip1 belong to the bimC class of microtubule motors that have been demonstrated to have roles in spindle formation and spindle elongation in other organisms (Kashina et al., 1997). The third motor, Kip3, is a novel kinesin that does not easily fit into the known kinesin subfamilies but has been shown to be important for spindle positioning (Cottingham and Hoyt, 1997; DeZwaan et al., 1997). Multiple other microtubule motor proteins have been shown to be involved in spindle positioning, assembly and elongation. The minus end directed motor Kar3 antagonizes the activity of Cin8/Kip1 to ensure proper spindle assembly and elongation (Saunders and Hoyt, 1992) and is also thought to participate in the positioning of the spindle (Cottingham and Hoyt, 1997; DeZwaan et al., 1997). In addition to the kinesin family of proteins, dynein has also been shown to have a roles in spindle positioning, assembly and elongation (Carminati and Stearns, 1997; Heald et al., 1997; Li et al., 1993; Saunders et al., 1995; Shaw et al., 1997; Vaisberg et al., 1993; Yeh et al., 1995).

Separate roles for motors during anaphase.

Our results show that Cin8 and Kip1 have distinct roles during anaphase. Previous studies have demonstrated that Cin8 and Kip1 have partially

UNIVERSITY OF TORONTO

redundant roles in exerting an outwardly directed force on the spindle pole bodies (Hoyt et al., 1992; Hoyt et al., 1993; Roof et al., 1992; Saunders et al., 1997; Saunders and Hoyt, 1992). We have shown that Cin8 functions early in the separation of the spindle pole bodies and is required for the proper execution of the rapid phase of anaphase spindle elongation. Unlike Cin8, Kip1 plays no role in controlling the rapid phase of spindle elongation. Cells deleted for Kip1 perform the initial phase of anaphase normally but are then compromised in their ability to execute the slower phase of spindle elongation.

The difference between the rates of the two phases of anaphase B in wild type cells could be explained in many ways. One is that the rate of the rapid phase is set by the rate at which motors slide the microtubules from opposite poles of the spindle past each other and that of the slow phase is set by the rate of the microtubule growth required to maintain an overlap zone as the spindle extends. In the rapid phase, Cin8 would move microtubules past each other more rapidly than Kip1, whereas in the slow phase the absence of Kip1, but not that of Cin8, would affect the rate at which the length of microtubules increased. Cut7, a fission yeast homolog of Cin8 and Kip1, localizes to the mid zone of the spindle during anaphase B (Hagan and Yanagida, 1992). Another possibility is that both rates are set by the speed of microtubule sliding and that Cin8 is a faster motor that is only active during early anaphase, whereas Kip1 is active throughout anaphase.

Cells lacking Kip3 delay spindle breakdown and their final spindles are so long that they are physically deformed when they run into the ends of the cell. Previous studies suggest that Kip3 may regulate the stability of microtubules (Cottingham and Hoyt, 1997). In our experiments, metaphase *kip3* Δ spindles were longer than those of wild type cells in agreement with spindle length measurements in hydroxyurea arrested cells (Cottingham and Hoyt, 1997). Once

UNIVERSITY OF TORONTO

anaphase began, the *kip3Δ* cells behaved exactly like wild type cells until the time of spindle breakdown: when wild type spindles broke down, *kip3Δ* spindles remained intact and continued to elongate. The ability of the spindle to elongate beyond the cell length has implications for the mechanism of spindle elongation. The final buckling of the spindle in *kip3Δ* means that some or all of the force elongating the spindle must be generated within the spindle, pushing the poles apart. If all of the forces were due to pulling force generated by interactions of astral microtubules with the cortex at the ends of the cell, the length of the spindle could not exceed that of the cell. In experiments in *Nectria haematococca* and in rat kangaroo kidney epithelial cells (PtK2 cells), severing the central spindle during anaphase increased the rate of spindle pole separation arguing that interactions in the central spindle were limiting the rate of spindle elongation (Aist et al., 1991; Aist et al., 1993). We do not know if this apparent discrepancy is due to different factors regulating the extent versus the speed of anaphase, or differences between the mechanism of spindle elongation in different organisms.

Regulation of spindle elongation.

In most organisms, the position of the metaphase spindle dictates the plane of cell division (Rappaport, 1996), ensuring that each daughter cell ends up with one set of chromosomes. In budding yeast, cell division occurs at the neck that separates mother and bud and this site is defined prior to spindle formation. As a result, cells must ensure that the anaphase spindle passes through the neck so that the mother receives one set of chromosomes and the bud the other. Studies of dynein mutants reveal a mechanism to achieve this: the anaphase

spindle does not break down until one of its poles and the associated set of chromosomes has entered the bud (Yeh et al., 1995).

Our analysis of kinesin mutants suggests that the regulation of spindle breakdown is complex. Compared to wild type cells, the spindles of *cin8Δ* break down at the same time after the onset of anaphase and at shorter final lengths, those of *kip1Δ* break down later but at the same final length those of *kip3Δ* cells break down later and at a greater final length. A simple interpretation of these results is that the timing of spindle breakdown is influenced both by the state of the cell cycle machinery and also by the effects of microtubule motors on microtubule dynamics.

We suggest that late in anaphase, some change in the cell cycle destabilizes nuclear microtubules leading to spindle breakdown. Possible changes include the inactivation of Cdc28 and the APC-mediated destruction of Ase1. Ase1 has been shown to regulate spindle breakdown: Ase1 localizes to the spindle midzone, *ase1Δ* mutants have unstable spindles in late anaphase, and indestructible Ase1 results in a delay in spindle breakdown producing a phenotype similar to *kip3Δ* (Juang et al., 1997; Pellman et al., 1995). In *cin8Δ* mutants, the cell cycle-induced destabilization would occur normally so that spindles broke down at the same time as they did in wild type. In contrast, Kip1 and Kip3 would be among the activities that were regulated in order to induce the microtubule depolymerization that destroys the spindle. In the absence of either of these activities, although the change in the cell cycle machinery would occur normally, it would take longer for this change to induce spindle breakdown. The difference in the final lengths of the *kip1Δ* and *kip3Δ* spindles would simply reflect the different rates of spindle elongation in these mutants. The increased length of astral microtubules in *kip3Δ* cells suggests that this motor does control microtubule dynamics. Experiments in isolated diatom

spindles suggest that the rate of spindle elongation is strongly influenced by factors that control the speed at which microtubules grow (Masuda and Cande, 1987).

It is likely that the fidelity of anaphase results from the regulation of multiple independent properties including cell cycle timing of spindle elongation, absolute spindle length, spindle microtubule dynamics, and motor protein activity. Determining how these properties are built into the chemistry of motor proteins and how they are regulated by the cell should be informative in understanding the regulation of anaphase.

Genetic Redundancy and Functional Overlap

The distinct phenotypes of *cin8Δ* and *kip1Δ* cells have important implications for the concepts of genetic redundancy and functional overlap between related genes. Groups of two or more genes are said to be redundant if deletion of a single member of the family produces little or no phenotype, but deletion of all members of the group is lethal. *KIP1* and *CIN8* are partially redundant since *kip1Δ* mutants have very mild phenotypes and mild overexpression of Kip1 suppresses the phenotype of *cin8Δ* (Hoyt et al., 1992). One interpretation of these observations is that the two motors perform essentially identical functions and differ only in their level of expression. If this were so, the phenotypes of *kip1Δ* and *cin8Δ* might differ quantitatively but not qualitatively. The observations that two mutants have distinct effects on different aspects of anaphase strongly argues that although the functions of the two motors overlap, they are clearly specialized for different roles. We believe that "genetic redundancy" is an artifact of studying the behavior of cells under a very limited set of conditions and using crude criteria like easily detectable

UNIVERSITY OF TORONTO

differences in overall growth rate to assess the phenotypes of mutants. As mutant phenotypes are investigated in more detail, we suspect that deleting individual members of gene families will produce phenotypes that have aspects that are clearly distinct from those of knocking out other genes within the same family.

The phenotypes of motor mutants highlight the distinction between minimal and full systems for performing complex cellular tasks like chromosome segregation. A minimal system is one that suffices to perform the task at a level that allows cells to reproduce indefinitely under optimal conditions. Cells lacking up to three motor proteins can function at this level. A full system is one that performs a task with high fidelity in the face of environmental, physiological, and genetic perturbations. For mitosis one criterion of the full system is a very low rate of errors in chromosome segregation. Lack of Cin8 disrupts the full system, since *cin8* mutants were first found because they lead to errors in chromosome segregation. A more general criterion for including a function in the full system is that loss of the function makes cells more susceptible to genetic perturbations. Mutations in any one of the mitotic motors (Cin8, Kip1, Kip3, Kar3, and dynein) make at least one of the remaining mitotic motors essential for cell proliferation (Cottingham and Hoyt, 1997; DeZwaan et al., 1997; Hoyt et al., 1992; Roof et al., 1992). Detailed analysis of the requirements for mitosis in budding yeast and other organisms should illuminate how minimal systems for chromosome segregation arose and were then evolved into the highly efficient and regulated machines found today.

UNIVERSITY OF CALIFORNIA

Experimental Procedures

Strains and Media

Yeast were grown either in YPD (10g/l yeast extract, 20g/l Bacto-Peptide, 20g/l Dextrose) supplemented with 50µg/l adenine-HCl and 50µg/l l-tryptophan or in complete synthetic medium lacking histidine (CSM-HIS) (Sherman et al., 1974) supplemented with 50µg/l adenine-HCl, 50µg/l l-tryptophan and 6.5g/l NaCitrate. Yeast strains are listed in Table I and are all isogenic to W303 (AFS34). Yeast transformations were performed using the lithium acetate method (Ito et al., 1983). Plasmids were propagated in E. coli strain TG1 (Sambrook et al., 1989) in medium containing 100µg/ml ampicillin except for Lac operator repeat plasmids which were propagated in E. coli STBL2 (Gibco/BRL). GFP-Lac repressor and GFP-Tubulin fusions were induced as described (Straight et al., 1996; Straight et al., 1997).

Plasmids and DNA manipulation

Construction of Motor Protein Deletions

The *cin8Δ::LEU2* deletion plasmid was provided by Andrew Hoyt (Hoyt et al., 1992). Cin8 was deleted in strain AFS34, then the *LEU2* marked Cin8 deletion was changed to *TRP1* by integrating the marker switching plasmid pLT7 from F. Cross (Cross, 1997).

Kip1 was amplified from yeast genomic DNA by PCR using the following oligonucleotide pair:

5'-GCTTGGTCGACGTCAAATGCAGACGGATACGAG-3'

5'-GCCAATTCGTATGGTGCTGCGGCCGTC AAC-3'

The PCR product was digested with Sall and EagI and cloned into Sall and EagI digested pBluescript (KS-) (Stratagene) to yield pAFS108. The complete open reading frame of *KIP1* was replaced by inserting an EcoRI-SphI fragment of *HIS3* into EcoRI-SphI digested pAFS108. The resulting deletion construct pAFS111 was digested with NotI and AatII and transformed into yeast strain AFS34.

Kip3 was amplified from yeast genomic DNA by PCR using the following oligonucleotide pair:

5'-GCGCTCGAGAACTGAACGTCATAGTTATAG-3'

5'-ACGTTATTCCTCCTCCTGTTCGCGGCCGCGCGC-3'

The PCR product was digested with XhoI and NotI and cloned into XhoI and NotI digested pBluescript (KS-) (Stratagene) to yield pAFS119. The NheI-HincII fragment of pAFS119 was replaced with an XbaI-SmaI fragment of *HIS3* to remove the open reading frame of *KIP3*. The deletion plasmid pAFS124 was then cut with EcoRV and NotI and transformed into yeast strain AFS34.

Mutagenesis of GFP-LacI fusions

GFP was fused to the Lac repressor as previously described (Straight et al., 1996).

The Ser65->Thr mutant of GFP (Heim and Tsien, 1996) was linked with XhoI and HindIII sites by PCR using the following oligonucleotide pair:

5'-CGCCTCGAGGAGATGAGTAAAGGAGAAGA ACTT-3'

5'-GGCATGGATGAACTATACAAATAAGCTTCGC-3'.

The XhoI-HindIII digested PCR product was cloned into SalI-HindIII digested pQE9 (Qiagen) to generate a 6-histidine fusion to GFP (pAFS97). Mutant GFP molecules were generated by PCR shuffling (Stemmer, 1994), expressed in *E. coli* at 37°C then sorted by Fluorescence Activated Cell Sorting to isolate cells that fluoresced strongly at 37°C. These mutant GFP molecules were then screened for fluorescence intensity relative to the Ser65->Thr mutant of GFP and the brightest molecule was sequenced. The brightest GFP (GFP12) was mutated at codon 163 from GTT to GCT changing Val163 to Ala163. This change resulted in the same amino acid change described by Siemering et. al. for the GFP-B mutant (Siemering et al., 1996) but utilized a different codon. Based on the work of Siemering et. al we then combined our GFP12 mutant with the Ser175->Gly mutation to give GFP13 (S65T, V163A, and S175G).

Certain mutations in the lac repressor cause increased affinity between the repressor and operator DNA (Miller and Reznikoff, 1980). We mutated the GFP-lac repressor fusion contained in pAFS78 from Pro3->Tyr3 to give the *lacI-I12* mutation (Schmitz et al., 1978). This Lac repressor mutant was then fused to the GFP12 and GFP13 sequences exactly as described for pAFS78 to give pAFS135 and pAFS144 respectively. Plasmids pAFS135 and pAFS144 were linearized with NheI and transformed into yeast strain AFS34 for expression of GFP-LacI fusions in yeast. Lac operators were introduced at the centromere of chromosome III as previously described using pAFS59 (Straight et al., 1996). GFP-Tubulin was expressed by integration of pAFS91 as previously described (Straight et al., 1997).

Time Lapse Microscopy and Image Analysis

Images were acquired as described (Straight et al., 1997) except that the actual length of spindles in *kip3Δ* cells was calculated by tracing fluorescence intensities

in three dimensional image stacks using the program 3D Model that had been customized for length measurement (Chen et al., 1996). The data for wild type spindle elongation is previously published (Straight et al., 1997) and used only for comparison to the motor mutant data.

UNIVERSITY OF TORONTO

References

Aist, J. R., Bayles, C. J., Tao, W. and Berns, M. W. (1991). Direct experimental evidence for the existence, structural basis and function of astral forces during anaphase B in vivo. *J Cell Sci* 100, 279-88.

Aist, J. R., Liang, H. and Berns, M. W. (1993). Astral and spindle forces in PtK2 cells during anaphase B: a laser microbeam study. *J Cell Sci* 104, 1207-16.

Carminati, J. L. and Stearns, T. (1997). Microtubules orient the mitotic spindle in yeast through dynein-dependent interactions with the cell cortex. *J Cell Biol* 138, 629-41.

Chen, H., Hughes, D. D., Chan, T. A., Sedat, J. W. and Agard, D. A. (1996). IVE (Image Visualization Environment): a software platform for all three-dimensional microscopy applications. *J Struct Biol* 116, 56-60.

Cottingham, F. R. and Hoyt, M. A. (1997). Mitotic spindle positioning in *Saccharomyces cerevisiae* is accomplished by antagonistically acting microtubule motor proteins. *J Cell Biol* 138, 1041-53.

Cross, F. R. (1997). 'Marker swap' plasmids: convenient tools for budding yeast molecular genetics. *Yeast* 13, 647-53.

UNIVERSITY OF TORONTO

DeZwaan, T. M., Ellingson, E., Pellman, D. and Roof, D. M. (1997). Kinesin-related KIP3 of *Saccharomyces cerevisiae* is required for a distinct step in nuclear migration. *J Cell Biol* 138, 1023-40.

Endow, S. A., Kang, S. J., Satterwhite, L. L., Rose, M. D., Skeen, V. P. and Salmon, E. D. (1994). Yeast Kar3 is a minus-end microtubule motor protein that destabilizes microtubules preferentially at the minus ends. *Embo J* 13, 2708-13.

Eshel, D., Urrestarazu, L. A., Vissers, S., Jauniaux, J. C., van Vliet-Reedijk, J. C., Planta, R. J. and Gibbons, I. R. (1993). Cytoplasmic dynein is required for normal nuclear segregation in yeast. *Proc Natl Acad Sci U S A* 90, 11172-6.

Geiser, J. R., Schott, E. J., Kingsbury, T. J., Cole, N. B., Totis, L. J., Bhattacharyya, G., He, L. and Hoyt, M. A. (1997). *Saccharomyces cerevisiae* genes required in the absence of the CIN8-encoded spindle motor act in functionally diverse mitotic pathways. *Mol Biol Cell* 8, 1035-50.

Goffeau, A., Barrell, B. G., Bussey, H., Davis, R. W., Dujon, B., Feldmann, H., Galibert, F., Hoheisel, J. D., Jacq, C., Johnston, M., Louis, E. J., Mewes, H. W., Murakami, Y., Philippsen, P., Tettelin, H. and Oliver, S. G. (1996). Life with 6000 genes. *Science* 274, 546, 563-7.

Hagan, I. and Yanagida, M. (1992). Kinesin-related cut7 protein associates with mitotic and meiotic spindles in fission yeast. *Nature* 356, 74-6.

Hagan, I. M. and Hyams, J. S. (1996). Forces acting on the fission yeast anaphase spindle. *Cell Motil Cytoskeleton* 34, 69-75.

Heald, R., Tournebise, R., Habermann, A., Karsenti, E. and Hyman, A. (1997). Spindle assembly in *Xenopus* egg extracts: respective roles of centrosomes and microtubule self-organization. *J Cell Biol* 138, 615-28.

Heim, R. and Tsien, R. Y. (1996). Engineering green fluorescent protein for improved brightness, longer wavelengths and fluorescence resonance energy transfer. *Curr Biol* 6, 178-82.

Hoyt, M. A., He, L., Loo, K. K. and Saunders, W. S. (1992). Two *Saccharomyces cerevisiae* kinesin-related gene products required for mitotic spindle assembly. *J. Cell Biol.* 118, 109-120.

Hoyt, M. A., He, L., Totis, L. and Saunders, W. S. (1993). Loss of function of *Saccharomyces cerevisiae* kinesin-related CIN8 and KIP1 is suppressed by KAR3 motor domain mutations. *Genetics* 135, 35-44.

Hoyt, M. A., Stearns, T. and Botstein, D. (1990). Chromosome instability mutants of *Saccharomyces cerevisiae* that are defective in microtubule-mediated processes. *Mol Cell Biol* 10, 223-34.

Inoue, S. and Salmon, E. D. (1995). Force generation by microtubule assembly/disassembly in mitosis and related movements. *Mol Biol Cell* 6, 1619-40.

Ito, H., Fukuda, Y., Murata, K. and Kimura, A. (1983). Transformation of Intact Yeast Cells Treated with Alkali Cations. *J Bacteriol* 153, 163-168.

Juang, Y. L., Huang, J., Peters, J. M., McLaughlin, M. E., Tai, C. Y. and Pellman, D. (1997). APC-mediated proteolysis of Ase1 and the morphogenesis of the mitotic spindle. *Science* 275, 1311-4.

Kahana, J. A., Schnapp, B. J. and Silver, P. A. (1995). Kinetics of spindle pole body separation in budding yeast. *Proc Natl Acad Sci U S A* 92, 9707-11.

Kashina, A. S., Rogers, G. C. and Scholey, J. M. (1997). The bimC family of kinesins: essential bipolar mitotic motors driving centrosome separation. *Biochim Biophys Acta* 1357, 257-71.

Li, Y. Y., Yeh, E., Hays, T. and Bloom, K. (1993). Disruption of mitotic spindle orientation in a yeast dynein mutant. *Proc Natl Acad Sci U S A* 90, 10096-100.

Lillie, S. H. and Brown, S. S. (1992). Suppression of a myosin defect by a kinesin-related gene. *Nature* 356, 358-61.

Lillie, S. H. and Brown, S. S. (1994). Immunofluorescence localization of the unconventional myosin, Myo2p, and the putative kinesin-related protein, Smy1p, to the same regions of polarized growth in *Saccharomyces cerevisiae*. *J Cell Biol* 125, 825-42.

Lombillo, V. A., Nislow, C., Yen, T. J., Gelfand, V. I. and McIntosh, J. R. (1995). Antibodies to the kinesin motor domain and CENP-E inhibit microtubule depolymerization-dependent motion of chromosomes in vitro. *J Cell Biol* 128, 107-15.

Masuda, H. and Cande, W. Z. (1987). The role of tubulin polymerization during spindle elongation in vitro. *Cell* 49, 193-202.

McIntosh, J. R. and Pfarr, C. M. (1991). Mitotic Motors. *115*, 577-585.

Meluh, P. B. and Rose, M. D. (1990). *KAR3*, a kinesin-related gene required for yeast nuclear fusion. *Cell* 60, 1029-1041.

Miller, J. H. and Reznikoff, W. S. (1980). The Operon. Cold Spring Harbor. Cold Spring Harbor Laboratory

Miller, R. K. and Rose, M. D. (1998). Kar9p is a novel cortical protein required for cytoplasmic microtubule orientation in yeast. *J. Cell Biol.* 140,

Nicklas, R. B. (1997). How cells get the right chromosomes. *Science* 275, 632-7.

Pellman, D., Bagget, M., Tu, Y. H., Fink, G. R. and Tu, H. (1995). Two microtubule-associated proteins required for anaphase spindle movement in *Saccharomyces cerevisiae*. *J Cell Biol* 130, 1373-85.

Rappaport, R. (1996). Cytokinesis in animal cells. New York, NY. Cambridge University Press

Rodionov, V. I., Gyoeva, F. K., Tanaka, E., Bershinsky, A. D., Vasiliev, J. M. and Gelfand, V. I. (1993). Microtubule-dependent control of cell shape and

pseudopodial activity is inhibited by the antibody to kinesin motor domain. *J Cell Biol* 123, 1811-20.

Roof, D. M., Meluh, P. B. and Rose, M. D. (1991). Multiple kinesin-related proteins in yeast mitosis. *Cold Spring Harb Symp Quant Biol* 56, 693-703.

Roof, D. M., Meluh, P. B. and Rose, M. D. (1992). Kinesin-related proteins required for assembly of the mitotic spindle. *J. Cell Biol.* 118, 95-108.

Rudner, A. D. and Murray, A. W. (1996). The spindle assembly checkpoint. *Curr Opin Cell Biol* 8, 773-80.

Sambrook, J., Fritsch, E. F. and Maniatis, T. (1989). *Molecular cloning : a laboratory manual*. Cold Spring Harbor, NY. Cold Spring Harbor Laboratory

Saunders, W., Lengyel, V. and Hoyt, M. A. (1997). Mitotic spindle function in *Saccharomyces cerevisiae* requires a balance between different types of kinesin-related motors. *Mol Biol Cell* 8, 1025-33.

Saunders, W. S. and Hoyt, M. A. (1992). Kinesin-related proteins required for structural integrity of the mitotic spindle. *Cell* 70, 451-8.

Saunders, W. S., Koshland, D., Eshel, D., Gibbons, I. R. and Hoyt, M. A. (1995). *Saccharomyces cerevisiae* kinesin- and dynein-related proteins required for anaphase chromosome segregation. *J Cell Biol* 128, 617-24.

Schmitz, A., Coulondre, C. and Miller, J. H. (1978). Genetic studies of the lac repressor. V. Repressors which bind operator more tightly generated by suppression and reversion of nonsense mutations. *J Mol Biol* 123, 431-54.

Shaw, S. L., Yeh, E., Maddox, P., Salmon, E. D. and Bloom, K. (1997). Astral microtubule dynamics in yeast: a microtubule-based searching mechanism for spindle orientation and nuclear migration into the bud. *J. Cell Biol.* 139, 985-994.

Sherman, F., Fink, G. and Lawrence, C. (1974). *Methods in Yeast Genetics*. Cold Spring Harbor, New York. Cold Spring Harbor Laboratory Press

Siemering, K. R., Golbik, R., Sever, R. and Haseloff, J. (1996). Mutations that suppress the thermosensitivity of green fluorescent protein. *Curr Biol* 6, 1653-63.

Stemmer, W. P. (1994). Rapid evolution of a protein in vitro by DNA shuffling. *Nature* 370, 389-91.

Straight, A. F., Belmont, A. S., Robinett, C. C. and Murray, A. W. (1996). GFP tagging of budding yeast chromosomes reveals that protein-protein interactions can mediate sister chromatid cohesion. *Curr Biol* 6, 1599-608.

Straight, A. F., Marshall, W. F., Sedat, J. W. and Murray, A. W. (1997). Mitosis in living budding yeast: anaphase A but no metaphase plate. *Science* 277, 574-8.

Vaisberg, E. A., Koonce, M. P. and McIntosh, J. R. (1993). Cytoplasmic dynein plays a role in mammalian mitotic spindle formation. *J Cell Biol* 123, 849-58.

Vernos, I. and Karsenti, E. (1996). Motors involved in spindle assembly and chromosome segregation. *Curr. Opin. Cell Biol.* 8, 4-9.

Walczak, C. E., Mitchison, T. J. and Desai, A. (1996). XKCM1: a *Xenopus* kinesin-related protein that regulates microtubule dynamics during mitotic spindle assembly. *Cell* 84, 37-47.

Yeh, E., Skibbens, R. V., Cheng, J. W., Salmon, E. D. and Bloom, K. (1995). Spindle dynamics and cell cycle regulation of dynein in the budding yeast, *Saccharomyces cerevisiae*. *J Cell Biol* 130, 687-700.

UNIVERSITY OF
MICHIGAN

Figure Legends

Table I - Yeast Strains

All strains are isogenic to AFS34 (W303-1a from the laboratory of R. Rothstein). Only the genotype that differs from AFS34 is shown.

Table II - Spindle and chromosome dynamics in wild type cells and kinesin mutants

Rates of spindle elongation were calculated using linear regression analysis in the same time intervals used to calculate the wild type rates for the fast and slow phases of anaphase. All measurements shown in bold are significantly different from wild type rates. The average breakdown length and the average duration of anaphase were calculated using the final timepoint prior to spindle disassembly. The total number of records analyzed for measurements of WT, *cin8Δ*, *kip1Δ*, and *kip3Δ* are n=6, n=5, n=5, and n=7 respectively.

Figure 1 - *cin8Δ* cells are defective in the fast phase of anaphase B

Comparison of spindle elongation and centromere separation in wild type and *cin8Δ* cells. Cells of yeast strain AFS426(*cin8Δ*) were arrested in G1 with α -factor then released from G1 and recorded as they progressed through mitosis. Twelve optical sections at 0.5 μ m intervals were acquired every 26 seconds. The distances between the spindle poles and the distances between the centromeres were measured in 3-dimensional space. (A) Distance between spindle pole

bodies versus time. (B) Distance between centromeres versus time. The time of sister chromatid separation is indicated by $t = 0$.

Figure 2 - Motor mutants affect the duration of anaphase

Duration of anaphase in wild type cells and motor mutants. The average time between the separation of sister chromatids and the breakdown of the spindle was calculated from video records of strains AFS403 (WT), AFS426 (*cin8Δ*), AFS404 (*kip1Δ*) and AFS417 (*kip3Δ*).

Figure 3 - *kip1Δ* cells are defective in the slow phase of anaphase B and prolong anaphase

kip1Δ cells (yeast strain AFS404) were recorded as described in Figure 1. (A) Distance between spindle pole bodies versus time. (B) Distance between centromeres versus time. The time of sister chromatid separation is indicated by $t = 0$.

Figure 4 - Motor mutations alter the length of the metaphase spindle

Metaphase spindle length in wild type cells and motor mutants. The length of the bipolar spindle was measured in the 20-30 minute interval prior to the initiation of anaphase in strains AFS403 (WT), AFS426 (*cin8Δ*), AFS404 (*kip1Δ*) and AFS417 (*kip3Δ*).

Figure 5 - The length of the spindle and the duration of anaphase are regulated by Kip3.

Cells deleted for Kip3 (AFS417) were recorded as described in Figure 1. (A) Distance between spindle pole bodies versus time. (B) Centromere separation versus time. (C) Measurement of actual spindle length in 3-dimensions. Asterisk represents the total length of the spindle as compared to the distance between the spindle pole bodies. (D) Bent spindle at the end of anaphase *inkip3Δ* cell. Twelve 0.5μm axial sections through a *kip3Δ* cell were projected onto two dimensions (left panel), a schematic of the cell is also shown (right panel).

Figure 6 - Motors regulate the final length of the anaphase spindle

Spindle breakdown length in wild type and motor mutants. The final breakdown length of the anaphase spindle was calculated using the timepoint prior to spindle breakdown in strains AFS403 (WT), AFS426 (*cin8Δ*), AFS404 (*kip1Δ*) and AFS417 (*kip3Δ*).

Figure 7 - Motor mutants delay anaphase onset

cin8Δ causes a delay in the entry into anaphase. Strains AFS501 (WT), AFS426 (*cin8Δ*), AFS404 (*kip1Δ*) and AFS417 (*kip3Δ*) were synchronized in G1 by treatment with 10μg/ml α-factor. Cells were released from the block and were assayed for sister chromatid separation at 15 minute intervals as previously described (Straight et al., 1996). The percentage of cells with separated sister chromatids versus time is shown.

UNIVERSITY OF CALIFORNIA

Table I - Yeast Strains

Strain Number	Relevant Genotype	Plasmid
AFS34(W303-1a)	<i>MATa ade2-1 can1-100 ura3-1 leu2-3,112 his3-11,15 trp1-1</i>	pAFS78
AFS403	<i>MATa his3-11,15::GFP-LacI-HIS3 leu2-3,112::lacO-LEU2 ura3-1::GFP-TUB1-URA3</i>	pAFS59 pAFS91
AFS426	<i>MATa cin8Δ::TRP1 his3-11,15::GFP-LacI-HIS3 leu2-3,112::lacO-LEU2 ura3-1::GFP-TUB1-URA3</i>	"
AFS404	<i>MATa kip1Δ::HIS3 his3-11,15::GFP-LacI-HIS3 leu2-3,112::lacO-LEU2 ura3-1::GFP-TUB1-URA3</i>	"
AFS417	<i>MATa kip3Δ::HIS3 his3-11,15::GFP-LacI-HIS3 leu2-3,112::lacO-LEU2 ura3-1::GFP-TUB1-URA3</i>	"
AFS501	<i>MATa his3-11,15::GFP13-LacI-HIS3 leu2-3,112::lacO-LEU2 ura3-1::GFP-TUB1-URA3</i>	pAFS144 pAFS59 pAFS91

Table II Spindle dynamics in wild type and kinesin mutants

	Fast Phase $\mu\text{m}/\text{min}$	Slow Phase $\mu\text{m}/\text{min}$	Breakdown Length μm	Anaphase Duration	AnaphaseA
WT	0.54\pm0.02	0.21\pm0.01	9.52\pm0.49	26.6\pm1.6	1.33$\mu\text{m}/\text{min}$
cin8Δ	0.28\pm0.02	0.19\pm0.02	6.95\pm0.68	26.7\pm2.4	ND
kip1Δ	0.51\pm0.03	0.12\pm0.03	9.79\pm0.43	43.0\pm3.1	ND
kip3Δ	0.56\pm0.04	0.17\pm0.02	12.31\pm0.25	38.5\pm3.1	1.30$\mu\text{m}/\text{min}$

A

cin8 Δ Pole Separation

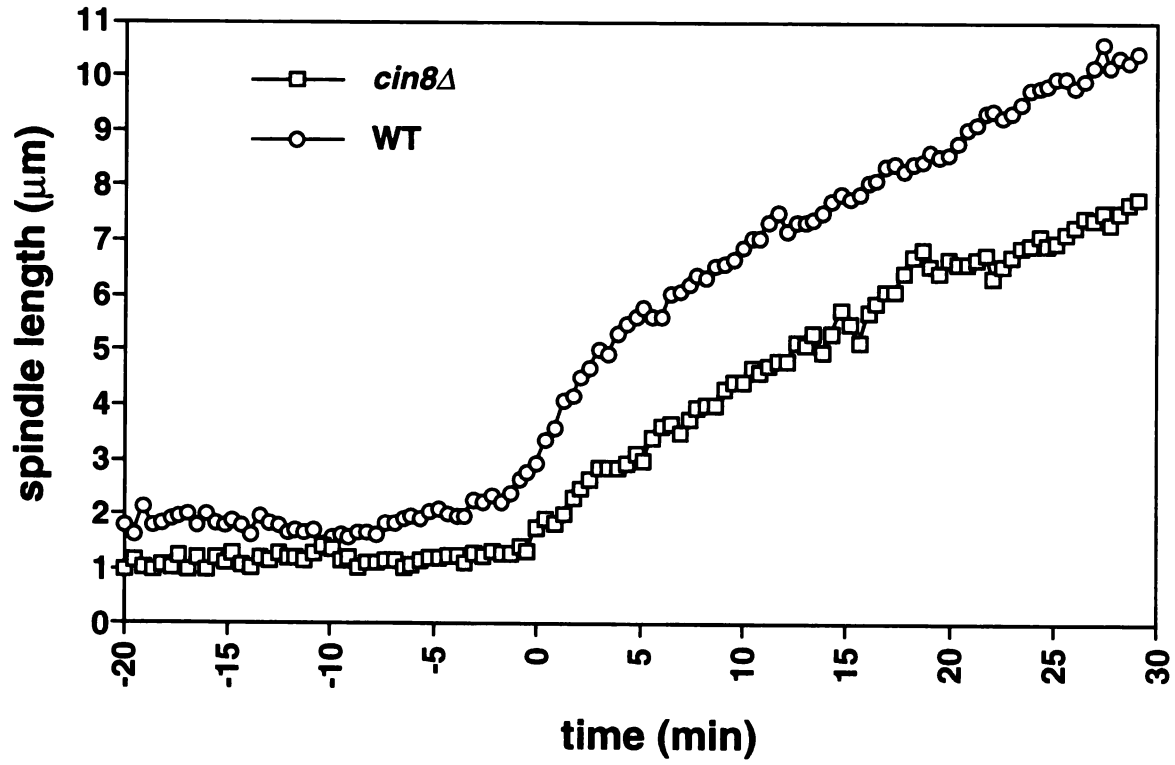


Figure 1. Straight et al.

B

*cin8*Δ Centromere Separation

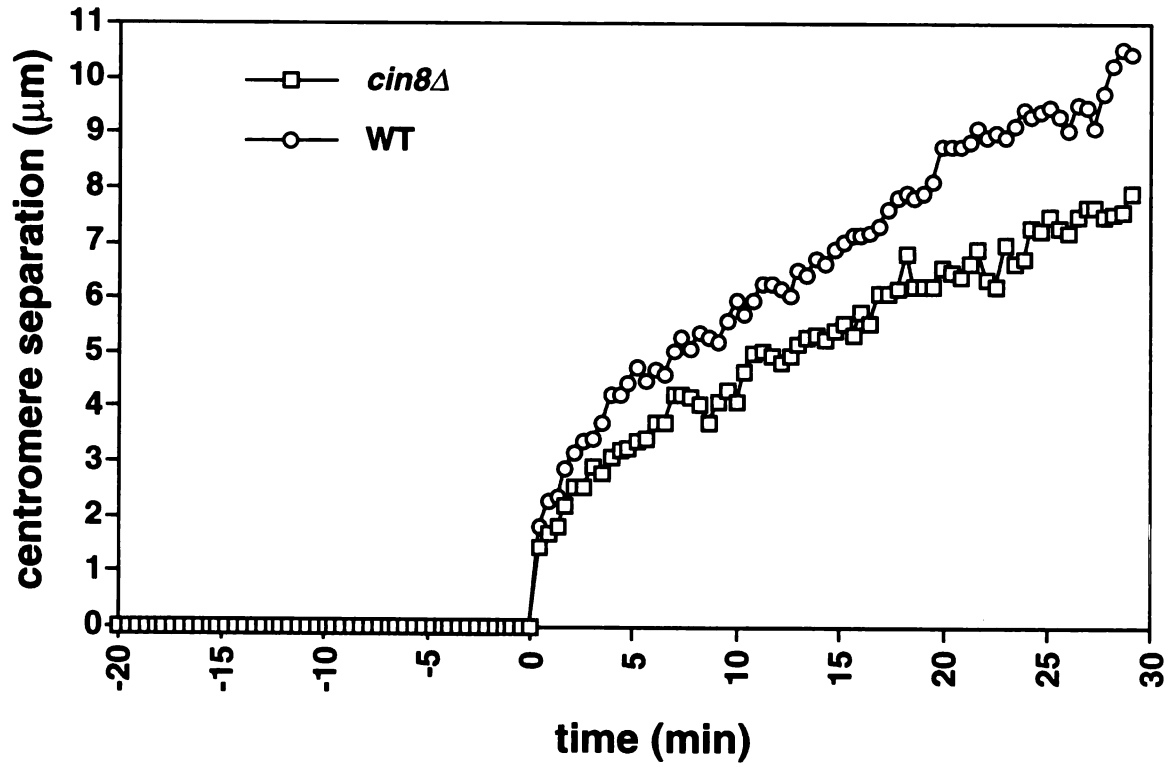
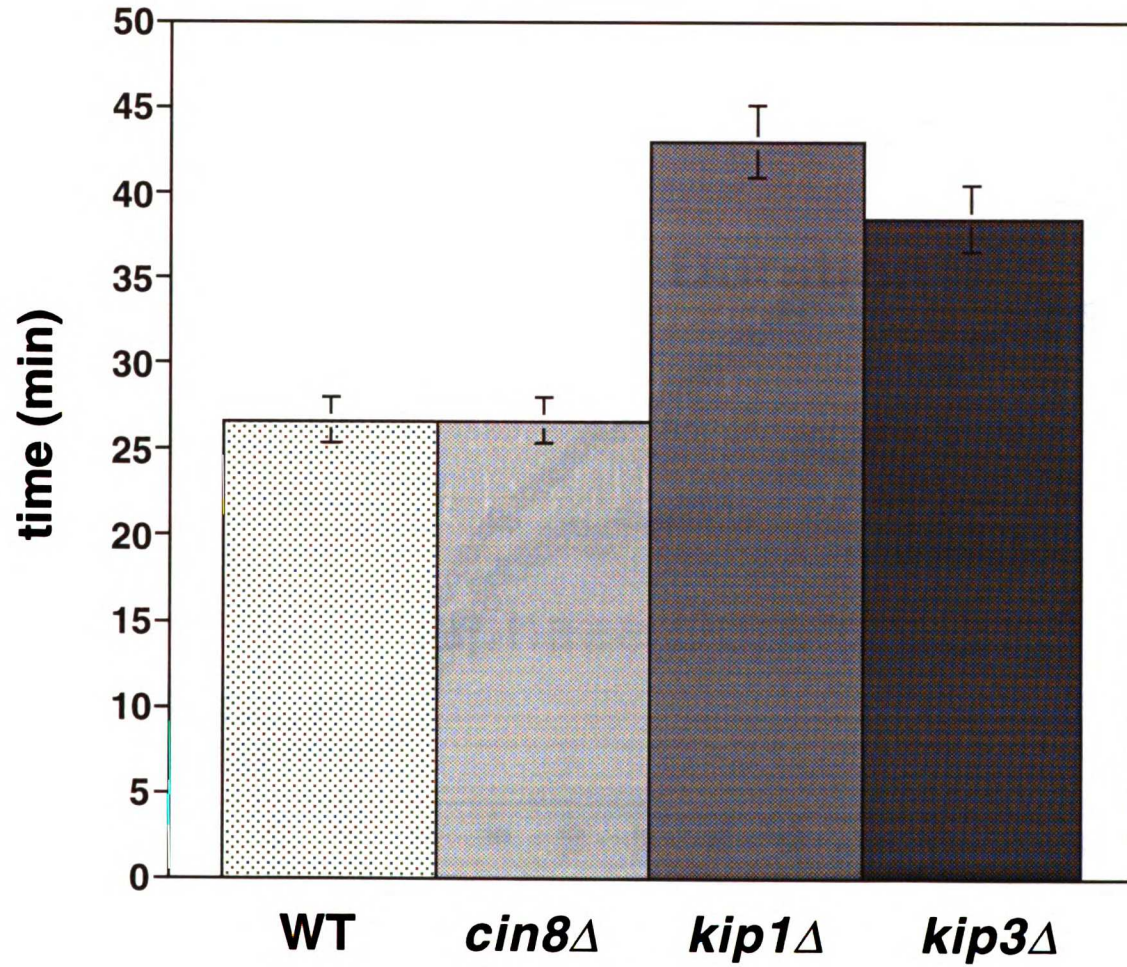


Figure 1. Straight et al.

Anaphase Duration



UWI LIBRARY

Figure 2. Straight et al.

A

kip1 Δ Pole Separation

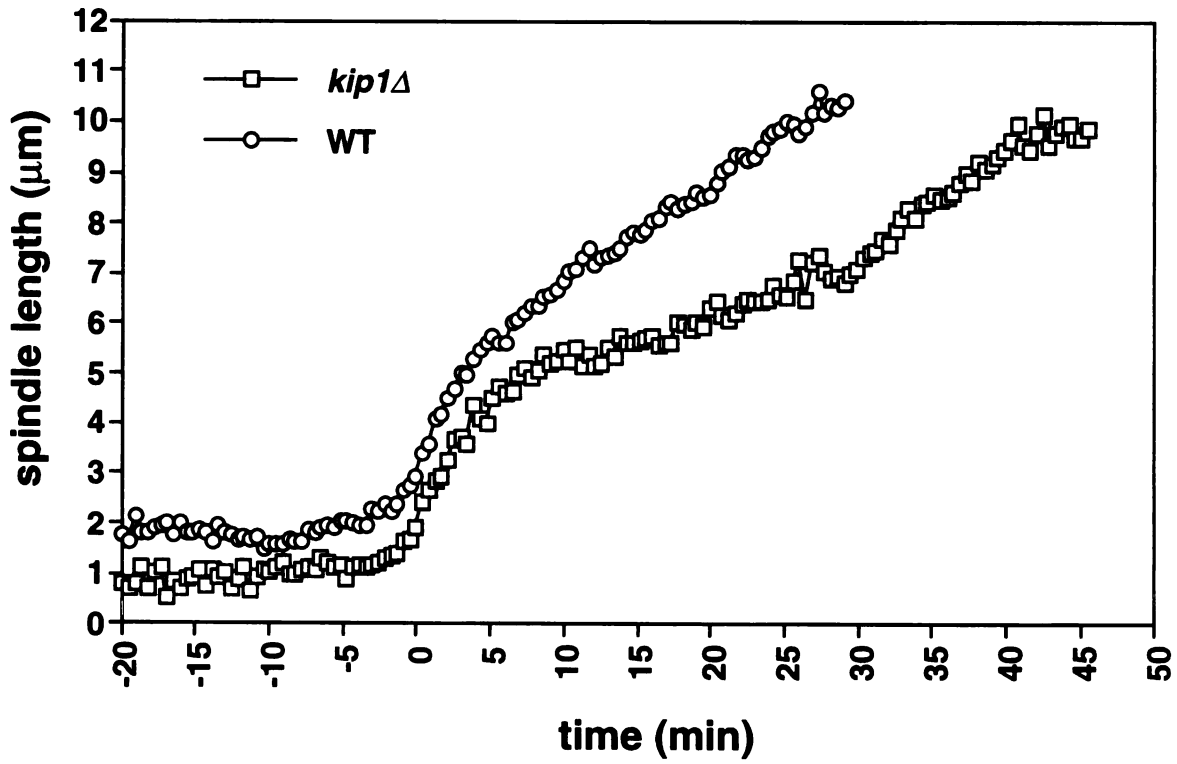
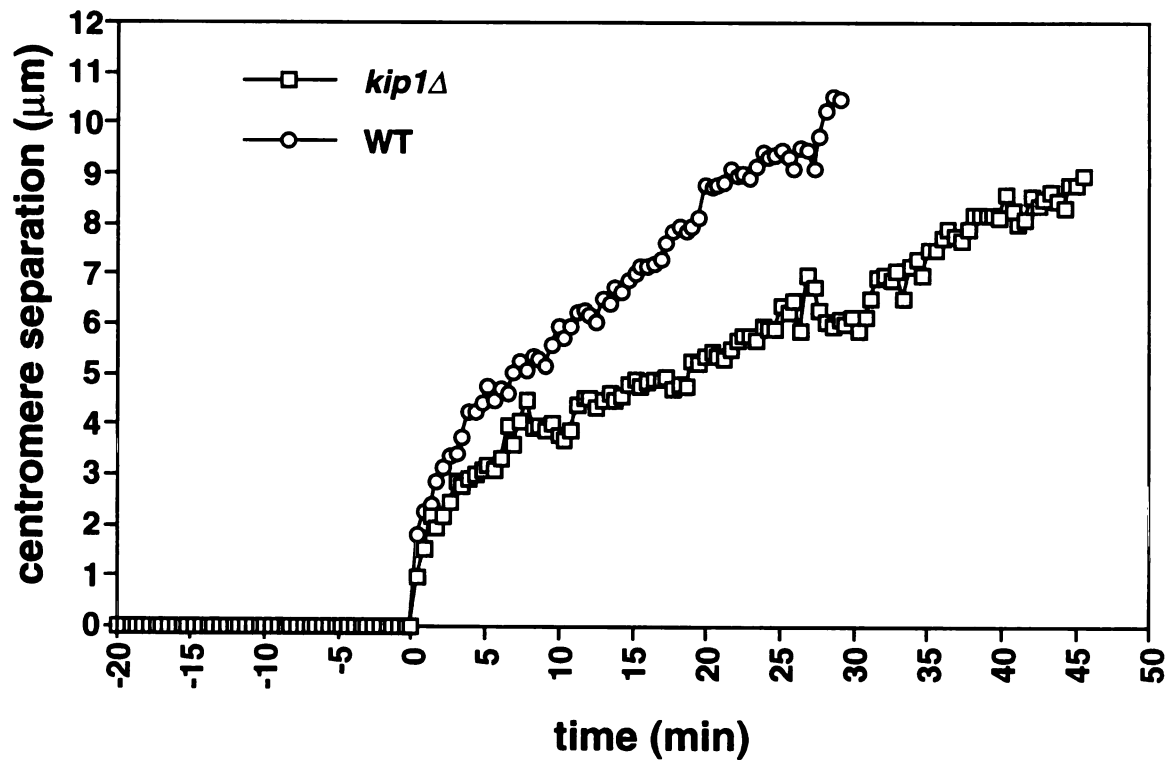


Figure 3. Straight et al.

B

*kip1*Δ Centromere Separation



UVA LUMINA

Figure 3. Straight et al.

Preanaphase Spindle Length

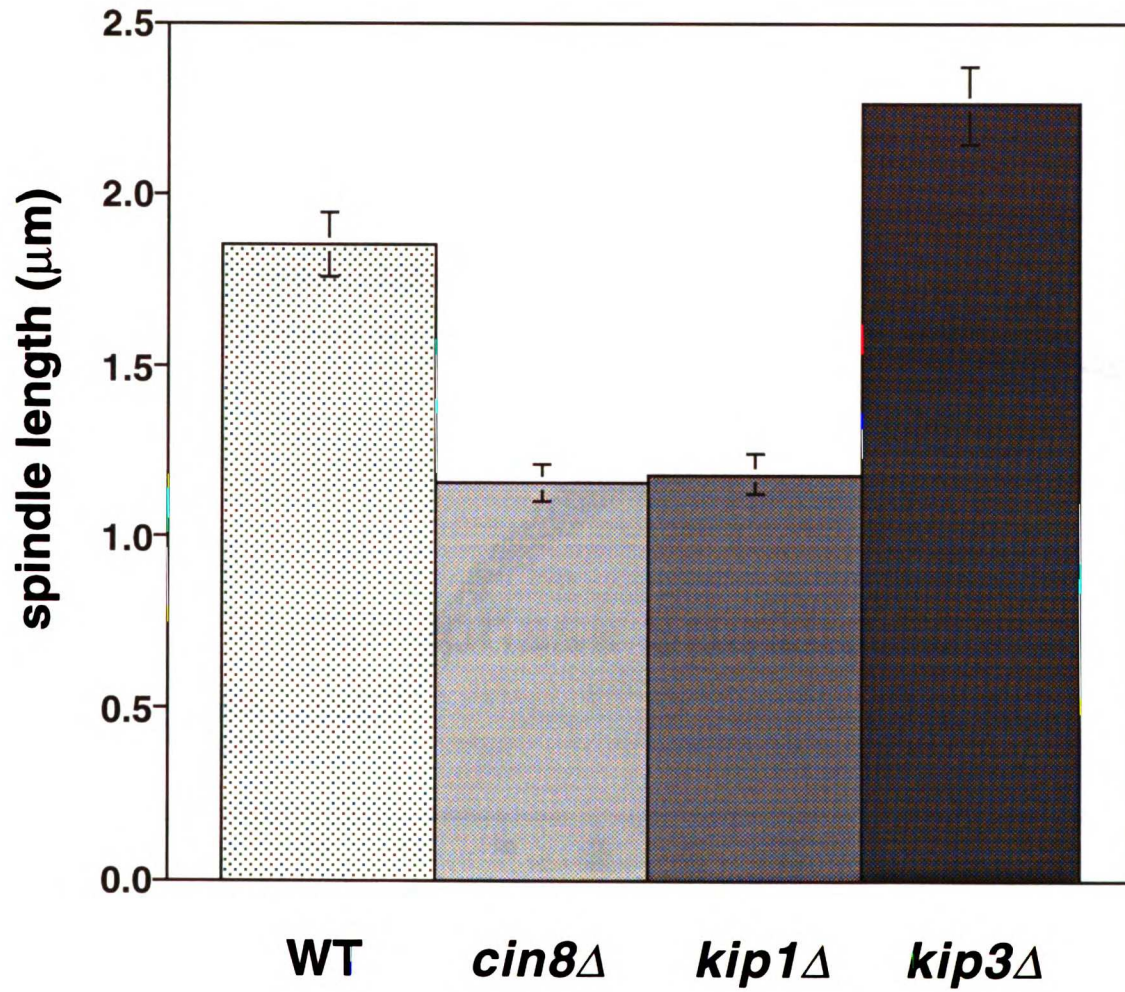


Figure 4 Straight et al.

A

kip3 Δ Pole Separation

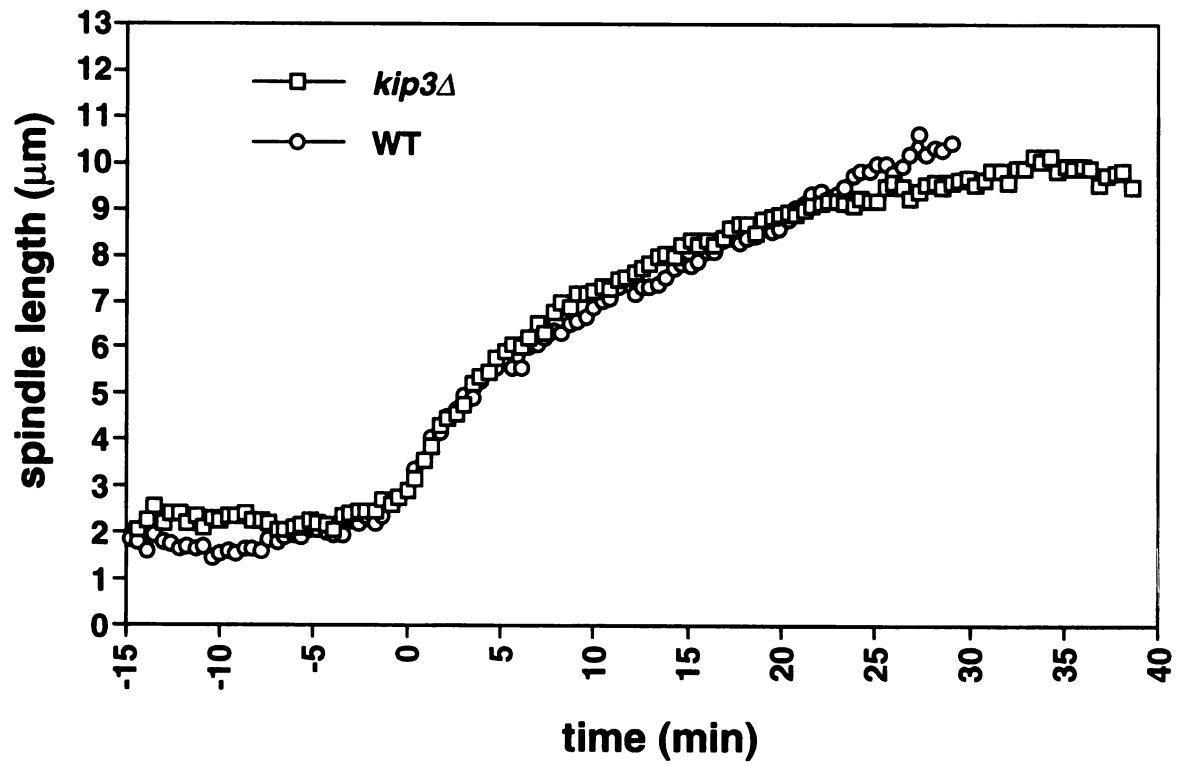


Figure 5. Straight et al.

B

kip3 Δ Centromere Separation

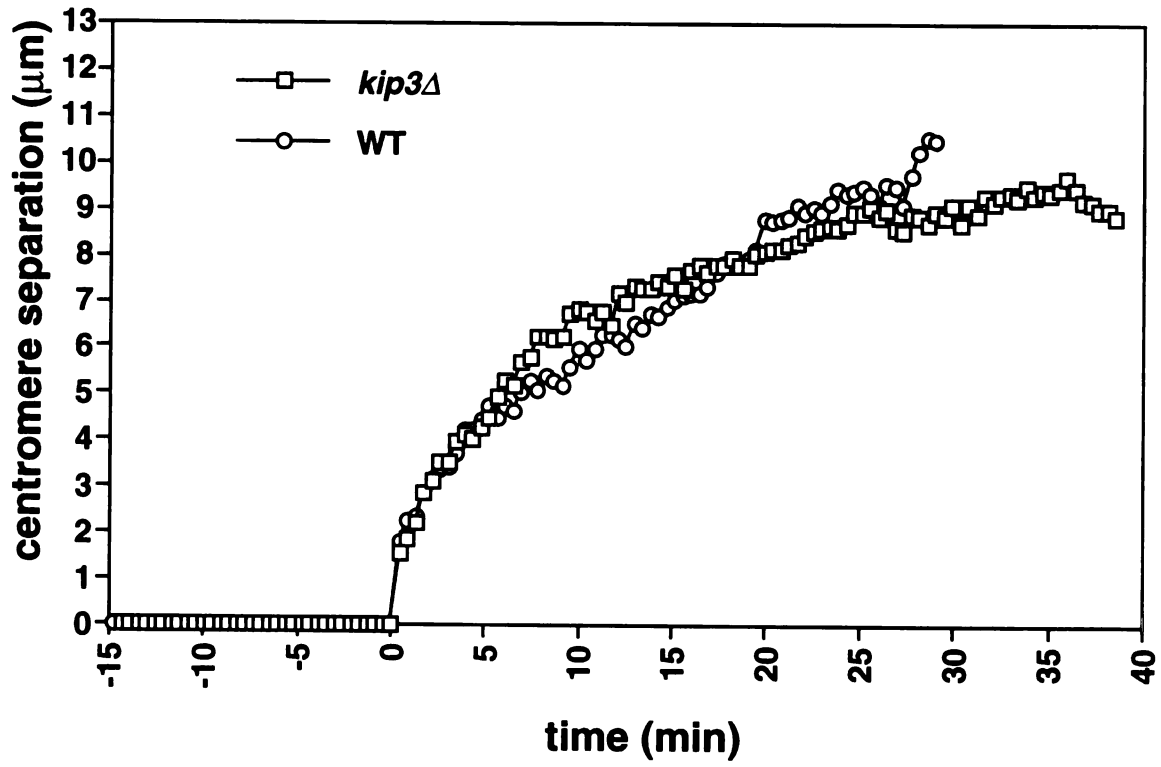


Figure 5. Straight et al.

UVU LIBRARY

C

kip3 Δ Spindle Length

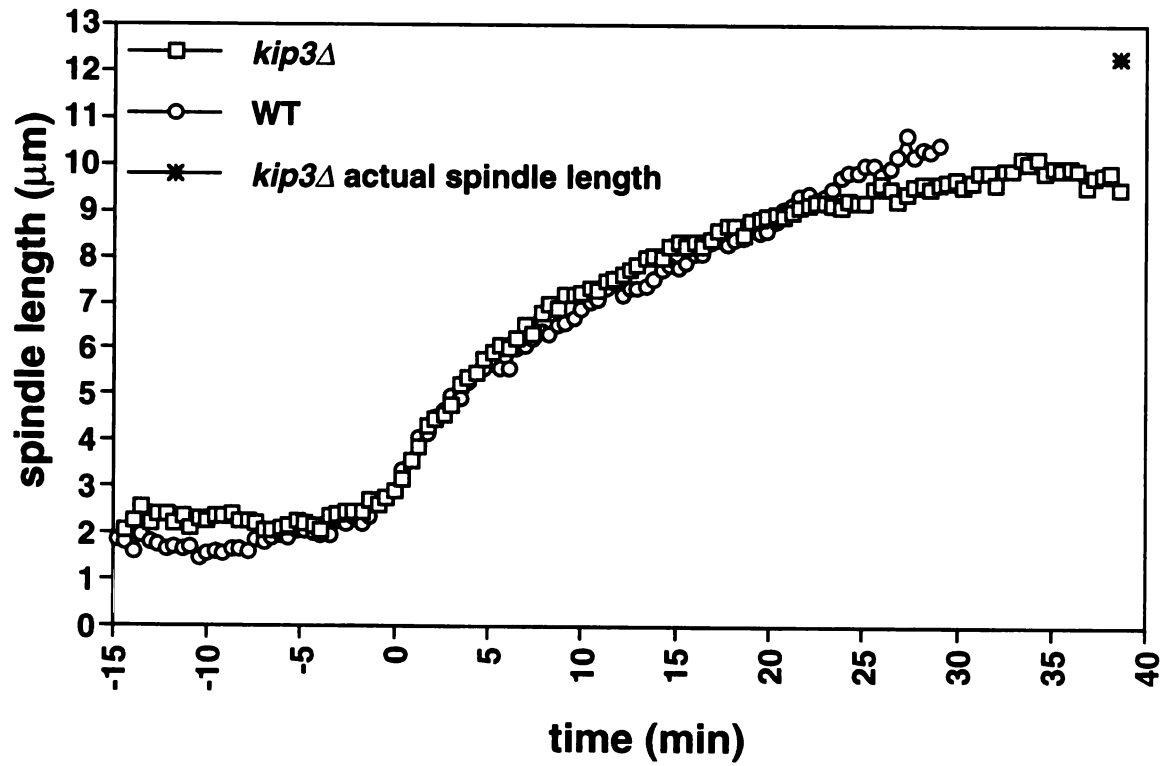


Figure 5. Straight et al.

UVAI 11111111

D

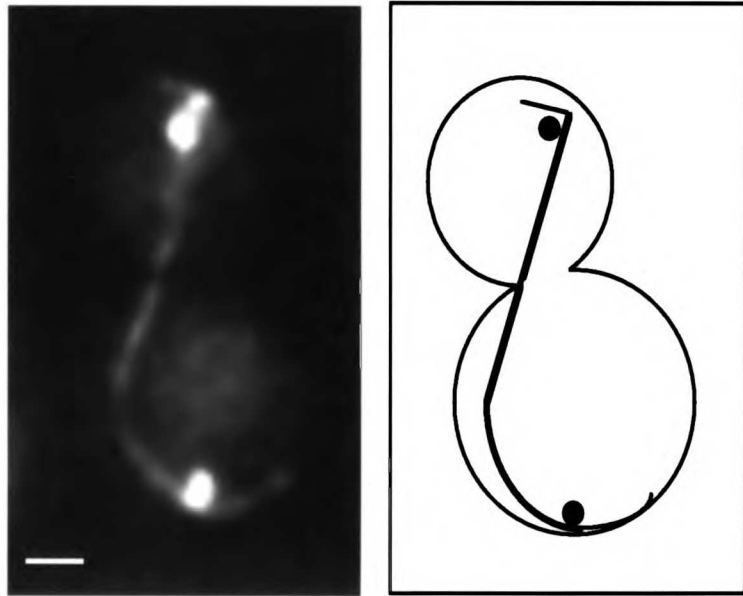


Figure 5. Straight et al.

Spindle Breakdown Length

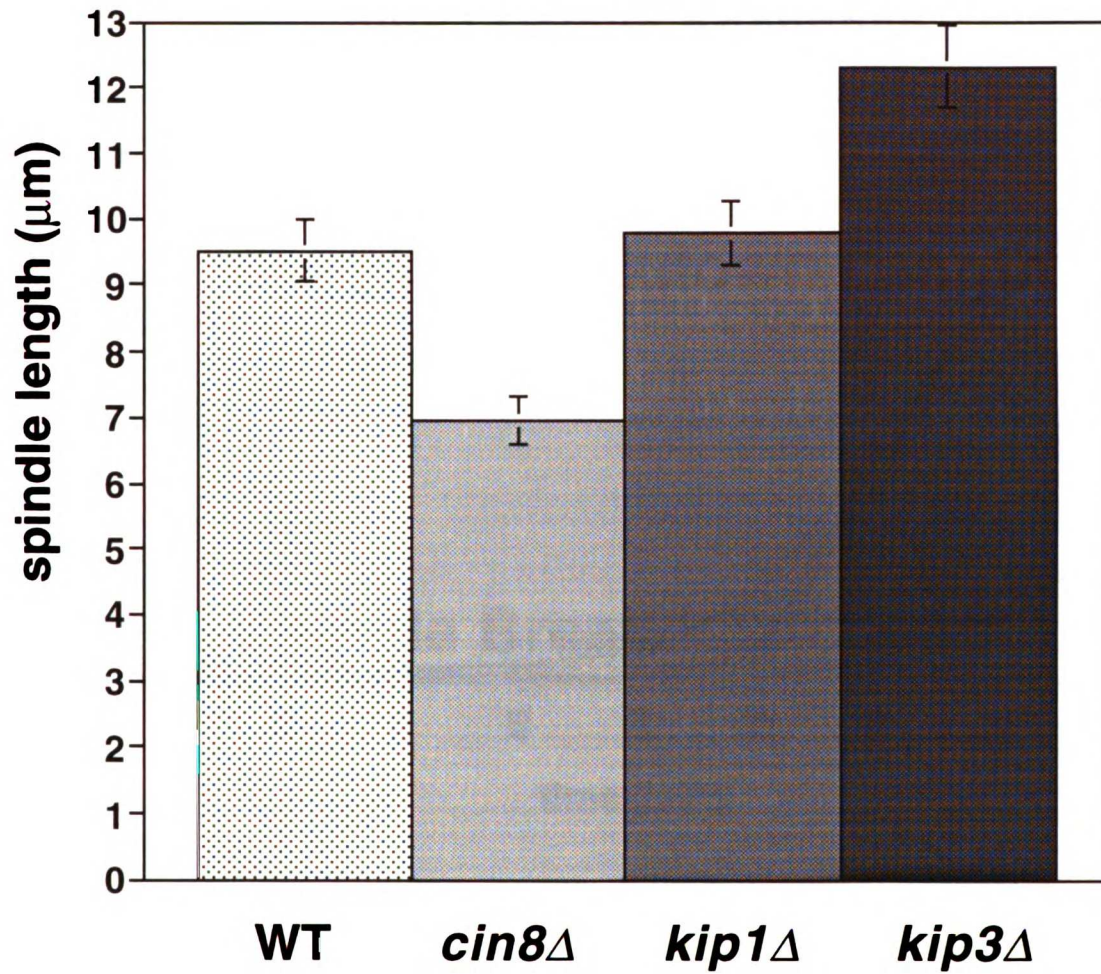


Figure 6 Straight et al.

www.lipidworld.com

cin8 Δ Delays Anaphase

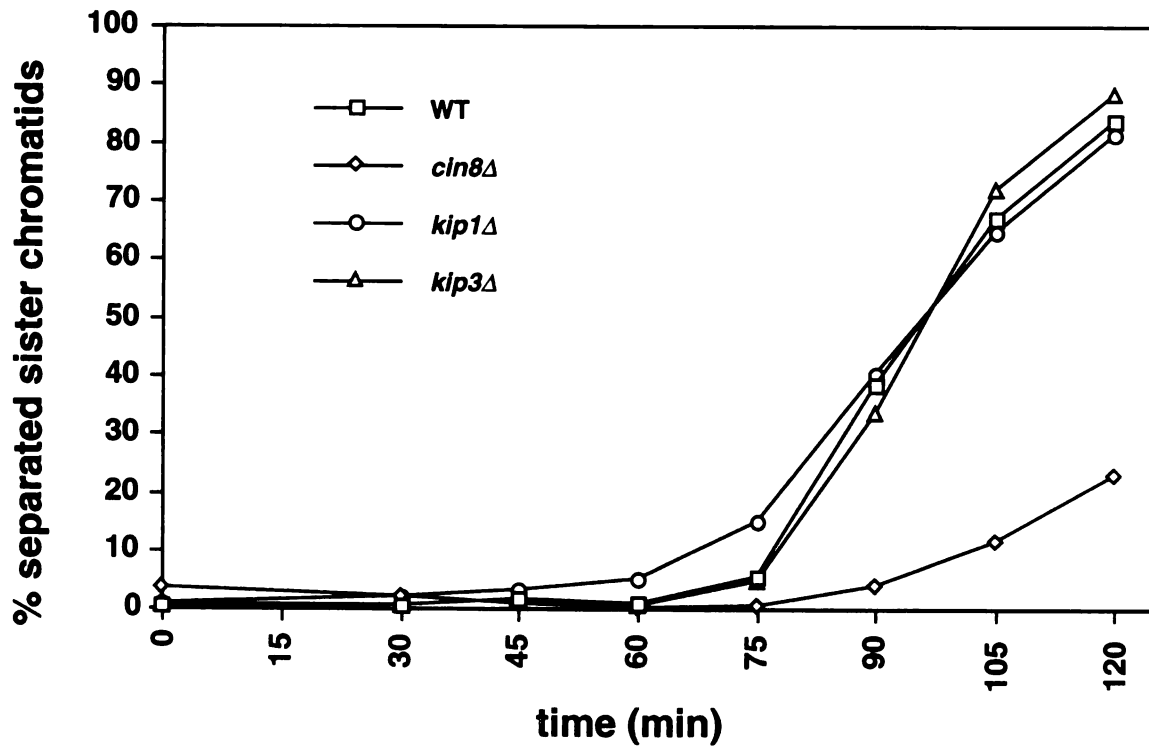


Figure 7. Straight et al.

Appendix A

Identification of Cyclosome/APC substrates by regular expression pattern matching of protein families.

UNIVERSITY OF CALIFORNIA

Appendix A

Identification of Cyclosome/APC substrates by regular expression pattern matching of protein families.

Introduction

The ordered events of the cell cycle are controlled by two mechanisms: activation of cyclin dependent kinases (CDKs) that drive cell cycle transitions, and destruction of proteins important for cell cycle transitions. The activity of CDKs is regulated by activating and inhibitory phosphorylations of the kinase molecules, by the synthesis and destruction of activating subunits of the kinases called cyclins, and by the induction and destruction of inhibitor subunits of the kinase called CKIs. The regulation of CDK activity is best understood during mitosis. Prior to the entry into mitosis, mitotic cyclins (A and B-type cyclins) are synthesized and form active kinase complexes with CDC2, the mitotic CDK (Deshaies, 1997; Fisher, 1997; King et al., 1996a). These active kinase complexes initiate the events leading to nuclear envelope breakdown, bipolar spindle assembly, and metaphase chromosome alignment. Once cells have properly formed a mitotic spindle and all the chromosomes are aligned on the metaphase plate, the transition from metaphase to anaphase is signalled and cells complete chromosome separation and spindle elongation.

The transition from metaphase to anaphase requires the inhibition of CDK kinase activity. The primary mechanism of CDK inhibition is through the proteolysis of the activating cyclin subunits of the CDK complex. When

the transition from metaphase to anaphase is signalled, the cyclins are targeted for destruction by the conjugation of ubiquitin to the cyclin molecule. Once a polyubiquitin chain has been added to the cyclin molecule, the cyclins become substrates for the proteasome and are degraded. The enzyme that accomplishes the conjugation of ubiquitin to the cyclin N-terminus is called the Cyclosome/APC (Hershko, 1996). The exact mechanism of cyclin recognition by the Cyclosome/APC is unclear, however, it is known that ubiquitination of cyclin requires a short amino acid motif in the N-terminus of the cyclin molecule called the destruction box.

The destruction box was first identified because deletions in the N-terminus of cyclins stabilized the cyclin protein. The sequence responsible for destabilization was identified as nine amino acid sequence (Glotzer et al., 1991). In this nine amino acid sequence, all destruction boxes identified to date contain arginine at the first position. The fourth position is also highly conserved and in the vast majority of destruction boxes is leucine. Other positions in the destruction box sequence have a greater degree of variation (King et al., 1996b; Yamano et al., 1996).

Recent work has implicated destruction box dependent proteolysis in the destabilization of more than just cyclin substrates. In particular, as cells exit mitosis they must separate their sister chromatids and must disassemble their spindle so that they can properly proceed through the cell cycle. Evidence in frog egg extracts suggested that proteins other than cyclins had to be destroyed in order for sister chromatids to properly separate. Addition of cyclin N-terminus to extracts going through mitosis prevented the proper separation of sister chromatids but allowed spindle elongation. This suggested that the N-terminus of cyclin overwhelmed the ubiquitin-mediated proteolysis pathway, blocking the degradation of other substrates required for

sister chromatid separation (Holloway et al., 1993). Analysis of sister chromatid separation in fission and budding yeast identified proteins that had to be proteolyzed in order for sister chromatids to separate. These proteins, CUT2 and PDS1 respectively, contain sequences homologous to the cyclin destruction box. These sequences were shown in both cases to be required for the proper destruction of these proteins as cells passed through anaphase (Cohen-Fix et al., 1996; Funabiki et al., 1996a; Funabiki et al., 1996b; Funabiki et al., 1997; Yamamoto et al., 1996a; Yamamoto et al., 1996b). In addition, studies of spindle breakdown in budding yeast identified another protein, ASE1, that had to be destroyed in order for the mitotic spindle to properly disassemble. The destruction of ASE1 was also shown to be dependent on the presence of a sequence homologous to the destruction box (Juang et al., 1997; Pellman et al., 1995).

Other proteins required for the proper execution of mitosis and the transition from mitosis to interphase are likely to be destroyed by the Cyclosome/APC. Identification of these proteins is difficult since there is no simple biochemical assay for their activity. One possible approach is to use homology to the destruction box to identify potential substrates of the Cyclosome/APC. The destruction box is short and highly degenerate so that conventional homology searching, using programs such as BLAST or FASTA, is unlikely to find specific destruction box containing proteins. We wanted to use an alternative approach to find destruction box containing proteins based on the properties of known destruction boxes. We used an approach similar to the approach described by Gribskov et al. (Gribskov et al., 1990) to search for novel destruction box containing proteins. We constructed a matrix that reflected the likelihood that a particular amino acid would occur at an individual position in a destruction box. We then aligned this matrix

with every position in the yeast proteome to find those proteins containing the most likely destruction boxes. From this search we identified all the known destruction box containing proteins in yeast as well as numerous candidate proteins as novel Cyclosome/APC substrates.

Methodology

We first constructed an alignment of known destruction boxes in the yeasts *Saccharomyces cerevisiae* and *Schizosaccharomyces pombe* (Figure 1A). The destruction boxes of the B-type cyclins in *S. cerevisiae* CLB1-4, the B-type cyclin *cdc13* of *S. pombe* and three other known destruction box containing proteins: *S. pombe* *cut2*, *S. cerevisiae* ASE1 and *S. cerevisiae* PDS1, were aligned with one another (Figure 1A). Following alignment of the destruction box sequences we constructed a matrix containing the number of times an amino acid appeared in each position of the destruction box (Figure 1B). For example, position four of the destruction box is leucine in eight out of the nine sequences aligned and is phenylalanine in the ninth destruction box. Thus leucine at position four receives a score of eight, phenylalanine a score of one and all other amino acids a score of zero (Figure 1B). From this type of matrix, one can construct an 'ideal' destruction box representing the amino acids that give the highest score at each position (Figure 1B, Best Box). We have also made alignments of destruction boxes from the majority of the known A- and B-type cyclins and all other proteins containing destruction boxes. For simplicity, we show the destruction boxes, the accession numbers of the sequences, and the names and origins of the sequences (Figure 2).

Identification of destruction box containing proteins in *S. cerevisiae*.

We used the matrix representation of the destruction box to identify other destruction box containing proteins in budding yeast. The recent sequencing of the entire yeast genome allowed us to search all the encoded proteins in yeast. Furthermore, yeast have the advantage that candidate destruction box containing proteins can be easily tested using yeast genetic approaches. Conventional search algorithms such as FASTA and BLAST are extremely rapid and efficient when comparing longer and less degenerate sequences against large databases (Altschul et al., 1994; Altschul et al., 1990; Pearson, 1990). Since we wanted to compare a short highly degenerate sequence family against a large database we needed a more sensitive search method so that we could accurately search all potential yeast sequences for destruction boxes. One highly sensitive method for matching patterns utilizes regular expression pattern matching. Regular expressions use generalized representations of language characters to scan for matching patterns (Friedl, 1997). For example, a regular expression character such as "." will match any alphanumeric character when compared against a set of characters. We could therefore represent a nine amino acid destruction box as merely a set of nine alphabetic characters. The only disadvantage to the use of regular expressions is that they are more computationally expensive than conventional fast searching methods. However, our primary concern was sensitivity and we had unlimited computational resources.

A simple PERL program for matrix construction and database searching.

The Practical Extraction and Report Language (PERL) was ideal for our purposes (Wall and Schwartz, 1991). PERL implements tools for data

manipulation and extraction and also contains an efficient implementation of regular expression pattern matching routines (Friedl, 1997). We wrote a simple program that, when given a list of destruction boxes and a database to search against would compile a matrix based on those destruction boxes and pattern match the destruction box matrix against the database. The complete source code for the program is listed in Figure 3. In order to ensure complete coverage of the genome, we allowed any position to contain any amino acid and we searched every nine amino acid block in the yeast genome. Each block was scored using the matrix constructed from the input destruction box sequences. Following scoring, the destruction boxes were ranked according to their scores and then identified using the information published by the Saccharomyces Genome Database (SGD). Identification was done based on the most current version of the file "ORF_table.text" available by ftp from genome-ftp.stanford.edu.

Results

Identification of destruction box containing proteins.

The top ten scoring destruction boxes from searching the yeast genome are displayed in Figure 4. Figure 4A shows the results from searching the yeast genome with a matrix containing the four *S. cerevisiae* B-type cyclins (CLB1-4), ASE1, PDS1, the *S. pombe* cyclin cdc13 and the cut2 protein. The destruction box prediction program detects the four budding yeast B-type cyclins as the highest scoring destruction boxes in the genome. This is in contrast to the FASTA search results shown in Figure 4C where only one of the four B-type cyclins ranked in the top ten search results. The results of this

type of matrix searching are entirely dependent on the sequences used to build the matrix. We therefore altered the destruction box matrix to include all the destruction boxes listed in Figure 2. Results from this search are shown in Figure 4B. The searching program still scored three of the four yeast B-type cyclins in the top ten but CLB2 fell to position number seventeen in the results. The rearrangement in scores is accounted for by the difference in the destruction box matrix representing the majority of cyclins versus the matrix representing only yeast proteins. As a further comparison we constructed a 'profile' from the yeast proteins and searched this profile against the same yeast database using the profilesearch method developed by Gribskov et al (Gribskov et al., 1990; Gribskov et al., 1987). The Gribskov method was also effective, finding three out of the four B-type cyclins. The profile searching approach, however, gave significantly different results apart from the cyclins (Figure 4D). The divergence between the results using our regular expression matching approach and the profilesearch method may be explained by a number of differences between the methods. The profilesearching method normalizes scores as a function of their length. Thus, a high scoring destruction box in a long amino acid sequence will receive a lower score. In addition, score assignment is also modified using predicted evolutionary distances between amino acids. Using the Dayhoff evolutionary distance matrix, scores are positively or negatively weighted based on the likelihood that a change between two amino acids would occur during evolution (Dayhoff, 1965). The differences between our linear scoring scheme versus the weighted scheme used by Gribskov et al. may account for the differences in results.

New candidates for Cyclosome/APC mediated proteolysis.

We examined the results from our database searching method to determine whether specific proteins ranked highly using different destruction box matrices. We describe four potential candidates that gave high scores using different matrices and have some known function. The first candidate protein, known as Hsl1, was isolated because mutations in the gene cause cells with mutations in histone H3 to die (Ma et al., 1996). The isolation of the gene revealed that it was homologous to the nim1 protein kinase that promotes the entry into mitosis in *S. pombe* (Coleman et al., 1993; Parker et al., 1993; Tang et al., 1993; Wu and Russell, 1993). Destruction of the Hsl1 protein at the metaphase to anaphase transition would inhibit mitosis and thus help drive cells through anaphase and ensure that cells exit mitosis properly. We have attempted to detect Hsl1 protein levels in cells by tagging the Hsl1 protein with an epitope recognized by a monoclonal antibody against the influenza hemagglutinin protein. Even when overexpressed under control of the GAL1-10 promoter we were unable to detect the Hsl1 protein (data not shown).

A second protein that consistently scored well in our matrix searching approach was the Sir4 protein. The Sir4 protein is required for the establishment and maintenance of silent heterochromatin at telomeres in yeast (Laurenson and Rine, 1992). Sir4 was recently shown to interact tightly with Sir2, Sir3 and two other proteins. One of the other proteins was shown to be a deubiquitinating enzyme that inhibits telomeric silencing (Moazed and Johnson, 1996; Moazed et al., 1997). The Sir4 protein has been shown to oscillate during the cell cycle much like the Clb2 protein in yeast. In addition, mutations in components of the Cyclosome/APC cause stabilization of the Sir4 protein. Finally, mutation of two potential destruction boxes in the Sir4

protein causes stabilization of Sir4 protein (D. Moazed and A. Johnson, unpublished data). It may be that destruction of a silencing protein like Sir4 is required to remove and then reestablish the silent chromatin state during the cell cycle. It is known progression through replication is required to reestablish silencing in *S. cerevisiae*. Establishment of silencing may reflect the resynthesis of Sir4 after passage through mitosis and Start.

The third protein, YPL183, was recently identified in a screen for proteins that caused death to a cell lacking the kinesin motor Cin8 (Geiser et al., 1997). The PAC1/LIS-1 protein was found to be homologous to a gene implicated in the neurological disorder Miller-Deiker Lissencephaly (Dobyns et al., 1993). Recent work has identified this protein as having a role in stabilizing microtubules. In the presence of the LIS1 protein the catastrophe rate of microtubules decreases, resulting in longer, less dynamic microtubules (Sapir et al., 1997). Destruction of this protein at the end of mitosis would cause the destabilization of microtubules as cells enter into interphase. However, this is inconsistent with the known changes in microtubule dynamics in cells that normally undergo a transition from dynamic mitotic microtubule arrays to stable interphase microtubule arrays (Mitchison, 1989). An alternative possibility is that destabilization of microtubules at the end of anaphase may be required for the disassembly of the mitotic spindle prior to cytokinesis.

The yeast Rad52 protein is also an interesting candidate for proteolysis. Rad52 is involved in double strand break repair and recombination (Friedberg et al., 1991). In two hybrid interaction screens using the human Rad52 protein, Rad52 interacts with the ubiquitin like protein Ubl1/Smt3 and with the ubiquitin conjugating enzyme Ubc9 (Shen et al., 1996a; Shen et al., 1996b). Rad52 has also been reported to have high protein levels in S and G2/M and

low levels in other cell cycle phases. Cells with DNA damage arrest in response to the damage and prevent the proteolysis of B-type cyclins. If proteolysis is blocked in a DNA damage arrest, Rad52 might be stabilized allowing the cell to repair the damaged DNA. It is unclear why Rad52 would need to be proteolyzed after mitosis. One possibility is that there is a deleterious effect of the presence of Rad52 in late anaphase or prior to the initiation of S-phase.

Conclusion

The proteolysis of substrates important for the passage through mitosis is regulated by a short, degenerate amino acid sequence called the destruction box. Using a sensitive pattern matching technique we have identified a number of proteins that contain potential destruction boxes. Preliminary biochemical data suggests that at least one candidate is a true substrate of the Cyclosome/APC. The ability to distinguish true destruction boxes from destruction box like sequences will be strengthened as biochemical data verifies or rejects the candidate destruction box containing proteins. Once a more widespread family of proteins that contain true destruction boxes is known we can strengthen our analysis by including new sequences into the matrix used to search databases. Our analysis is not limited to destruction boxes. Any family of sequences can be used to construct a searching matrix to use against any database. We hope that an iterated approach to searching and identification of destruction box containing proteins will lead to the identification of novel substrates for the Cyclosome/APC.

References

- Altschul, S. F., Boguski, M. S., Gish, W. and Wootton, J. C. (1994). Issues in searching molecular sequence databases. *Nat Genet* 6, 119-29.
- Altschul, S. F., Gish, W., Miller, W., Myers, E. W. and Lipman, D. J. (1990). Basic local alignment search tool. *J Mol Biol* 215, 403-10.
- Cohen-Fix, O., Peters, J. M., Kirschner, M. W. and Koshland, D. (1996). Anaphase initiation in *Saccharomyces cerevisiae* is controlled by the APC-dependent degradation of the anaphase inhibitor Pds1p. *Genes Dev* 10, 3081-93.
- Coleman, T. R., Tang, Z. and Dunphy, W. G. (1993). Negative regulation of the wee1 protein kinase by direct action of the nim1/cdr1 mitotic inducer. *Cell* 72, 919-29.
- Dayhoff, M. O. (1965). Atlas of protein sequence and structure. Silver Spring, Md. National Biomedical Research Foundation
- Deshaies, R. J. (1997). Phosphorylation and proteolysis: partners in the regulation of cell division in budding yeast. *Curr Opin Genet Dev* 7, 7-16.

Dobyns, W. B., Reiner, O., Carrozzo, R. and Ledbetter, D. H. (1993).

Lissencephaly. A human brain malformation associated with deletion of the LIS1 gene located at chromosome 17p13. *Jama* 270, 2838-42.

Fisher, R. P. (1997). CDKs and cyclins in transition (s). *Curr Opin Genet Dev* 7, 32-8.

Friedberg, E. C., Siede, W. and Cooper, A. J. (1991). Cellular responses to DNA damage in yeast. In *The molecular and cellular biology of the yeast Saccharomyces, genome dynamics, protein synthesis, and energetics*, ed. Broach, J. R., Jones, E. W. and Pringle, J. R., Cold Spring Harbor Laboratory Press, Cold Spring Harbor, N.Y. Vol. 1, pp. 147-92

Friedl, J. E. F. (1997). *Mastering regular expressions : powerful techniques for Perl and other tools*. Cambridge. O'Reilly

Funabiki, H., Kumada, K. and Yanagida, M. (1996a). Fission yeast Cut1 and Cut2 are essential for sister chromatid separation, concentrate along the metaphase spindle and form large complexes. *Embo J* 15, 6617-28.

Funabiki, H., Yamano, H., Kumada, K., Nagao, K., Hunt, T. and Yanagida, M. (1996b). Cut2 proteolysis required for sister-chromatid separation in fission yeast. *Nature* 381, 438-41.

Funabiki, H., Yamano, H., Nagao, K., Tanaka, H., Yasuda, H., Hunt, T. and Yanagida, M. (1997). Fission yeast Cut2 required for anaphase has two destruction boxes. *Embo J* 16, 5977-87.

Geiser, J. R., Schott, E. J., Kingsbury, T. J., Cole, N. B., Totis, L. J., Bhattacharyya, G., He, L. and Hoyt, M. A. (1997). *Saccharomyces cerevisiae* genes required in the absence of the CIN8-encoded spindle motor act in functionally diverse mitotic pathways. *Mol Biol Cell* 8, 1035-50.

Glotzer, M., Murray, A. W. and Kirschner, M. W. (1991). Cyclin is degraded by the ubiquitin pathway. *Nature* 349, 132-138.

Gribskov, M., Luthy, R. and Eisenberg, D. (1990). Profile analysis. *Methods Enzymol* 183, 146-59.

Gribskov, M., McLachlan, A. D. and Eisenberg, D. (1987). Profile analysis: detection of distantly related proteins. *Proc Natl Acad Sci U S A* 84, 4355-8.

Hershko, A. (1996). Mechanisms and regulation of ubiquitin-mediated cyclin degradation. *Adv Exp Med Biol* 389, 221-7.

Holloway, S. L., Glotzer, M., King, R. W. and Murray, A. W. (1993). Anaphase is initiated by proteolysis rather than by the inactivation of MPF. *Cell* 73, 1393-1402.

Juang, Y. L., Huang, J., Peters, J. M., McLaughlin, M. E., Tai, C. Y. and Pellman, D. (1997). APC-mediated proteolysis of Ase1 and the morphogenesis of the mitotic spindle. *Science* 275, 1311-4.

King, R. W., Deshaies, R. J., Peters, J. M. and Kirschner, M. W. (1996a). How proteolysis drives the cell cycle. *Science* 274, 1652-9.

King, R. W., Glotzer, M. and Kirschner, M. W. (1996b). Mutagenic Analysis of the Destruction Signal of Mitotic Cyclins and Structural Characterization of Ubiquitinated Intermediates. *M.B.O.C.* 7, 1343-1357.

Laurenson, P. and Rine, J. (1992). Silencers, silencing, and heritable transcriptional states. *Microbiol Rev* 56, 543-60.

Ma, X. J., Lu, Q. and Grunstein, M. (1996). A search for proteins that interact genetically with histone H3 and H4 amino termini uncovers novel regulators of the Swe1 kinase in *Saccharomyces cerevisiae*. *Genes Dev* 10, 1327-40.

Mitchison, T. J. (1989). Mitosis: basic concepts. *Curr Opin Cell Biol* 1, 67-74.

Moazed, D. and Johnson, D. (1996). A deubiquitinating enzyme interacts with SIR4 and regulates silencing in *S. cerevisiae*. *Cell* 86, 667-77.

Moazed, D., Kistler, A., Axelrod, A., Rine, J. and Johnson, A. D. (1997). Silent information regulator protein complexes in *Saccharomyces cerevisiae*: a SIR2/SIR4 complex and evidence for a regulatory domain in SIR4 that inhibits its interaction with SIR3. *Proc Natl Acad Sci U S A* 94, 2186-91.

Parker, L. L., Walter, S. A., Young, P. G. and Piwnicka-Worms, H. (1993). Phosphorylation and inactivation of the mitotic inhibitor Wee1 by the nim1/cdr1 kinase. *Nature* 363, 736-8.

Pearson, W. R. (1990). Rapid and sensitive sequence comparison with FASTP and FASTA. *Methods Enzymol* 183, 63-98.

Pellman, D., Bagget, M., Tu, Y. H., Fink, G. R. and Tu, H. (1995). Two microtubule-associated proteins required for anaphase spindle movement in *Saccharomyces cerevisiae*. *J Cell Biol* 130, 1373-85.

Sapir, T., Elbaum, M. and Reiner, R. (1997). Reduction of microtubule catastrophe events by LIS1, platelet-activating factor acetylhydrolase subunit. *Embo J* 16, 6977-84.

Shen, Z., Pardington-Purtymun, P. E., Comeaux, J. C., Moyzis, R. K. and Chen, D. J. (1996a). Associations of UBE2I with RAD52, UBL1, p53, and RAD51 proteins in a yeast two-hybrid system. *Genomics* 37, 183-6.

Shen, Z., Pardington-Purtymun, P. E., Comeaux, J. C., Moyzis, R. K. and Chen, D. J. (1996b). UBL1, a human ubiquitin-like protein associating with human RAD51/RAD52 proteins. *Genomics* 36, 271-9.

Tang, Z., Coleman, T. R. and Dunphy, W. G. (1993). Two distinct mechanisms for negative regulation of the Wee1 protein kinase. *Embo J* 12, 3427-36.

Wall, L. and Schwartz, R. L. (1991). *Programming Perl*. Sebastopol. O'Reilly

Wu, L. and Russell, P. (1993). Nim1 kinase promotes mitosis by inactivating Wee1 tyrosine kinase. *Nature* 363, 738-41.

Yamamoto, A., Guacci, V. and Koshland, D. (1996a). Pds1p is required for faithful execution of anaphase in the yeast, *Saccharomyces cerevisiae*. *J. Cell Biol.* 133, 85-97.

Yamamoto, Y., A., Guacci, V. and Koshland, D. (1996b). Pds1p, an inhibitor of anaphase in budding yeast, plays a critical role in the APC and checkpoint pathway (s). *J. Cell Biol.* 133, 99-110.

Yamano, H., Gannon, J. and Hunt, T. (1996). The role of proteolysis in cell cycle progression in *Schizosaccharomyces pombe*. *Embo J* 15, 5268-79.

Figure Legends

Figure 1 - Matrix representation of destruction box sequences

Destruction box sequences can be aligned to create a matrix representing the frequency of amino acid appearance at each position. (A) Alignment of all known yeast (*S. cerevisiae* and *S. pombe*) destruction box sequences. (B) Matrix representing the number of times each amino acid appears at each position in the destruction box. The "ideal" destruction box is listed below the matrix.

Figure 2 - List of known destruction boxes in eukaryotes

All sequences of cyclin destruction boxes were retrieved from the genbank, pir, swissprot, and EMBL databases and checked for redundancy. Column1, 2 and 3 contain the sequences of the destruction boxes, the accession numbers for the destruction boxes and the name of the cyclin and genus and species of the organism. The last four sequences represent functional destruction boxes in non-cyclin proteins.

Figure 3 - A PERL program to compare destruction boxes against sequence databases

The PERL source code of the destruction box prediction program. The source was written and run using PERL version 5.01 on a DEC station alpha OSF1 running UNIX BSD v3.2. The same source has been run on a Macintosh running system MacOS 7.6 or 8.0 using MacPERL v5.

Figure 4 - Comparison of different search methods

Different search methods were used to identify destruction box sequences in the yeast genome database. In each case Column 1, 2, 3 and 4 represent the score from the database search, the destruction box sequence identified, the open reading frame designation of the destruction box containing protein and the identity (if known) of the open reading frame. (A) Results from searching a matrix comprised of only yeast destruction box containing sequences represented in Figure 1 against the yeast database. (B) Results from searching a matrix comprised of all destruction box containing sequences represented in Figure 2 against the yeast database. (C) FASTA search results using the "ideal" destruction box sequence shown in Figure 1. (D) Results of the Profilesearch method using the known yeast destruction boxes from Figure 1.

A

Gene Name	Pos 1	Pos 2	Pos 3	Pos 4	Pos 5	Pos 6	Pos 7	Pos 8	Pos 9
ASE1	R	Q	L	F	P	I	P	L	N
PDS1	R	L	P	L	A	A	K	D	N
CLB1	R	T	I	L	G	N	V	T	N
CLB2	R	L	A	L	N	N	V	T	N
CLB3	R	V	A	L	S	D	V	T	N
CLB4	R	V	A	L	G	D	V	T	S
CDC13	R	H	A	L	D	D	V	S	N
CUT2-1	R	A	P	L	G	S	T	K	Q
CUT2-2	R	T	V	L	G	G	K	S	T

B

Amino Acid	Pos 1	Pos 2	Pos 3	Pos 4	Pos 5	Pos 6	Pos 7	Pos 8	Pos 9
------------	-------	-------	-------	-------	-------	-------	-------	-------	-------

A	0	1	4	0	1	1	0	0	0
C	0	0	0	0	0	0	0	0	0
D	0	0	0	0	1	3	0	1	0
E	0	0	0	0	0	0	0	0	0
F	0	0	0	1	0	0	0	0	0
G	0	0	0	0	4	1	0	0	0
H	0	1	0	0	0	0	0	0	0
I	0	0	1	0	0	1	0	0	0
K	0	0	0	0	0	0	2	1	0
L	0	2	1	8	0	0	0	1	0
M	0	0	0	0	0	0	0	0	0
N	0	0	0	0	1	2	0	0	6
P	0	0	2	0	1	0	1	0	0
Q	0	1	0	0	0	0	0	0	1
R	9	0	0	0	0	0	0	0	0
S	0	0	0	0	1	1	0	2	1
T	0	2	0	0	0	0	1	4	1
V	0	2	1	0	0	0	5	0	0
W	0	0	0	0	0	0	0	0	0
Y	0	0	0	0	0	0	0	0	0

Best Box	R	LTV	A	L	G	D	V	T	N
----------	---	-----	---	---	---	---	---	---	---

Figure 1.

Dest Box	Acc #	Name and Species
RRALSDIKN	D57742	cyclin III maize (Zea mays)
RRALGDIGN	S49904	cyclin common tobacco (Nicotiana tabacum)
RAVLGDISN	S53003	cyclin rape (Brassica napus)
RAPLGNITN	S53004	cyclin rape (Brassica napus)
RRALGVINQ	S56679	cyclin III alfalfa (Medicago sativa)
RASVGSIGN	C57742	cyclin II maize (Zea mays)
RRALGVINQ	CG1B_MEDVA	cyclin B (Medicago varia)
RRALGDIGN	CG21_ANTMA	cyclin A/B garden snapdragon (Antirrhinum majus)
RRALGDIGN	CG22_ANTMA	cyclin A/B garden snapdragon (Antirrhinum majus)
RQYLGDVSN	CG21_CANAL	cyclin B1 (Candida albicans)
RAALGDVSN	CG21_EMENI	cyclin B (Aspergillus nidulans)
RKALGDIGN	CG21_SOYBN	cyclin B soybean (Glycine max)
RTILGNVTN	CG21_YEAST	cyclin B CLB1 budding yeast (Saccharomyces cerevisiae)
RLALNNVTN	CG22_YEAST	cyclin B CLB2 budding yeast (Saccharomyces cerevisiae)
RVALSDVTN	CG23_YEAST	cyclin B CLB3 budding yeast (Saccharomyces cerevisiae)
RVALGDVTS	CG24_YEAST	cyclin B CLB4 budding yeast (Saccharomyces cerevisiae)
RRALTDVPV	CGS5_YEAST	cyclin B CLB5 budding yeast (Saccharomyces cerevisiae)
RTVLSDVSN	CG22_SCHPO	cyclin B Cig2/Cyc17 fission yeast (Schizosaccharomyces pombe)
RHALDDVSN	CG23_SCHPO	cyclin B Cdc13 fission yeast (Schizosaccharomyces pombe)
RVVLGVLTE	CG2A_CARAU	cyclin A goldfish (Carassius auratus)
RAALGTVGE	CG2A_CHICK	cyclin A chicken (Gallus gallus)
RVVLGEISN	CG2A_DAUCA	cyclin A carrot (Daucus carota)
RSILGVIQS	CG2A_DROME	cyclin A fruit fly (Drosophila melanogaster)
RAALAVLKS	CG2A_HUMAN	cyclin A human (Homo sapiens)
RAALKTGNA	CG2A_MESAU	cyclin A golden hamster (Mesocricetus auratus)
RSALGTITN	CG2A_PATVU	cyclin A common limpet (Patella vulgata)
RAALGVITN	CG2A_SPISO	cyclin A atlantic surf-clam (Spisula solidissima)
RQVLGDIGN	CG2B_ARATH	cyclin A/B mouse-ear cress (Arabidopsis thaliana)
RAALGNISN	CG2B_ARBPU	cyclin B sea urchin (Arbacia punctulata)
RCALENISN	CG2B_ASTPE	cyclin B starfish (Asterina pectinifera)
RAALGEIGN	CG2B_CARAU	cyclin B goldfish (Carassius auratus)
RTALSNISN	CG2B_CHLVR	cyclin B hydra (Chlorohydra viridissima)

Figure 2.

RGALSDLTN	CG2B_DICDI	cyclin B CLB1 slime mold (<i>Dictyostelium discoideum</i>)
RAALGDLQN	CG2B_DROME	cyclin B fruit fly (<i>Drosophila melanogaster</i>)
RGALENISN	CG2B_MARGL	cyclin B spiny starfish (<i>Marthasterias glacialis</i>)
RRALGGINQ	CG2B_MEDVA	cyclin B (<i>Medicago varia</i>)
RSALGDIGN	CG2B_PATVU	cyclin B common limpet (<i>Patella vulgata</i>)
RNTLGDIGN	CG2B_SPIISO	cyclin B atlantic surf-clam (<i>Spisula solidissima</i>)
RTVLGVIGD	CGA1_XENLA	cyclin A1 african clawed frog (<i>Xenopus laevis</i>)
RTVLGVLTE	CGA1_MOUSE	cyclin A1 mouse (<i>Mus musculus</i>)
RTVLGVLOE	CGA2_XENLA	cyclin A2 african clawed frog (<i>Xenopus laevis</i>)
RTALGDIGN	CGB1_CRILO	cyclin B1 chinese hamster (<i>Cricetulus longicaudatus</i>)
RTALGDIGN	CGB1_HUMAN	cyclin B1 human (<i>Homo sapiens</i>)
RTALGDIGN	CGB1_MESAU	cyclin B1 golden hamster (<i>Mesocricetus auratus</i>)
RTALGDIGN	CGB1_MOUSE	cyclin B1 mouse (<i>Mus musculus</i>)
RTALGDIGN	CGB1_RAT	cyclin B1 rat (<i>Rattus norvegicus</i>)
RTALGDIGN	CGB1_XENLA	cyclin B1 african clawed frog (<i>Xenopus laevis</i>)
RAVLEEIGN	CGB2_CHICK	cyclin B2 chicken (<i>Gallus gallus</i>)
RAVLEEIGN	CGB2_MESAU	cyclin B2 golden hamster (<i>Mesocricetus auratus</i>)
RAVLEEIGN	CGB2_MOUSE	cyclin B2 mouse (<i>Mus musculus</i>)
RAALGEIGN	CGB2_XENLA	cyclin B2 african clawed frog (<i>Xenopus laevis</i>)
RSAFGDITN	CGB3_CHICK	cyclin B3 chicken (<i>Gallus gallus</i>)

Dest Box	Acc #	Name and Species
RQLFPIPLN	ASE1_YEAST	ASE1 budding yeast (<i>Saccharomyces cerevisiae</i>)
RLPLAAKDN	PDS1_YEAST	PDS1 budding yeast (<i>Saccharomyces cerevisiae</i>)
RAPLGSTKQ	CUT2_SCHPO	CUT2-1 fission yeast (<i>Schizosaccharomyces pombe</i>)
RTVLGGKST	CUT2_SCHPO	CUT2-2 fission yeast (<i>Schizosaccharomyces pombe</i>)

Figure 2. (cont.)


```

#!/usr/local/bin/perl
#####
#This program searches a database by constructing a matrix
#from an input family of related sequences (See Gribskov Meth Enz,
1996
#266:198-212) then uses regular expression pattern matching to search
#the database.
#
#Database format is fasta format with each sequence terminated
#by an asterisk.
# e.g.      >comment
#          ASEDRTYFHGILK*
#This is the current yeast genome database format see http://genome-
#ftp.stanford.edu/ the current yeast database name is
orf_trans.fasta #for all the translated ORF's.
#There is also a companion program "Getnames" that will identify the
#sequences by name and print out descriptions of their known
functions.
#####
#The following sequences are the default matrix
#ASE1      RQLFPIPLN
#PDS1      RLPLAAKDN
#CLB1      RTILGNVTN
#CLB2      RLALNNVTN
#CLB3      RVALSDVTN
#CLB4      RVALGDVTS
#CDC13     RHALDDVSN
#CUT2-1    RAPLGSTKQ
#CUT2-2    RTVLGGKST
#####

@weightedarray = ();
print "Enter family of sequences separated by colons [e.g.
RQLFPIPLN:RLPLAAKDN]\n";
print "Default Family = <CR>\n";
print "\tASE1      RQLFPIPLN\n\tPDS1      RLPLAAKDN\n\tCLB1
RTILGNVTN\n\tCLB2      RLALNNVTN\n\tCLB3      RVALSDVTN\n\tCLB4
RVALGDVTS\n\tCDC13     RHALDDVSN\n\tCUT2-1    RAPLGSTKQ\n\tCUT2-2
RTVLGGKST\n";

chop ($sequences = <>);
print "\nWhich database to search?\n";
chop ($database = <>);
print "\nWhat name for output file?\n";
chop ($outfile = <>);

unless ($sequences) {
    $sequences =
"RQLFPIPLN:RLPLAAKDN:RTILGNVTN:RLALNNVTN:RVALSDVTN:RVALGDVTS:RHALDDVSN
:RAPLGSTKQ:RTVLGGKST";
}

```

Figure 3.

```

# $sequences =
"RRALSDIKN:RRALGDIGN:RAVLGDISN:RAPLGNITN:RRALGVINQ:RASVGS LGN:RRALGVINQ
:RRALGDIGN:RRALGDIGN:RQYLG DVS N:RAALGDVSN:RKALGDIGN:RTILGNVTN:RLALNNVTN
:RVALSDVTN:RVALGDVTS:RRALTDVPV:RTVLS DVS N:RHALDDVSN:RVVLGVLTE:RAALGTVGE
:RVVLGEISN:RSILGVIQS:RAALAVLKS:RAALKTGNA:RSALGTITN:RAALGVITN:RQVLGDIGN
:RAALGNISN:RCALENISN:RAALGEIGN:RTALSNISN:RGALSDLTN:RAALGDLQN:RGALENISN
:RRALGGINQ:RSALGDIGN:RNTLGDIGN:RTVLGVIGD:RTVLGVLTE:RTVLGVLQE:RTALGDIGN
:RTALGDIGN:RTALGDIGN:RTALGDIGN:RTALGDIGN:RAVLEEIGN:RAVLEEIGN
:RAVLEEIGN:RAALGEIGN:RSAFGDITN:RQLFPIPLN:RLPLAAKDN:RAPLGSTKQ:RTVLGGKST
"; #this is all destruction boxes
}
$sequences =~ tr/a-z/A-Z/;
@family = split /:/, $sequences;
print "\nFamily members\n";
foreach $member (@family){
print "$member\n";
@residues = split//, $member;
push @aminoarray, [ @residues ];

#construct array of hashes to use as scoring matrix
$lastres = $#residues;
foreach $res (0 .. $lastres) {
    foreach $m (A .. Z){
        undef $$m;
    }
    for $k (0 .. $#aminoarray){
        for $j (A .. Z) {
            if ("$j" =~ /$aminoarray[$k][$res]/){
                $$j++;
            }
        }
        $scoringmatrix[$res]{$j}="$$j";
    }
}

#print out scoring matrix
undef $maximum;
for $i ( 0 .. $#scoringmatrix ) {
    undef @maxscore;
    for $donut ( keys %{$scoringmatrix[$i] } ) {
        print "$i$donut=$scoringmatrix[$i]($donut) ";
        push (@maxscore, "$scoringmatrix[$i]($donut)");
    }
    @newmaxscore = sort {$b <=> $a} @maxscore;
    $maximum = $newmaxscore[0] + $maximum;
    print "\n";
}
print "\nThe maximum possible score = $maximum\n";
print "\nWhat cutoff score? [Default = 1/2 maximum score]\n";
chop ($cutoff = <>);

```

Figure 3. (cont.)

```

unless ($cutoff) {
    $cutoff = $maximum/2;
}

#search database with amino acid window
open (DATABASE, "$database");
open (OUTFILE, ">$outfile");
while (<DATABASE>) {
    if (/>/) { #gets sequence name
        $matchstring = ();
        $sequencename = $';
        next;
    }else{ #concatenates sequence file into single line
        chop($_);
        $matchstring .= $_;
        next until /\*/;
    }
    while ($matchstring =~ /\w/ig){ #matches each amino acid
        $firstmatch = $&;
        $matchnext = substr($',0,$lastres);
        if ($matchnext =~ /[A-Z]{$lastres}/ig){ #matches next
8 residues
            @weightedarray = split(/ */, $&);
            unshift (@weightedarray, $firstmatch);
            undef $weight;
            for $position (0 .. $lastres) {
                $residueweight =
$scoringmatrix[$position][$weightedarray[$position]];
                $weight = $weight + $residueweight;
#score assignment
            }
            if ($weight > $cutoff){
                push (@namefile, "$weight $firstmatch$&
$sequencename");
            }
        }
    }
}
@sortedlist = sort {$b <=> $a} @namefile; # rank boxes in order of
score
print OUTFILE @sortedlist;
close (DATABASE);
close (OUTFILE);

```

Figure 3. (cont.)

A

BOXSEARCH YEAST ONLY

42 RVALSDVTN YDL155W CLB3
41 RTILGNVTN YGR108W CLB1
41 RLALNNVTN YPR119W CLB2
40 RVALGDVTS YLR210W CLB4
36 RAALSDITN YKL101W HSL1
34 RHALENVTS YNL118C PSU1
34 RTWLHLVTN YLR342W FKS1
34 RDYLGVVSN YIL013C PDR11
33 RLSLDDVTT YDR332W
33 RLILPGVGN YBR248C HIS7

C

FASTA

114.7 RAWGGDVGN YNL277W MET2
113.7 PESIGDVGN YAL009W SPO7
111.6 RAEVSDVGN YAL038W CDC19
111.5 RAEVSDVGN YOR347C ALD7
109.3 LYATGDLGN YCR100C
109.2 RATIGLLGN YPL059W
107.0 RRSLRDIGN YDR130C NoHom
106.3 RVALGDVTS YLR210W CLB4
106.0 QGVLDIGD YOR003W YSP3
106.0 VRHVGDMGN YJR104C SOD1

B

BOXSEARCH

276 RAALSDITN YKL101W HSL1
241 RTILGPIKN YLR163C MAS1
240 RVALSDVTN YDL155W CLB3
240 RAALGKARN YOR019W (YDR474)
239 RRSLRDIGN YDR130C NoHom
238 RKALGVITH YGR002C Sp,At
236 RVALGDVTS YLR210W CLB4
232 RTILGNVTN YGR108W CLB1
230 RPQLGEIPN YDR227W SIR4
230 RMALVNINN YEL046C GLY1

D

PROFILESEARCH

15.40 RTILGNVTNN YGR108W CLB1
15.26 RVALGDVTS YLR210W CLB4
15.08 RVALSDVTN YDL155W CLB3
14.45 RNALGEVS YLR091W
13.43 RQALGSL YJR038C
13.86 RKGLGDLTS YGR226C
13.13 RLVLGKL YDL009C
14.65 RTILGPIKN YLR163C MAS1
12.86 RRRLGD YNL211C
13.31 RATIGLLGN YPL059W

Figure 4.

Appendix B

**Methods for studying the spindle assembly
checkpoint in budding yeast.**

Studying the Spindle Assembly Checkpoint in Budding Yeast

Aaron F. Straight and Andrew W. Murray

Address: Department of Physiology Box0444
School of Medicine
University of California San Francisco
San Francisco, CA 94143-0444

Correspondence: A. Straight
E-mail: straight@cgl.ucsf.edu
Phone: (415) 476-6970
Fax: (415) 476-4929

1. The first part of the document discusses the importance of maintaining accurate records of all transactions and activities. It emphasizes the need for transparency and accountability in financial reporting.

2. The second part of the document outlines the various methods and techniques used to collect and analyze data. It includes a detailed description of the experimental procedures and the tools used for data collection.

3. The third part of the document presents the results of the study, including a comparison of the different methods and techniques used. It discusses the strengths and weaknesses of each method and provides a summary of the findings.

4. The fourth part of the document discusses the implications of the study and provides recommendations for future research. It highlights the need for further investigation into the effectiveness of the different methods and techniques used.

5. The fifth part of the document concludes the study and provides a final summary of the findings. It emphasizes the importance of maintaining accurate records and the need for transparency and accountability in financial reporting.

The results of the study show that the use of the proposed method significantly improves the accuracy and reliability of the data collected. This is particularly evident in the case of the more complex and dynamic systems, where the traditional methods often fail to capture the full range of behavior.

The study also demonstrates that the proposed method is highly flexible and can be adapted to a wide range of different systems and environments. This makes it a valuable tool for researchers and practitioners alike, who are looking for more effective ways to collect and analyze data.

In conclusion, the study has shown that the proposed method is a highly effective and reliable way to collect and analyze data. It is particularly well-suited to the study of complex and dynamic systems, and its use can significantly improve the accuracy and reliability of the data collected.

Introduction

As cells proceed through cycles of growth and division they are often challenged by environmental insult and injury as well as spontaneous errors in cellular processes. The response to cell damage requires that cells sense the damage, arrest the cell cycle, and attempt to repair the lesion. This general process is known as checkpoint control and is a key mechanism cells employ to ensure accuracy and fidelity during cell division (Hartwell and Weinert¹). Recent work demonstrates that a checkpoint regulates mitosis to ensure the faithful construction of the mitotic spindle and the proper segregation of the chromosomes. This mitotic checkpoint, known as the spindle assembly checkpoint, monitors defects in the assembly of the mitotic spindle and failure of the kinetochores of paired sister chromatids to attach to opposite poles of the spindle. In response to spindle depolymerization or incorrect attachment of chromosomes to microtubules, the spindle assembly checkpoint arrests cells at metaphase (reviewed in (Wells²)). By preventing the onset of anaphase until spindle assembly and chromosome alignment are complete, the checkpoint helps to ensure that each daughter cell will receive an equal chromosomal complement.

Studies in the budding yeast, *Saccharomyces cerevisiae*, have genetically defined the spindle assembly checkpoint. A wild type yeast cell will arrest prior to the initiation of anaphase in response to spindle depolymerizing drugs such as nocodazole or benomyl. Li and Murray, and Roberts and Hoyt first identified components of the yeast spindle assembly checkpoint by isolating mutants that could no longer sense spindle depolymerization (*mad1,2* and *3* and *bub1,2* and *3* respectively), and thus

continued through the cell cycle in the absence of a spindle, resulting in death(Li and Murray³, Hoyt, et al.⁴). Two complementary approaches, studies on populations of cells and careful analysis of individual cells, have elucidated the roles of *MAD* and *BUB* genes in sensing and responding to spindle damage and have helped to classify the biochemical and morphological hallmarks of the spindle assembly checkpoint. We describe both types of analysis in the following sections.

Studying the Spindle Assembly Checkpoint in Yeast

The advantage of studying the spindle assembly checkpoint in budding yeast is that mutations exist that abrogate the response to spindle depolymerization. When the spindle is depolymerized, wild type yeast strains fail to initiate anaphase and arrest as large budded cells with a G2 DNA content. This arrest is thought to be due to the inactivation of the machinery that degrades B-type cyclins and proteins involved in holding sister chromatids together(Funabiki, et al.⁵, Yamamoto, et al.⁶, Yamamoto, et al.⁷). The stabilization of B-cyclins results in cells maintaining high Cdc28 kinase activity which prevents the exit from mitosis.

Populations assays for the spindle assembly checkpoint

The plate assay for benomyl sensitivity-

The most easily scored phenotype of a spindle assembly checkpoint mutant is its sensitivity to spindle depolymerizing drugs such as benomyl. This phenotype alone, however is not sufficient to classify a

mutant as checkpoint defective, since many mutants that affect microtubule assembly are also benomyl sensitive (Stearns, et al.⁸). The original checkpoint mutants *mad1*, *mad2*, *mad3*, *bub1*, *bub2* and *bub3* were isolated by looking for cells that would not grow on YPD plates containing benomyl (Li and Murray³, Hoyt, et al.⁴). In order to accurately assay a yeast strain's sensitivity to benomyl it is best to test it on plates containing a range of drug concentrations. YPD plates are made containing 7.5, 10, 12.5 and 15 µg/ml benomyl. Benomyl is very insoluble so the drug must be added to hot YPD media. Benomyl is added from a 10 mg/ml stock in DMSO to YPD agar immediately after autoclaving. Twofold serial dilutions of cells are made starting with a liquid culture at an OD₆₀₀ of 1.0 and equivalent amounts of cells (approximately 20 µl) are "frogged" onto the YPD +benomyl plates using a multiwell inoculating tray and a pronged metal inoculator for transferring reproducible volumes of cell suspensions to an agar plate. (Figure 1A, DanKar Scientific). The plates are incubated at 23°C for 24-48 hours before scoring the growth of the transferred cells as a measure of their sensitivity to the drug. It is best to apply cells in to the benomyl plates as drops of cell suspensions rather than by replica plating since thick patches of cells often give results that are difficult to interpret. This is most likely due to different cells in the patch being exposed to different effective concentrations of the drug. Furthermore, choosing the proper strain background can facilitate later analysis since different strain backgrounds exhibit different sensitivities to benomyl. For example, the A364a strain background is much less sensitive to benomyl than is W303. Figure 1B shows the sensitivities of three different W303 background strains (wild type, *mad2-1* and *tub1-801*) to benomyl. The three strains grow equally well on rich medium lacking benomyl (Figure 1B (top panel)). In the presence of 7.5 µg/ml and 10 µg/ml benomyl the wt strain is still able to grow.

The *mad2-1* strain dies since it cannot respond to the depolymerization of the spindle and continues through mitosis and the *tub1-801* strain dies since it cannot recover from spindle depolymerization and rebuild a proper spindle (Figure 1B middle and lower panels).

The rapid death assay for nocodazole sensitivity-

Although the plate assay isolates cells that are sensitive to spindle depolymerizing drugs it does not distinguish between checkpoint mutations and other mutations that cause drug sensitivity. Unlike *mad* or *bub* mutants, nocodazole sensitive mutants that affect microtubule stability cannot proliferate in the presence of benomyl but are not involved directly in the checkpoint (Straight, et al.⁹). One way to distinguish between checkpoint and microtubule assembly mutants is to assay the rates at which they die when exposed to nocodazole. Starting with cells that are logarithmically growing (OD₆₀₀ = 0.3-0.6), the cells are harvested and resuspended in YPD containing 15µg/ml nocodazole. Nocodazole is much more soluble than benomyl and is also more effective in activating the checkpoint in liquid medium than benomyl. Two hundred cells are plated on a YPD plate at 0, 3 and 6 hours after nocodazole addition. Once colonies have formed, viability after exposure to nocodazole is calculated by dividing the number of colonies formed at time 0, 3 or 6 hours by the number formed at time 0. Strains that aggregate should be lightly sonicated to disperse cell clumps before plating. The rate of death in the presence of nocodazole is an excellent indicator of checkpoint deficiency. Wild type cells maintain high viability over the 6 hour period of exposure to nocodazole. Checkpoint mutants die very rapidly often showing a 75% or greater loss of viability after three hours and a greater

than 95% loss of viability after 6 hours. Mutants that decrease microtubule stability, such as tubulin mutants, however, die more slowly when exposed to nocodazole, with significant inviability only apparent 6 hours after exposure (Figure 2). The rapid rate of death of a checkpoint mutant presumably reflects its passage through mitosis in the absence of a spindle. Although treatment of *mad* mutants with benomyl leads to a high frequency of chromosome loss, it is not possible to rigorously demonstrate that death is due to errors in chromosome segregation.

Analysis of Cyclin levels and Cdc28 kinase activity-

Wild type yeast arrest in mitosis upon exposure to nocodazole or benomyl. This arrest is maintained through the stabilization of the B-type cyclins and the elevation of cyclin B-associated Cdc28 kinase activity. Analysis of the levels of Clb2 protein (the primary mitotic cyclin in yeast) and the activity of Clb2-associated Cdc28 kinase activity serves as an excellent marker for checkpoint arrest. Logarithmically growing yeast cells are arrested in G1 by treating them with 10 μ g/ml α -factor in YPD for 3 hours at 24°C. Cells are then released from α factor into YPD containing 15 μ g/ml nocodazole and 1.5ml samples are harvested every 10 minutes, pelleted by centrifugation for 10 seconds in an eppendorf centrifuge and the cells pellets are frozen in liquid nitrogen. α factor is added back to the medium 60 minutes after the initial α factor release to ensure that cells do not proceed into a second cell cycle. Harvested samples are lysed in 170 μ l lysis buffer (50mM Hepes pH 7.6, 50mM Na-beta-glycerolphosphate, 150mM KCl, 50mM NaF, 1mM EDTA, 1mM EGTA, 0.2% Tween-20, 1mM PMSF, and 10 μ g/ml each of leupeptin, pepstatin and chymostatin) by mechanical disruption using glass beads. Cells



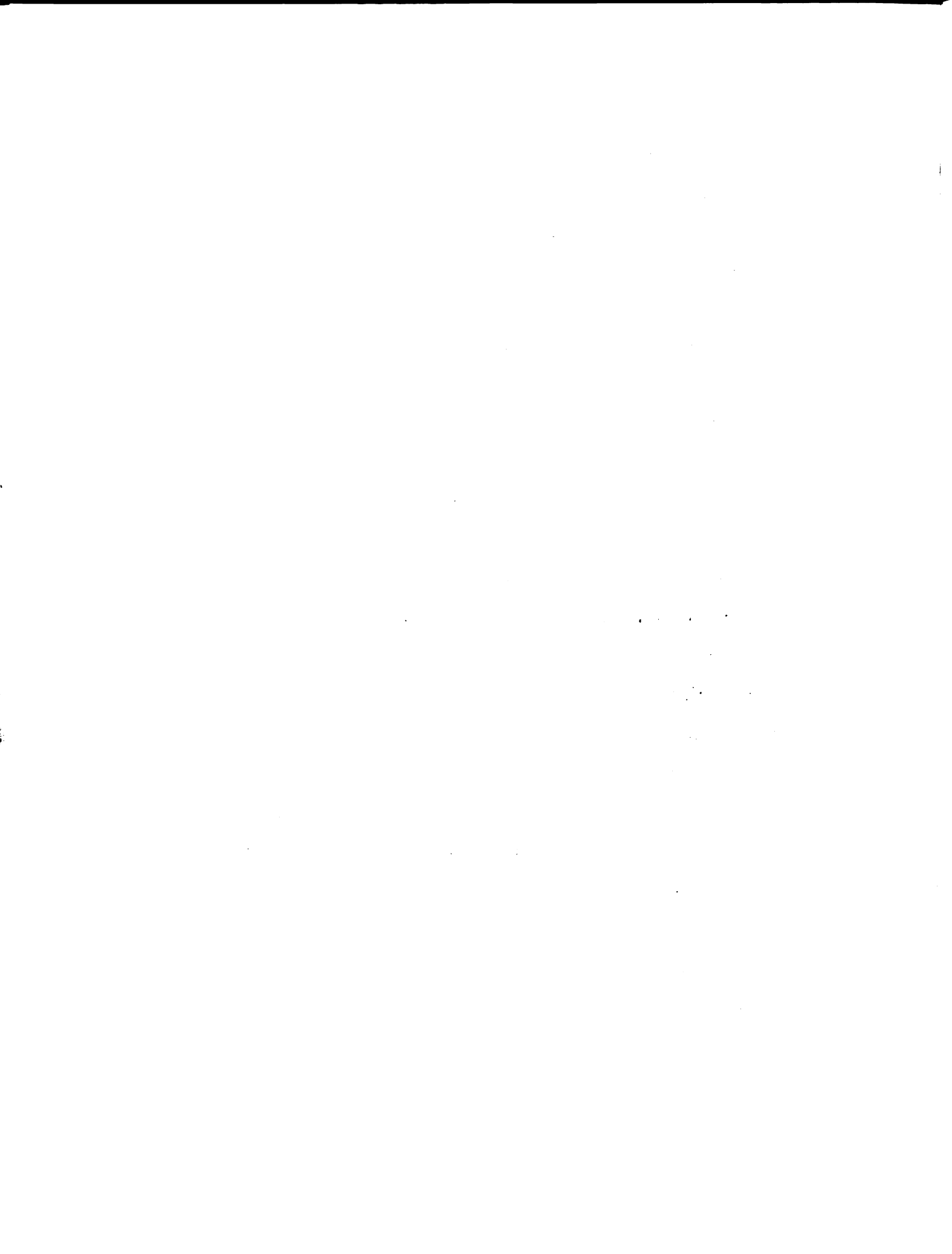
are disrupted by adding an approximately equal volume of acid washed glass beads to the yeast in lysis buffer and vigorously agitating the mixture of beads and yeast in a Bead Beater (Biospec Products) for 1-3 minutes. Lysates are spun for 5 minutes in a microfuge at top speed and supernatants transferred to a new tube. Samples are equalized for protein concentration by Bradford Assay (Bradford¹⁰) and 15-30 μ g of total protein is denatured in SDS-PAGE sample buffer for analysis of Clb2 protein levels by western blotting. Clb2 and the associated Cdc28 kinase are immunoprecipitated from 100-200 μ g of the remaining undenatured lysate and analyzed for kinase activity against histone H1. Clb2 antibody (0.5-1.0 μ g) is added to the lysate in a total volume of 400 μ l and incubated for 1 hour at 4°C to allow antibody binding. Once the antibody is bound, 10 μ l of ProteinA Sepharose beads (Pharmacia, Cat#17-0469-01) that have been equilibrated in lysis buffer are added and the mixture is incubated 1 hour at 4°C. The beads are spun out of the lysate and washed twice with 400 μ l wash buffer (50mM Hepes pH7.6, 50mM Na-beta-glycerolphosphate, 250mMKCl, 50mM NaF, 1mMEDTA, 1mM EGTA, and 0.1% NP-40). After the second wash, the beads are transferred to a new tube and washed once more with wash buffer. For H1 kinase assays, the beads are washed in 400 μ l kinase reaction buffer (80 mM Na-b-glycerophosphate pH 7.4, 15 mM MgCl₂, 20 mM EGTA) then resuspended in 10 μ l kinase reaction buffer containing 1mM DTT, 200 μ M ATP, 2.5 μ g histone-H1 (Boehringer-Mannheim), and 1 μ Ci of g-³²P-ATP. The mixture is incubated for 10 minutes at 30°C then the reaction is stopped by adding 10 μ l of 2X Laemmli sample buffer. The reactions are electrophoresed on a 15% SDS-polyacrylamide gel, dried, and autoradiographed.

Wild type cells released from alpha factor into nocodazole accumulate Clb2 and its associated kinase activity (Figure 3A left panel). However,

checkpoint deficient mutants do not sense that the spindle has been disrupted and continue through mitosis into the subsequent alpha factor block. This is clear from the drop in Clb2 (Figure 3A right panel) and Clb2 associated kinase levels (Figure 3B right panel)(Minshull, et al.¹¹). As it does in the rapid death assay, a tubulin mutant behaves like wild type in these assays maintaining high levels of Clb2 and Clb2-associated H1 kinase activity (data not shown). Thus it is clear that one of the primary defects in a checkpoint mutant is its inability to activate the mitotic arrest characteristic of wild type yeast cells.

Hyperphosphorylation of Mad1 protein-

Although the activation of Cdc28 and the high levels of Clb2 serve as general markers for cells in mitosis, the phosphorylation of the Mad1 protein serves as a specific marker for cells that have activated the mitotic checkpoint. The Mad1 protein is normally phosphorylated at a low level throughout the cell cycle. When the spindle assembly checkpoint is activated, the Mad1 protein becomes hyperphosphorylated and its mobility in SDS-PAGE gels decreases(Hardwick and Murray¹²). To assay the modification of Mad1, logarithmically growing cells are treated with 15µg/ml nocodazole for 3 hours at 23°C. Cells are then harvested by centrifugation and broken by mechanical shearing with glass beads in Laemmli sample buffer. Cell lysates are separated on an SDS-PAGE gel, transferred to nitrocellulose, and then blotted for Mad1 protein using Mad1-specific antibodies (Figure 4). Mad1 protein shows a dramatic shift in mobility in wild type cells that are treated with nocodazole indicating that the checkpoint has been activated. The hyperphosphorylation of Mad1 also serves as an excellent marker for epistatic ordering of genes involved in the checkpoint pathway. Examination of Mad1



hyperphosphorylation in *mad2*, *bub1*, *bub2* and *bub3* mutants suggests that the Bub1 and Bub3 proteins lie upstream of the Mad1 protein, that Mad2 functions upstream or in concert with Mad1, and that Mad3 functions downstream of the Mad1 protein in the spindle assembly checkpoint pathway (Figure 4).

FACS analysis of DNA content-

When the spindle assembly checkpoint is activated, yeast cells arrest with a 2C DNA content indicating that replication is complete but anaphase chromosome separation, cytokinesis, and initiation of the next round of DNA synthesis have not occurred. Checkpoint deficient mutants, however, continue through mitosis in the absence of a spindle and start another round of replication resulting in cells with 4C DNA content (Weiss and Winey¹³). The simplest assay for DNA content in yeast is by fluorescence activated cell scanning (FACS). A logarithmically growing population of cells is arrested in G1 before replication by treatment with 10µg/ml alpha factor for 3 hours at 23°C. Cells are then released from alpha factor into media containing 15µg/ml nocodazole and 1 ml samples are taken every 10 minutes to assay total cellular DNA content. At each timepoint, cells are harvested and fixed in 70% Ethanol for 1 hour. Samples are washed twice in 50mM Tris pH 7.5 then digested with 1mg/ml RNaseA in 50mM Tris pH 7.5 for 4 hours at 37°C followed by 40µg/ml Proteinase K for 1 hour at 55°C. Digested cells are then stained with 50µg/ml propidium iodide and lightly sonicated to separate aggregated cells. The cells are then analyzed by conventional flow cytometry to assay the DNA content. A wild type population of cells starts with a 1C DNA content and as it proceeds through replication increases to a 2C DNA

content. Cells then arrest with 2C DNA content before mitosis (Figure 5 (wild type)). Checkpoint deficient mutants proceed through replication as wild type cells do, but rather than arresting at mitosis, continue through the next G1 and replicate their DNA again (Figure 5 (*mps1-1* and *mad1-1*)). Since cell cycle progression occurs in the absence of a spindle, chromosomes are mis-segregated and the cells progress to 4C DNA content or become aploid.

Morphological and Single Cell Studies

Analysis of the behavior of single cells in response to spindle depolymerization reveals aspects of the spindle assembly checkpoint not observed in studies of cell populations.

The Rebudding Assay -

Wild type yeast cells arrest in response to checkpoint activation as large budded cells in mitosis (Figure 6A left panel). Because mutants in the checkpoint continue through the cell cycle in the absence of a spindle they eventually pass through the subsequent G1 and generate new buds (Hoyt, et al.⁴). This rebudding is clearly seen as cells that have two rather than one bud (Figure 6A right panel). Logarithmically growing cells are placed in the presence of 15µg/ml Nocodazole for 0, 3 and 6 hours. At each timepoint cells are fixed in 3.7% formaldehyde for 1 hour at room temperature. Cells are then vortexed vigorously or sonicated lightly to disperse cell clumps, examined by bright field, phase contrast, or DIC microscopy and categorized

into unbudded, large budded and multibudded groups. A wild type cell arrests in nocodazole and maintains greater than 80% of the cells as large budded even after 6 hours in nocodazole. *Mad* mutants, however, continue through the cell cycle and rebud as shown in Figure 6B.

Formation of Microcolonies -

A distinguishing characteristic of checkpoint mutants is that in the presence of activators of the checkpoint the mutants divide faster than wild type cells. These rapid divisions result in death but can be used as a valuable assay to monitor checkpoint defects. As *mad* or *bub* mutant cells go through rapid divisions on plates containing benomyl they give rise to microcolonies containing 5-50 cells. Wild type cells show a mitotic delay in the presence of benomyl, and thus proliferate slower, giving rise to microcolonies containing fewer cells (Li and Murray³). Logarithmically growing cultures of cells are arrested in G1 by treatment with a-factor for 3 hours then streaked in a narrow line onto a plate containing 7.5 μ g/ml of benomyl. From the streak of cells, 25-50 arrested cells are micromanipulated into a grid onto the rest of the plate (Figure 7A). After micromanipulation, each cell in the grid is scored every three hours for the number of cells produced from each progenitor. From these experiments it is clear that checkpoint mutants initially divide rapidly forming small but dead colonies (Figure 7B (*mad2-1*)). Wild type cells delay in mitosis (Figure 7B (wt)) but eventually recover from the delay and, after a day or two, form true colonies. Mutants in tubulin will arrest in mitosis but do not have the ability to recover from the arrest and thus remain as a single large budded cell (data not shown).

Pedigree Analysis of Mitotic Delays -

Most of the techniques employed to study the spindle assembly checkpoint in yeast depend on microtubule depolymerization to activate the checkpoint. Chromosome missegregation and kinetochore detachment from microtubules are also important activators of the spindle assembly checkpoint. Pedigree analysis of yeast chromosome segregation has been described previously (Murray and Szostak¹⁴). The use of pedigree analysis to monitor the delay caused by chromosome missegregation has helped to elucidate the role of the yeast kinetochore in the control of mitosis. Initial experiments by Wells and Murray monitored the cell cycle delay in cells containing a short linear minichromosome (a linear plasmid with a centromere, telomeres and a selectable marker) (Wells and Murray¹⁵). A logarithmically growing population of cells containing the minichromosome is streaked onto YPD plates. From the initial streak, small budded cells are micromanipulated into a line of individual cells separated by 5 mm from one another on another region of the plate. As cells complete cell separation, the mother and daughter cells are separated from one another and the daughter cell is moved to another location on the plate. This process is repeated for 4 divisions to generate a pedigree of 16 cells. The total time taken to traverse the cell cycle is recorded and the cells are allowed to grow into colonies. Colonies are then replica plated to selective medium to determine which divisions occurred in the presence or absence of the minichromosome (Figure 8A). These experiments demonstrate that wild type cells lacking the short linear minichromosome divide faster than wild type cells containing the minichromosome (Figure 8B (compare *MAD*, plasmid-free and plasmid-bearing cells)). If the same experiment is done in a checkpoint deficient

background, the delay caused by the linear minichromosome disappears demonstrating that the presence of the minichromosome activates the spindle assembly checkpoint (Figure 8B (compare *mad1*, 2 and 3 , plasmid-bearing cells to *MAD* , plasmid bearing cells)).

Visualization of Chromosome Separation -

A significant problem in the study of yeast mitosis is the inability to visualize individual yeast chromosomes by conventional microscopic techniques. Using a novel technique to specifically fluorescently label yeast chromosomes in living cells, we have examined the effect of checkpoint mutations on chromosome separation and segregation. A large tandem array of 256 Lac operator binding sites was constructed by Robinett et al (Robinett, et al.¹⁶). Taking advantage of the high specificity of Lac repressor binding to the Lac operator and the intrinsic fluorescence of the Green Fluorescent Protein (GFP), we constructed fusions of the Lac repressor, GFP, and the SV40 nuclear localization sequence (GFP-LacI). We then integrated the array of operator binding sites into the yeast genome near the centromere of chromosome III and expressed the GFP-LacI fusion under control of the yeast *HIS3* promoter in these yeast cells. Transcription from the yeast *HIS3* promoter is low in rich medium, induced to moderate levels in medium lacking histidine, and strongly induced in cells treated with the histidine analog 3-aminotriazole (Struhl and Kill¹⁷) allowing the levels of expression of the GFP-LacI fusion to be regulated. Once expressed, the GFP-LacI enters the nucleus, binds to the tandem array in the yeast genome and the chromosomal locus can be visualized by imaging the fluorescence from the GFP-LacI fusion by conventional fluorescence microscopy (Straight, et al.⁹, Robinett, et al.¹⁶).

Logarithmically growing cells containing the GFP-LacI fusion and the tandem lac operator array are induced with 10mM 3-aminotriazole for 30 minutes at 23°C in complete synthetic medium lacking histidine (CSM-HIS) to induce strong expression of the GFP-LacI fusion. Following GFP-LacI induction the cells are placed in YPD containing 15µg/ml nocodazole and timepoints are taken at 0, 3 and 6 hours. At each timepoint cells are fixed for 30 minutes in 3.7% formaldehyde then resuspended in phosphate buffered saline pH7.2 containing 1mM EDTA. Fixed cells are examined by conventional fluorescence microscopy and the number of cells with separated sister chromatids is quantified. When the spindle assembly checkpoint is activated in a wild type yeast cell, the cell arrests with a single large bud and its sister chromatids still linked, prior to anaphase chromosome separation (Figure 9A (wt) and 9B (top panel)). A nocodazole sensitive tubulin mutant also arrests in mitosis with unseparated sisters (Figure 9A (tub1-801) and 9B (middle panel)), demonstrating that the checkpoint is still intact. In a checkpoint deficient mutant, the sister chromatid linkage is dissolved as cells proceed through anaphase in the absence of a spindle. This is easily seen as the sister chromatids separate and two fluorescent spots appear rather than one (Figure 9A (*mad2-1*) and 9B (bottom panel)). Since there is no active segregation apparatus, the sister chromatids passively separate and remain in the mother cell.

Conclusions

The spindle assembly checkpoint has been best characterized in the budding yeast, *Saccharomyces cerevisiae*. Analysis of *mad* and *bub* mutants has revealed some of the biochemistry controlling checkpoint arrest and the

response to spindle depolymerization. The analysis of cell populations and single cells demonstrates that the cell cycle proceeds in spindle assembly checkpoint mutants and that the yeast cell is exquisitely sensitive to perturbations in the spindle and the kinetochore. It is still unclear why spindle assembly checkpoint mutants die so rapidly when the spindle is depolymerized. It may be that chromosome missegregation is the primary defect in checkpoint mutants exposed to spindle damage or there may be an as yet unidentified cell cycle event causing cell death. To date, the spindle assembly checkpoint has been primarily analyzed by studying the behaviors of cells and cell populations. However, the tools are now well established to begin unraveling the biochemical events underlying the spindle assembly checkpoint.

Acknowledgements

We wish to thank Hironori Funabiki, Sue Biggins, Marion Shonn, and Alison Farrell for assistance and critical review, and Mark Winey, Eric Weiss, Jeremy Minshull, Adam Rudner, Kevin Hardwick and Bill Wells for supplying data. This work was supported by grants from NIH, the Packard Foundation, and the March of Dimes to AWM. AWM is a David and Lucile Packard Fellow.

References

1. L.H. Hartwell and T.A. Weinert, Science, **246** 629 (1989).
2. W.A.E. Wells, Trends in Cell Biol., **6** 228 (1996).
3. R. Li and A.W. Murray, Cell, **66** 519 (1991).
4. M.A. Hoyt, L. Trotis and B.T. Roberts, Cell, **66** 507 (1991).
5. H. Funabiki, H. Yamano, K. Kumada, K. Nagao, T. Hunt and M. Yangida, Nature, **381** 438 (1996).
6. Y. Yamamoto, A., V. Guacci and D. Koshland, J. Cell Biol., **133** 99 (1996).
7. A. Yamamoto, V. Guacci and D. Koshland, J. Cell Biol., **133** 85 (1996).
8. T. Stearns, M. Hoyt, A. and D. Botstein, Genetics, **124** 251 (1990).
9. A.F. Straight, C.C. Robinett, A.S. Belmont and A.W. Murray, Curr. Biol., In press. (1996).
10. M. Bradford, Anal. Biochem., **72** 248 (1976).
11. J. Minshull, A. Straight, A. Rudner, A. Dernburg, A. Belmont and A.W. Murray, Curr. Biol., In press. (1996).
12. K. Hardwick and A.W. Murray, J. Cell Biol., **131** 709 (1995).
13. E. Weiss and M. Winey, J. Cell Biol., **132** 111 (1996).
14. A.W. Murray and J.W. Szostak, Cell, **34** 961 (1983).
15. W.A.E. Wells and A.W. Murray, J. Cell Biol., **133** 75 (1996).
16. C.C. Robinett, A.F. Straight, G. Li, C. Wilhelm, G. Sudlow, A.W. Murray and A. Belmont, J. Cell Biol., Submitted. (1996).
17. K. Struhl and D.E. Kill, Mol. Cell Biol., **7** 104 (1987).

Figure Legends

Figure 1 - *mad* and *tub* mutants are sensitive to benomyl.

A) The inoculating tray and stamp used to frog reproducible quantities of cells onto yeast plates. An aliquot of liquid culture of each strain is placed in the rightmost row of cavities, and serial dilutions are performed using the rows of cavities to the left of the one containing the initial aliquot. The 32 pronged metal device is used to transfer an aliquot of the cells in each cavity to the surface of an agar plate. B) Wild type, *mad2-1*, and *tub1-801*, cells were serially diluted twofold from a culture at OD₆₀₀=1.0, with the highest concentration of cells furthest to the right. Cells were stamped onto YPD plates or YPD plates containing benomyl. Wild type cells show growth on all plates while *mad2-1*, and *tub1-801*, cells do not grow on plates containing benomyl.

Figure 2 - *mad* mutants die rapidly in the presence of nocodazole.

Logarithmically growing cultures of wt, *mad2-1*, and *tub1-801* were treated with 15ug/ml of nocodazole in liquid YPD medium and cells were plated for viability at 0, 3 and 6 hours on YPD plates lacking nocodazole. The fraction of viable cells was calculated relative to the number of viable cells at time 0.

Figure 3 - Checkpoint deficient mutants fail to stabilize Clb2 and Clb2 associated H1 kinase in nocodazole.

Wild type or *mad2Δ* cells were released from a-factor arrest into nocodazole and timepoints were taken every thirty minutes (time 30 omitted). A) Western blot of Clb2 levels. The position of the Clb2 protein is indicated. B) Clb2-associated H1 kinase levels measured by a phosphorimager. Histone H1 was phosphorylated using the associated kinase from immunoprecipitations with anti-Clb2 antibodies.

Figure 4 - Mad1 is hyperphosphorylated when the checkpoint is activated.

Logarithmically growing wild type, *mad1, 2, and 3*, and *bub1, 2, and 3* cells were treated with 15 ug/ml benomyl for 3 hours then assayed for modification of Mad1 protein by western blotting. The presence or absence of benomyl is indicated by the + or - sign respectively. The Mad1 protein band is indicated.

Figure 5 - Checkpoint mutants proceed into another round of DNA replication in the presence of nocodazole.

Wild type *mps1-1*, and *mad1-1* cells were arrested in G1 by treatment with a-mating factor. Cells were then released at 37°C (the nonpermissive temperature for *mps1-1*) into medium containing 15ug/ml of nocodazole. Timepoints were taken every 30 minutes and analyzed by FACS. Arrows indicate G1 and G2 DNA content.

1. The first part of the document discusses the importance of maintaining accurate records of all transactions and activities. It emphasizes that this is crucial for ensuring transparency and accountability in the organization's operations.

2. The second part of the document outlines the various methods and tools used to collect and analyze data. It highlights the need for consistent and reliable data collection processes to support informed decision-making.

3. The third part of the document focuses on the role of technology in modern data management. It discusses how advanced software solutions can streamline data collection, storage, and analysis, leading to more efficient and accurate results.

4. The fourth part of the document addresses the challenges associated with data management, such as data quality, security, and privacy. It provides strategies to mitigate these risks and ensure that data is used responsibly and ethically.

5. The fifth part of the document concludes by summarizing the key findings and recommendations. It stresses the importance of ongoing monitoring and evaluation to ensure that data management practices remain effective and up-to-date.

Figure 6 - Checkpoint mutants continue to bud in the presence of nocodazole.

Logarithmically growing cultures of wild type, *mad2-1*, and *tub1-801* cells were treated with 15ug/ml of nocodazole and harvested at 0, 3 and 6 hours.

A) *mad2-1* cells continue to bud in the presence of nocodazole as shown by the presence of two buds rather than one, in this image taken 6 hours after the start of nocodazole treatment. B) The percentage of cells with multiple buds was calculated at 0, 3 and 6 hours.

Figure 7 - Checkpoint mutants divide faster than wild type cells in the presence of benomyl.

A) Cells were micromanipulated into a grid on a plate containing 7.5µg/ml benomyl. B) The number of cells and buds in each colony is counted at various times after micromanipulation. The number of colonies with greater than 2 cells plus buds/colony is shown at each timepoint.

Figure 8 - Checkpoint mutants fail to delay in the presence of linear centromere containing plasmids.

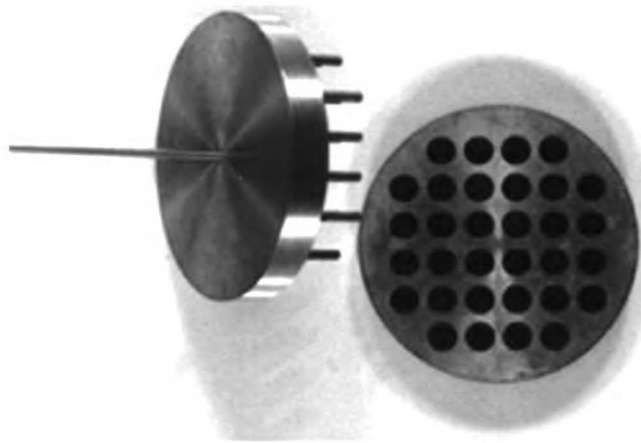
A) Cells containing a short linear minichromosome are micromanipulated into a line with each cell separated by 5mm. At each generation, daughter cells are separated from mother cells and moved to another region of the

plate (these movements are vertical on the figure as shown). After four generations the cells are allowed to form colonies and the presence or absence of the linear centromeric mini-chromosome is assayed by replica plating to selective medium. B) The total number of divisions with and without the linear minichromosome and the percentage of those divisions that exhibit a delay is shown for wild type, *mad1*, *mad2*, and *mad3* strains.

Figure 9 - Sister chromatids separate prematurely in checkpoint mutants.

A direct fluorescent method for analyzing sister chromatid separation. Wild type, *mad2-1*, and *tub1-801* cells containing chromosome III marked with the Lac operator array and expressing the GFP-Lac repressor fusion were treated with 15ug/ml of nocodazole and assayed for sister chromatid separation at 0, 3 and 6 hours. A) Separation of sister chromatids assayed as the percentage of cells with two fluorescent dots at 0, 3, and 6 hours after nocodazole treatment. B) GFP fluorescence (left panels) and DIC (differential interference contrast) images (right panels) are shown. WT yeast cells treated with nocodazole for 3 hours (top panels). Both cell pairs show a single fluorescent dot. *tub1-801* cells treated with nocodazole for 3 hours (center panels). Both cell pairs show a single fluorescent dot. *mad2-1* cells treated with nocodazole for 3 hours (bottom panels). Two cell pairs show two fluorescent dots and one shows a single dot.

A



B

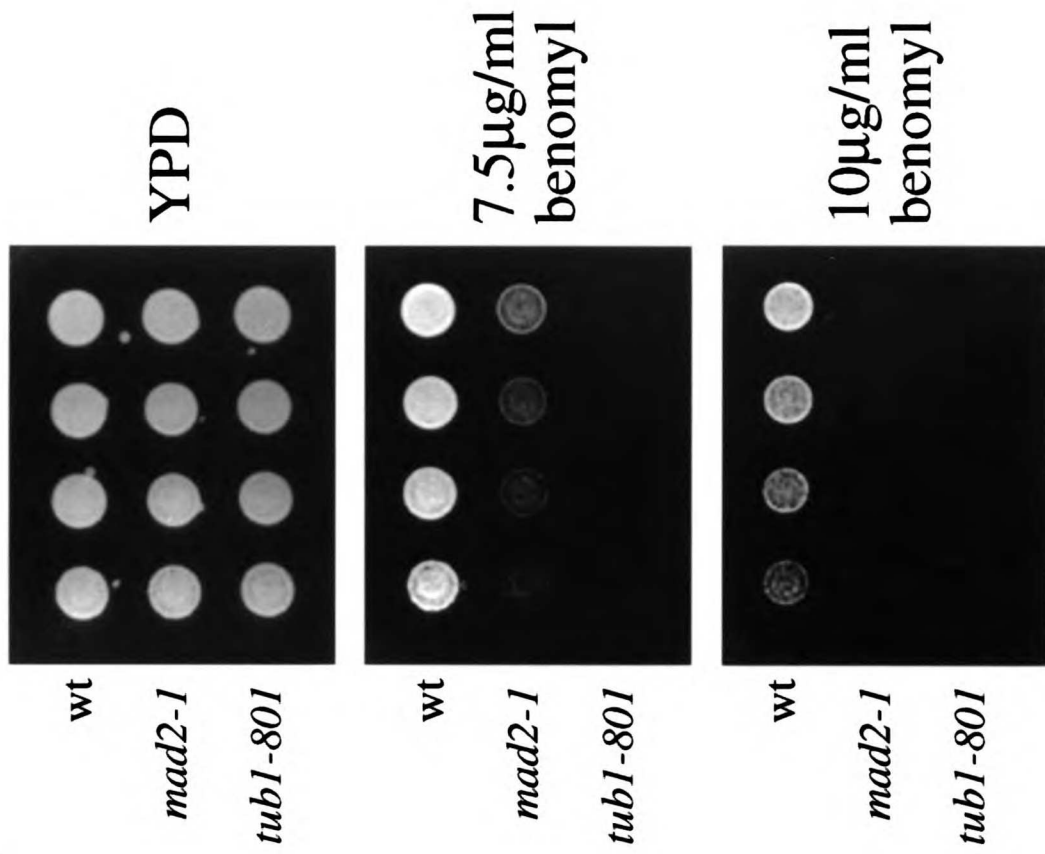


Figure 1. Straight and Murray

Rapid Death Assay

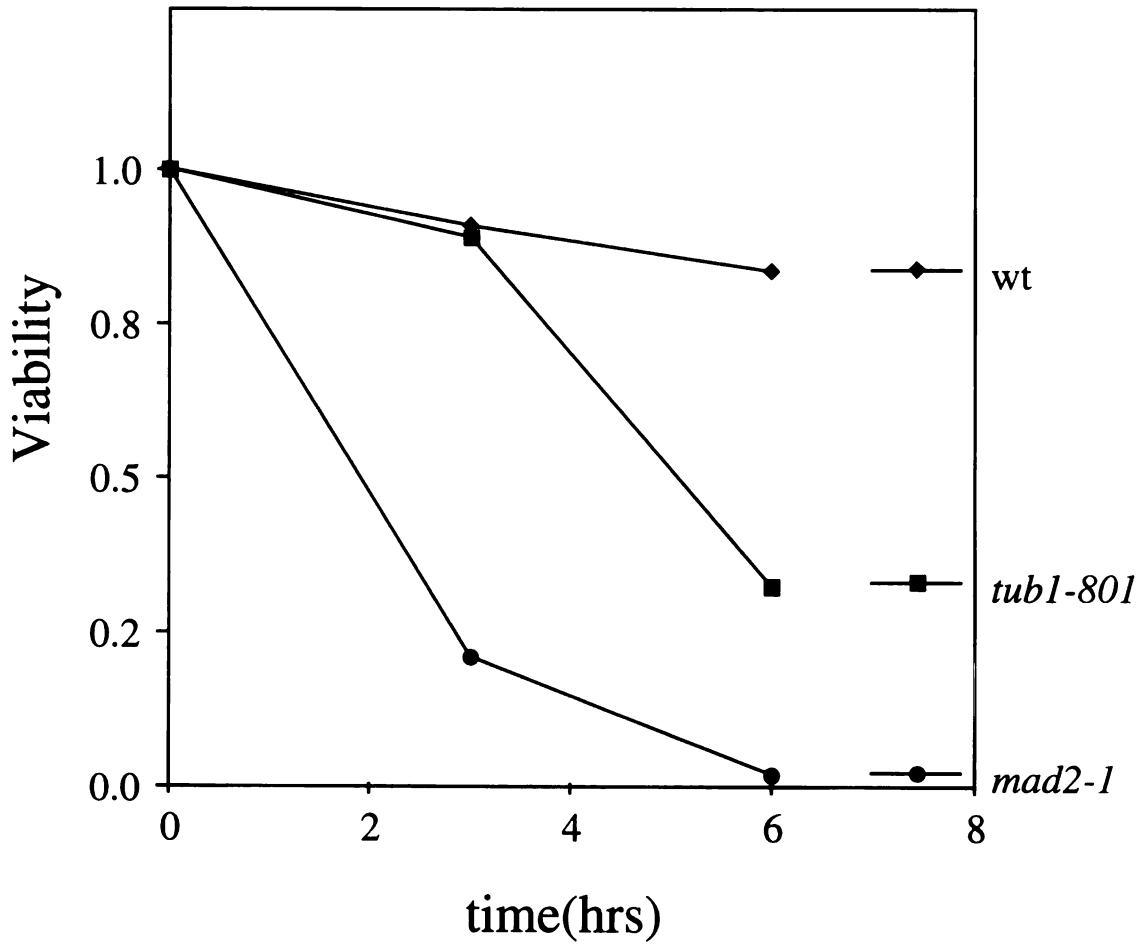


Figure 2. Straight and Murray

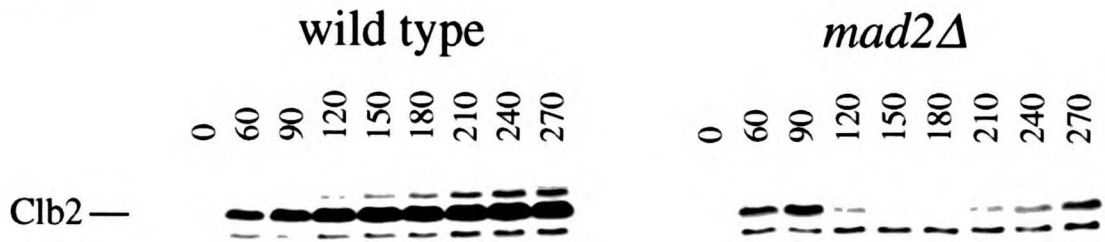
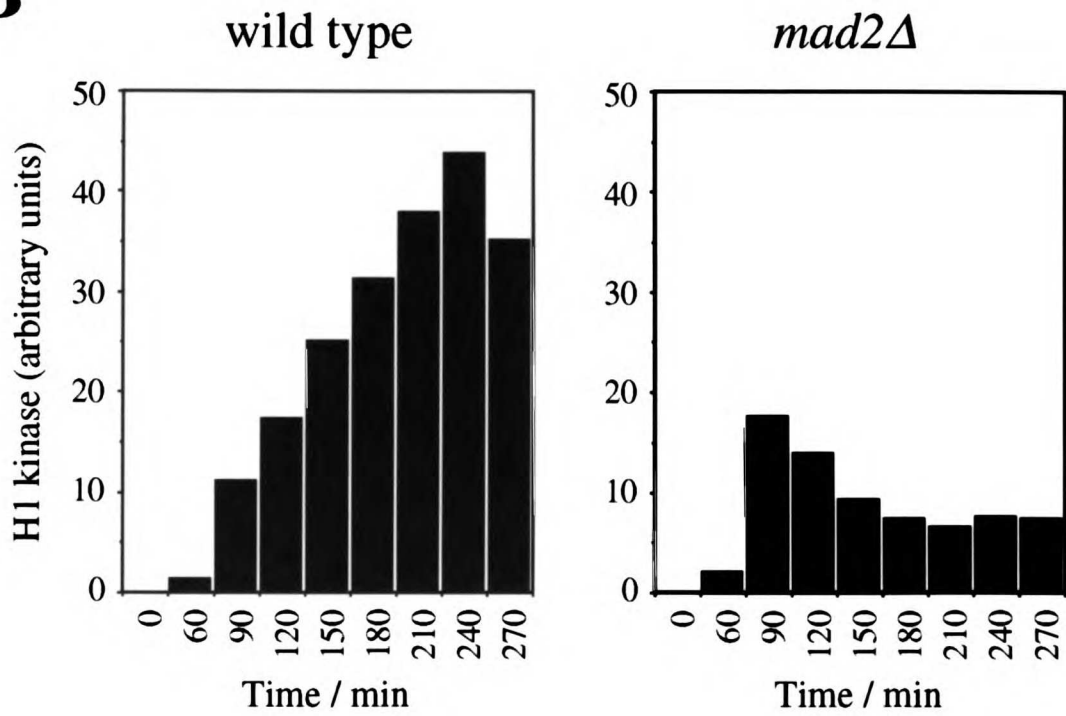
A**B**

Figure 3. Straight and Murray

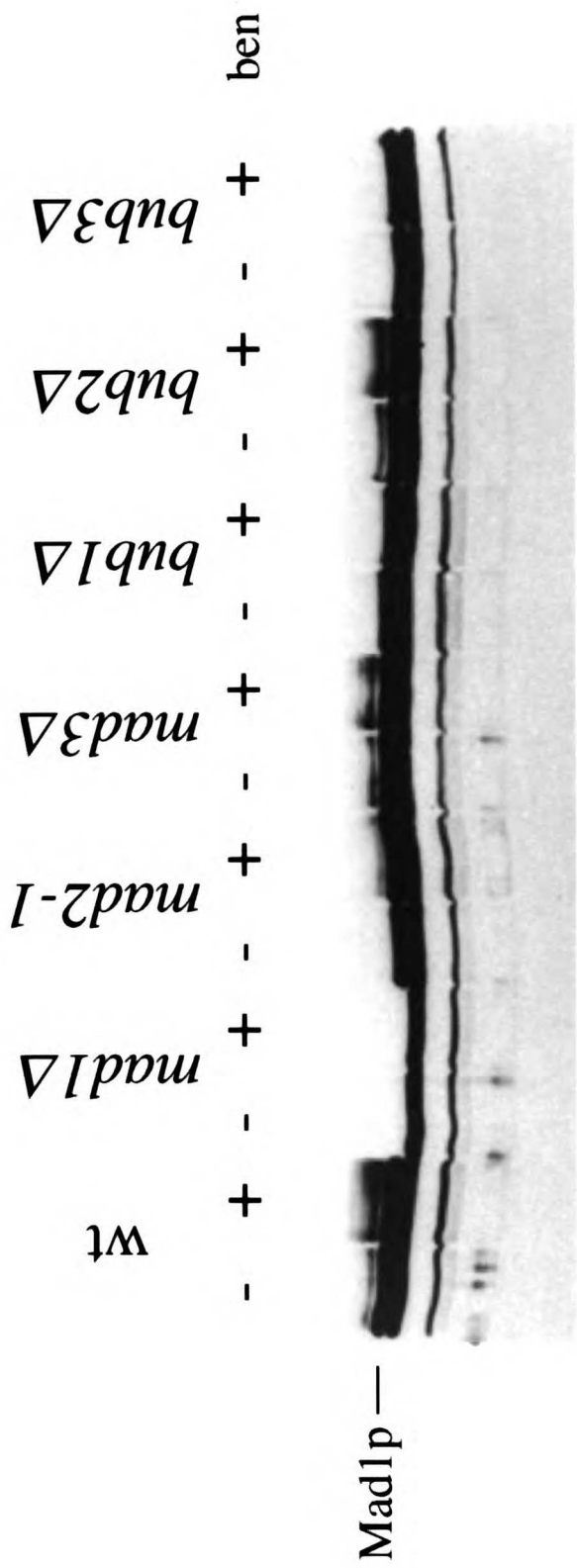


Figure 4. Straight and Murray

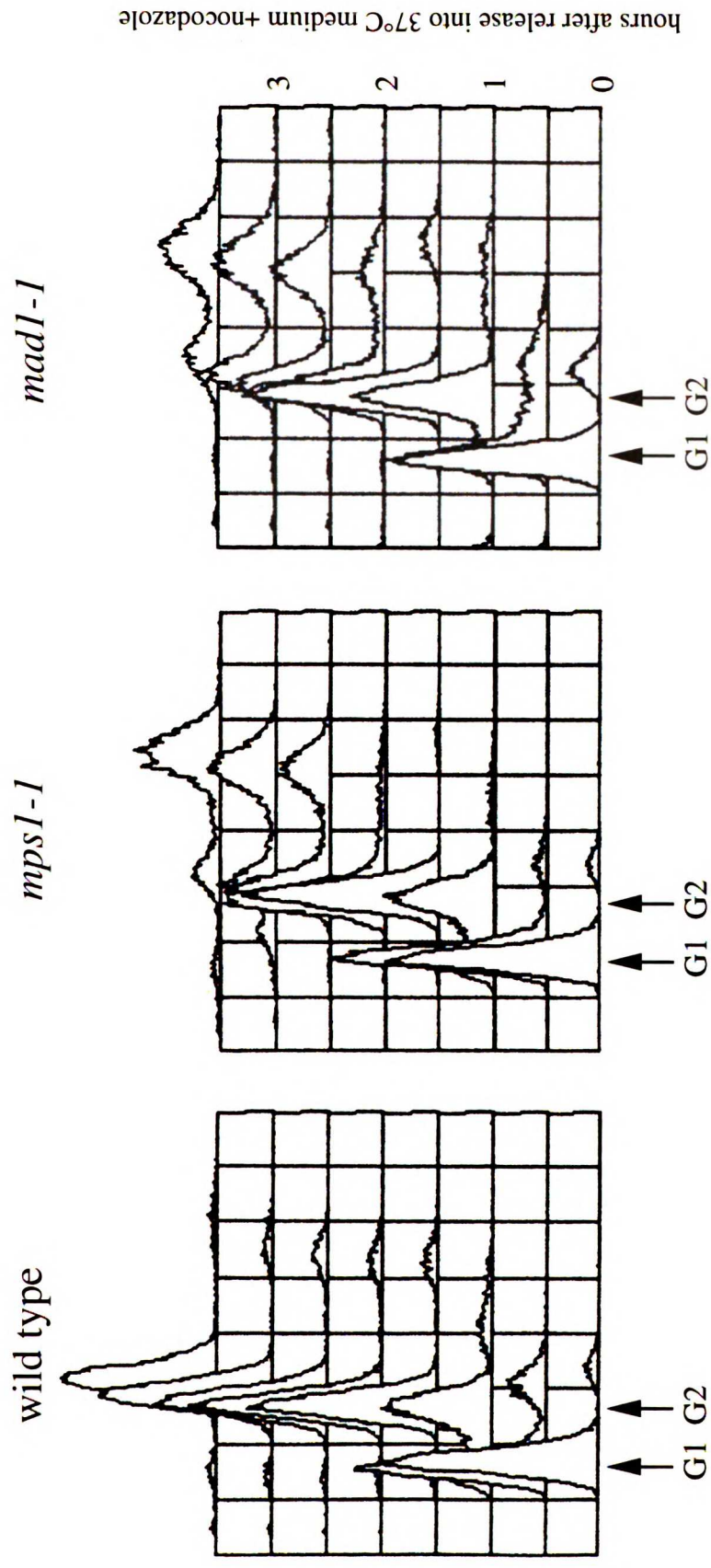


Figure 5. Straight and Murray

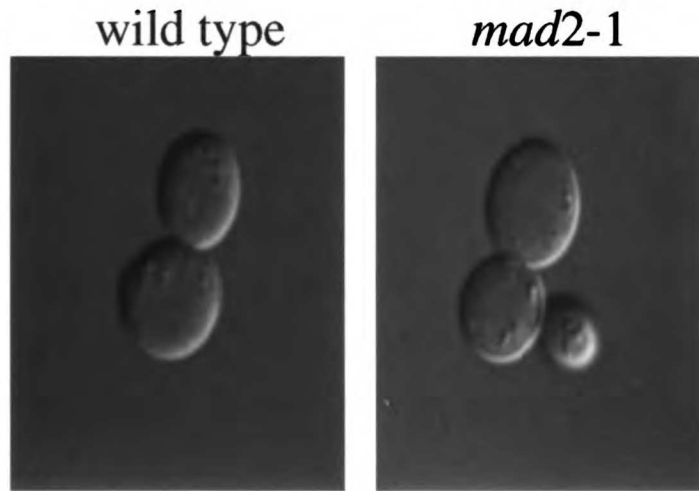
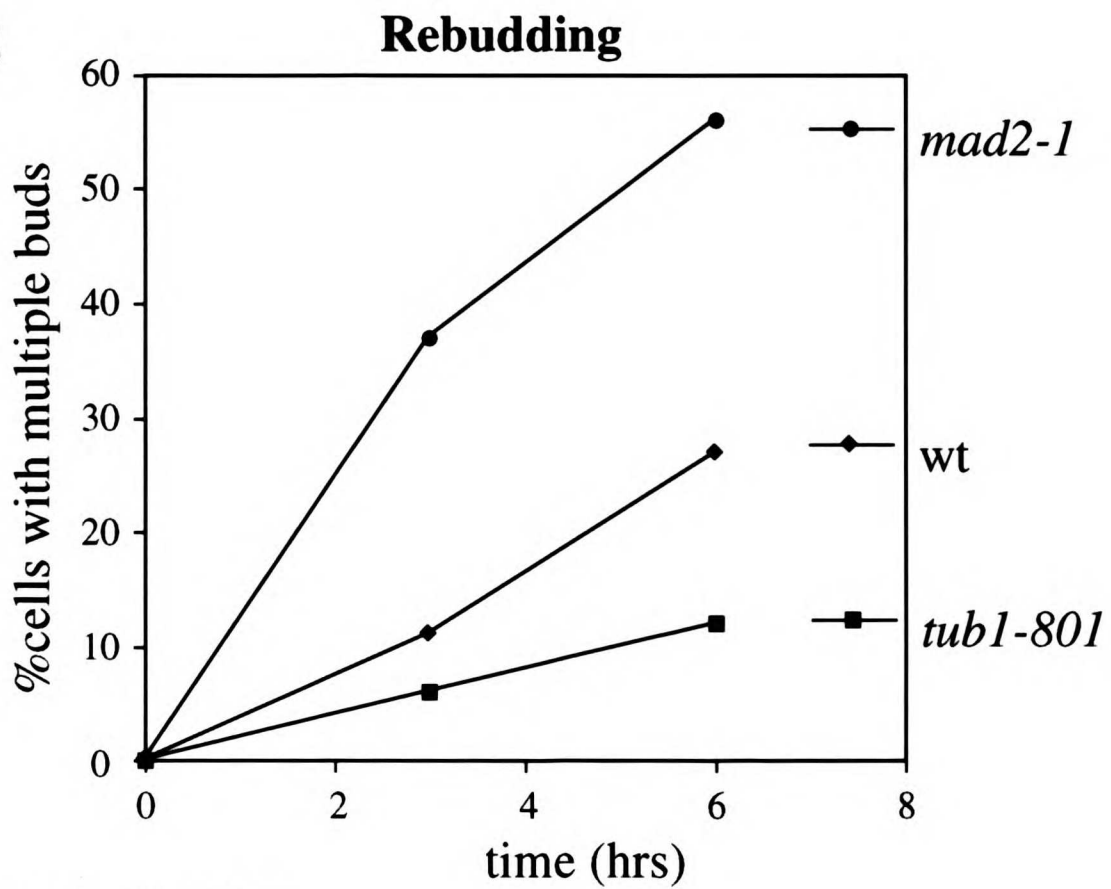
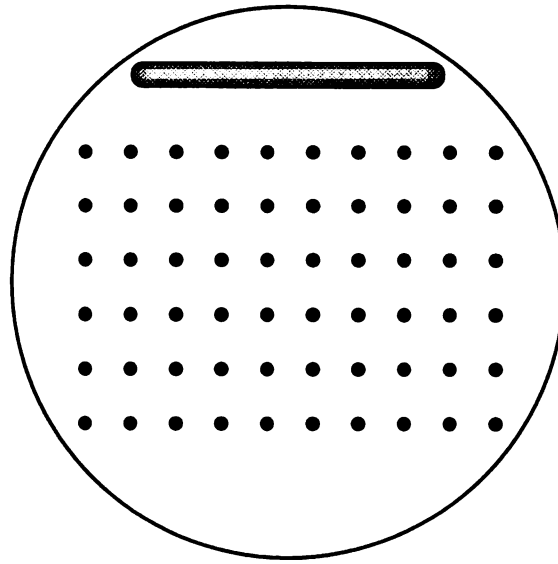
A**B**

Figure 6. Straight and Murray

A



B

Microcolony Assay

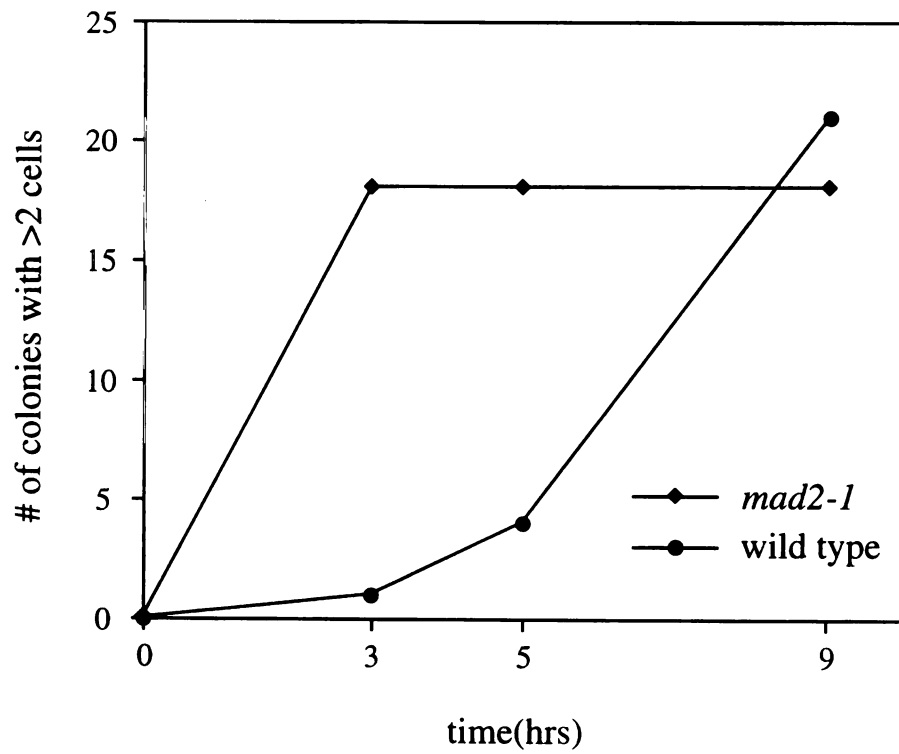
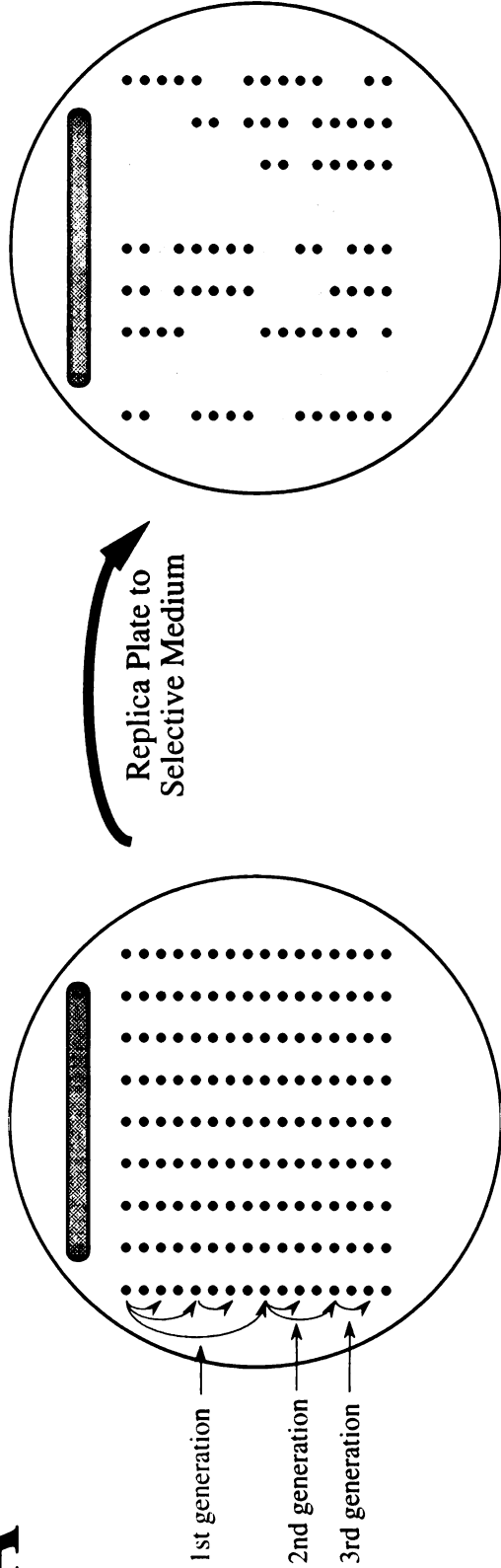


Figure 7. Straight and Murray

A



YPD Plate

-Leucine Plate

B

Checkpoint Genotype	Plasmid	Plasmid-bearing cells		Plasmid-free cells	
		Percent Delayed	No. Divisions	Percent Delayed	No. Divisions
MAD	pVL106 (CEN-linear)	61	147	1	233
<i>mad1</i>	pVL106 (CEN-linear)	2	330	3	38
<i>mad2</i>	pVL106 (CEN-linear)	1	284	2	54
<i>mad3</i>	pVL106 (CEN-linear)	4	400	0	42

Figure 8. Straight and Murray

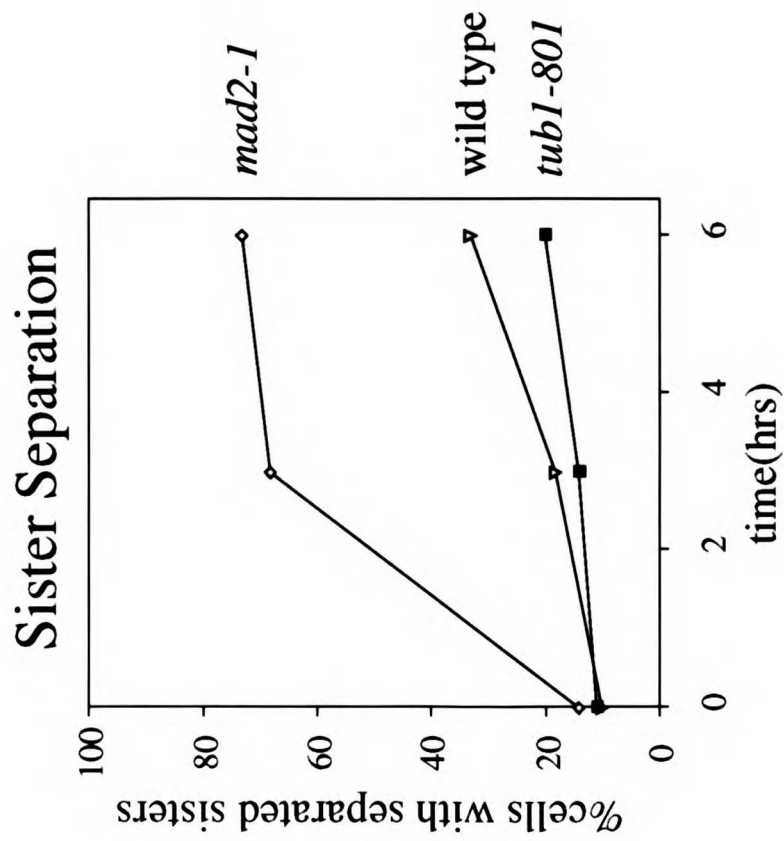
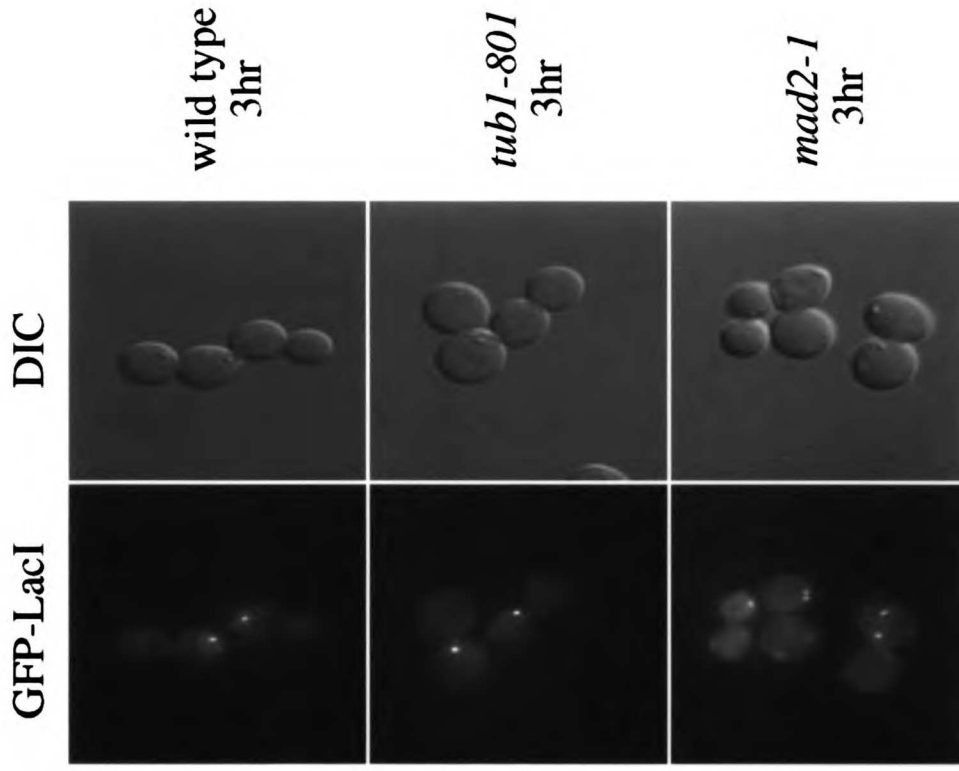
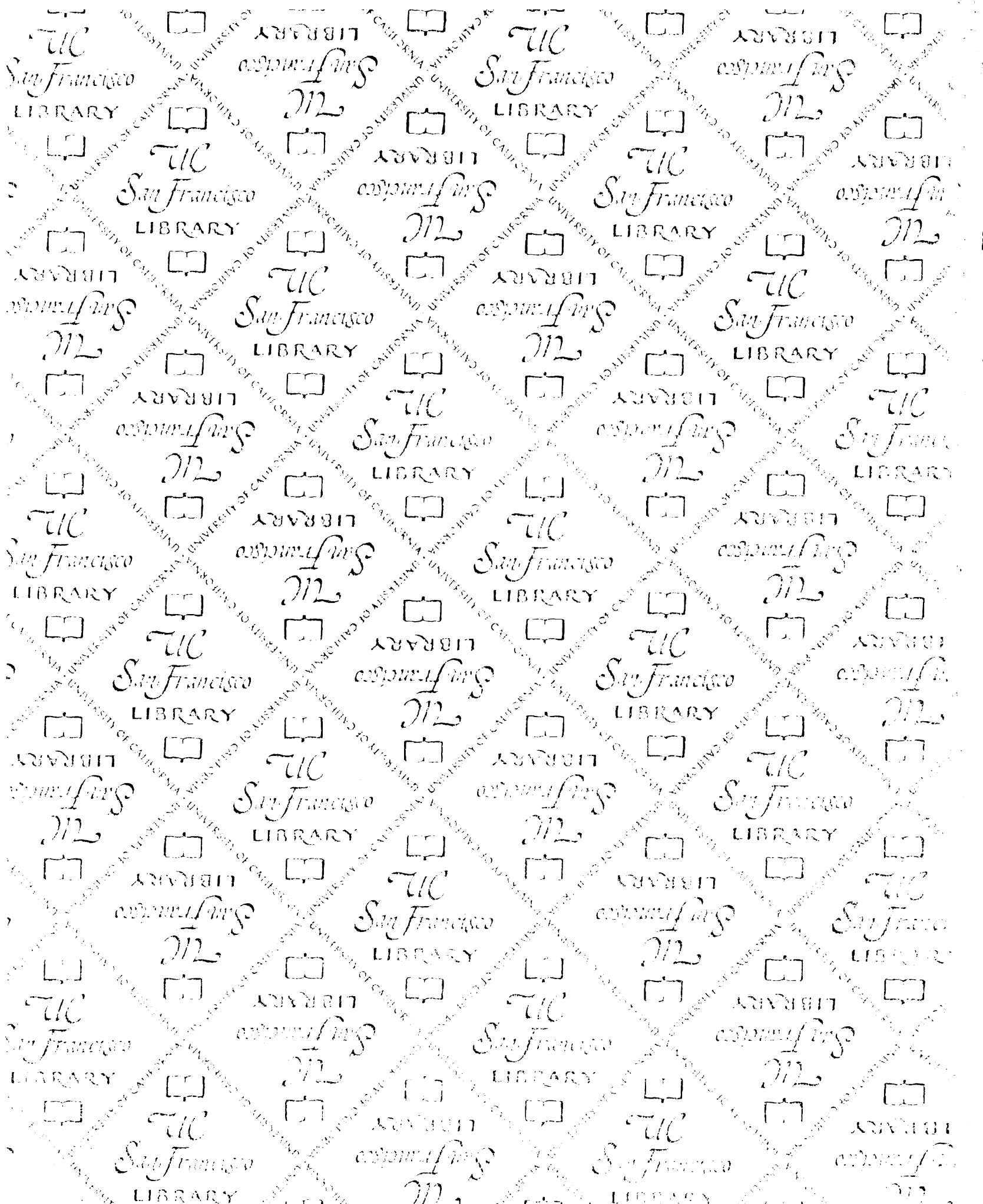
A**B**

Figure 9. Straight and Murray

Reagent Table

Reagent	Supplier	Catalog#	Stock Solution
Nocodazole	Sigma Chemical Co.	M1404	10mg/ml in DMSO
Benomyl	Sigma Chemical Co.	38,158-6	10mg/ml in DMSO
α -factor	Sigma Chemical Co.	T6901	10mg/ml in DMSO
Histone H1	Boehringer-Mannheim	1004875	10mg/ml in water
Bead Beater	Biospec Products, Mini- Beadbeater-8, Bartlesville, OK	693	
Multi Well Inoculating Tray	DanKar Scientific, Wilmington, MA	MC-32T	



For reference

Not to be taken
from the room.

